STATIC AND ULTRASONIC ELASTIC MODULI OF WOOL, MOHAIR AND KEMP FIBRES.

A Thesis submitted in fulfilment of the requirements for the degree of Master of Science in the Faculty of Physics at Rhodes University, Grahamstown

by

Neville Edwin King, B.Sc.(Hons.)

South African Wool Textile Research Institute,
PORT ELIZABETH.

December, 1968.

ACKNOWLEDGEMENTS

The author is indebted to Dr D.P. Veldsman, Director of S A W T R I, for permission to prepare this thesis.

Grateful thanks are expressed to Dr P.J. Kruger of S A W T R I and Professor J.A. Gledhill, joint promotors of this study, for their constructive criticism and encouragement.

The author wishes to acknowledge the help given by various members of S A W T R I staff, especially Messrs R. Slinger and A. Eichstadt.

---oOo---

CONTENTS

PART IV / .....

CONTENTS (Continued)

PART IV

TECHNIQUE OF TRANSMITTING SHORT ULTRASONIC PULSES THROUGH FIBRES

STATIC AND ULTRASONIC ELASTIC MODULI OF WOOL, MOHAIR AND KEMP FIBRES

General Introduction

Fibres used in textiles can be classified broadly into natural fibres and synthetic fibres. Natural fibres can be either animal, such as wool, mohair and camel hair, or vegetable such as cotton, flax and hemp. In the development of synthetic fibres numerous polymers have emerged which have no real natural counterpart and are unique in their mechanical and chemical behaviour. Often the synthetic counterpart of a natural fibre has properties with certain advantages from the textile point of view, but, simultaneously, may exhibit other properties which have disadvantages. Nylon 6 and nylon 6-6, for example, are extremely strong and generally easier to dye than animal fibres. On the other hand, they absorb relatively little water vapour and therefore do not give the buffering action characteristic of hygroscopic fibres, once they are woven or knitted into cloth.

All textile fibres belong to the chemical class of polymers, i.e. they are made up of repeating molecular units which are linked together to form long chains. In wool the chains are made up of amino-acids which cluster together to form protein chains. Three of these protein chains, coil around each other to form what is termed a proto-fibril. The proto-fibrils make up the micro-fibrils, each of these consisting of eleven of the three chain proto-fibrils. The micro-fibrils, in turn, pack together in bundles which run parallel to the length of the wool fibre and are termed macro-fibrils. Sulphur rich amino-acids fill up the spaces between the micro-fibrils forming a matrix which binds the system into a continuous material.

Wool fibres / .....

Wool fibres have certain inherent properties making them very desirable for textiles, particularly for clothing. A wool garment can absorb about 30% of its own weight of moisture without feeling damp or losing its shape. The absorption of water molecules by keratin is an exothermic reaction which assists the human body in its function of maintaining correct body temperatures. The wearer of a wool garment, for example can move from a warm dry atmosphere of his home to a cold damp atmosphere outside. In absorbing moisture from the atmosphere, the garment gives off heat, consequently the body is not subjected to a sudden change in temperature.

Furthermore, the scales on a wool fibre cause the fibre to possess anisotropic friction which is called the differential frictional effect (D.F.E.). The D.F.E. accounts for the feltability of wool, and hence its extensive use in the felt industry. This is also the reason for the wool staples felting during scouring which then results in severe fibre breakage during carding and combing. The extent of felting, however, depends on the bending properties of the fibres, the more pliable fibres exhibiting greater felting propensities. Fibre breakage during carding also depends on the flexibility and extensibility of the fibres.

Closely allied to wool is mohair, the fibre obtained from the fleece of Angora goats. Mohair is also made of keratin, the difference between it and wool being that wool contains a higher proportion of sulphur containing amino-acids. Since wool and mohair are closely allied, studies of mohair will

have some / .....

have some bearing on the properties of wool. Mohair is relatively difficult to process because of the lack of fibre cohesion resulting from the smooth surface of mohair fibres.

The evolution of fine mohair and wool fibres has been accomplished by selective and scientific breeding. Initially, the short, fine fibres were hidden by the thicker, longer and opaque primary fibres. These primary or kempy fibres to a great extent have been bred out of the goat fleece. In worsted yarns, kemp is undesirable since it is coarse and, although it can be dyed, has an opaque appearance due to the existence of cells in the centre of the fibre of a different nature to the rest of the fibre called the medulla.

It is clear from the above that the physical properties of fibres are extremely important and play a major rôle in determining the properties of the finished yarn of fabric; and is intuitively reasonable that the extension and bending moduli of the constituent fibre will influence the yarn or fabric properties to a large degree. The aim of this work was to determine Young's modulus for keratin fibres by static and dynamic methods. The opinion of earlier workers was that Young's modulus of keratin, both for bending and stretching, should be the same at all frequencies. However, they neglected the contribution of the viscoelastic nature of these fibres which, if included, leads one to expect a variation of modulus with frequency. Conflicting results were obtained in some cases and contrary opinions were expressed as to which of the two moduli should have the greater value. Differences between Young's modulus for bending and stretching at very low frequencies also yielded conflicting results. Results given in this thesis agree with conclusions of recent workers, namely that there is really no difference in Young's modulus for

bending and / .....

bending and stretching when measured statically.

Furthermore, a short, accurate method was sought by means of which one could measure elastic moduli of fibres. The methods used by earlier workers of cantilever bending and longitudinal stretching are tedious and the calculations involve a number of fibre parameters. If, however, a stress pulse is propagated through a fibre then the velocity of the pulse through the fibre will be a direct measure of the elastic properties of that fibre. By using compressional, shear and torsional stress pulses, the three corresponding elastic constants can be obtained on a single fibre by merely changing transducers. This is not as simple a task as it appears and certain concepts must be understood before pulse propagation can be applied successfully to the fibres dealt with here. The disjointed nature of the experiments conducted, have lead to the division of the thesis into four parts:

Part I - a summary of the literature relevent to the project.

Part II - a description of the determination of the static elastic modulus of the single fibres.

Part III - a summary of the relevant theory of wave-guide propagation, and

Part IV - a study of the technique of transmitting short ultrasonic pulses through fibres.

PART I

INTRODUCTION AND SUMMARY OF RELEVANT LITERATURE

1.1 The usefulness of elastic moduli measurements

During the various phases of processing of fibres, several mechanical processes are applied. It is therefore essential to understand the mechanical characteristics of textile fibres if certain responses are to be anticipated. The properties of a textile structure, such as a yarn or a fabric, depend on a complex inter-relation of fibre arrangement and fibre properties. The mechanical properties of a fibre are exhibited in a number of ways, all of which combine to determine the particular characteristics of the fibre. To obtain a certain end product it is necessary to find a type of fibre whose characteristics best suit the need of the required textile material.

Cloth properties such as drape, handle and wrinkle resistance, are governed to a large extent by the flexural properties of the individual fibres[1]. The bulkiness of a yarn and its hairiness depend partly on the torsional and flexural rigidity of the individual fibres. High tensile and shearing moduli of textile fibres confer on fabrics dimensional stability and resistance to laundering[2].

1.2 Difficulties encountered when examining elastic behaviour

Fibres are distinguished by the complexity of their mechanical properties, since they are highly deformable and show various elastic aberrations which make application of classical theory inappropriate.

The principal problems which are encountered in the experimental examination of the elastic behaviour of

fibres are:- / .....

fibres are:-

(i) fibres are very susceptible to environmental conditions during and prior to the experiment[3];

(ii) time effects occur to an extent which cannot be disregarded in most cases[4];

(iii) deformation is rarely, if ever, a reversible process. It involves permanent and transient changes in the properties of the material so that an experiment cannot be repeated on the same specimen, i.e. it is not purely elastic, but partly plastic.

Besides these difficulties the variability from fibre to fibre, and even along a single fibre, must be kept in mind. Finally, the external form of the fibre impresses severe limitations on the types of deformation which can be usefully studied; only Young's modulus and the rigidity modulus, of all the classical constants, can be measured with any accuracy. The behaviour of a material depends on its molecular structure which will not only vary from one type of material to another (wool to nylon say), but also from fibre to fibre within a sample. These effects must be taken into account when considering the results of a test. The difference between the behaviour of individual fibres must be investigated and on some occasions the range of results may be more important than the mean value.

1.3 Mechanical properties measured

Because of their shape, the most studied, and in many applications the most important mechanical properties

of textile / .....

of textile fabrics, are their tensile properties. The most commonly measured properties are breaking strength, breaking extension and work of rupture, which are all measurements of the ability of a fibre or yarn to remain intact when subjected to external forces. Elastic recovery, resilience, plasticity, creep and stress relaxation are all concerned with dimensional stability of a fabric or yarn, under the action of mechanical forces or constraints and are useful in evaluating, for example, the recovery from creasing. The static moduli of deformation and yield strains provide a measure of the resistance to change of shape or size, while dynamic modulus and internal friction are related, respectively, to the energy stored and the energy dissipated when rapidly varying stresses or strains are applied. These fibre parameters have a practical value in evaluating the performance of tyre cords, sewing threads, etc., and their theoretical value is in the elucidation of fibre and yarn structure.

1.4 Techniques used in measuring static and dynamic moduli

Bending moduli can be measured either statically or dynamically. Both static and dynamic bending moduli have been measured on fibres by a number of workers with the reported values of static bending modulus varying from greater to smaller than those obtained by extension. Dynamic bending methods have lead to values different from both, so that disagreement is complete. A partial explanation for these discrepancies is that animal fibres are heterogeneous and one can expect the results to differ depending on the experimental technique adopted

for measurement. / .....

for measurement. Differences between static and dynamic moduli are also to be expected due to the viscoelastic nature of keratin fibres which only really becomes important during dynamic measurements. Differences between static bending and static stretching have, however, been subjected to much discussion.

(a) Bending Techniques

Apparatus for bending measurements take many different forms. Sen[5], used a cantilever method for measuring static flexural rigidity of jute fibres while Khyatt and Chamberlain[6] used the same method for wool. The latter determined both bending and extension moduli and their results show that, in all cases, the value of the former was smaller than the latter, i.e. E_b is of the order of $0.5E_s$ to $0.75E_s$. (E_b and E_s are Young's modulus for bending and stretching respectively.)

Meredeth[7], on the other hand, held that E_b was greater than E_s. A randomly arranged mass of wool was compressed by van Wyk[8] and his results suggest a bending modulus of one-hundredth that of stretching. A number of other workers also used this technique[9,10,11]. Mitchell and Feughelman[12] used an apparatus in which fibres up to 3 mm in length were deflected by a brass cantilever to which a mirror was attached. They concluded that, within the limits of the experiment, Young's modulus obtained from bending was the same as obtained from extension. Simpson[13], who compared static moduli with those obtained by low frequency dynamic determinations, reported that differences can be accounted for by such factors as work hardening and, furthermore, that the

load-extension curve / .....

load-extension curve in the "Hookean" region is not entirely linear.

Measurements by Lochner[14] of Young's modulus by dynamic bending methods such as transverse vibrations in the frequency range 50-600 Hz of wool fibres held in a cantilever position, gave a modulus of about twice that obtained in extension, i.e. 7.47×10^{10} dynes/cm^2. Guthrie et al[15] measured the bending modulus of Merino wool fibres statically and dynamically over a frequency range of 40 Hz to 2 kHz. They concluded that bending rigidities of fibres measured by dynamic methods are always greater than the values obtained by the static method. Hermanne[16] also stated that values of the moduli at acoustic frequencies are invariably higher than those obtained quasi-statically. Kärrholm and Schröder[17] found with viscose rayon, as did Guthrie[15], that Young's modulus for bending is greater than that for stretching. From the variation in the methods used by the various workers mentioned, and the different experimental conditions used, it is not surprising to find that the conclusions differ to such an extent. It appears that only results of determinations carried out under similar circumstances and with similar experimental arrangements should be compared, which is also the view held by Simpson[13].

(b) Dynamic Techniques

Dynamic measurements consist of vibrating systems in which stress and strain vary (usually sinusoidally) with time.

Time effects in the elastic behaviour of fibres can be neglected or eliminated if the deformation is

rapid enough. / .....

rapid enough. This has led to sonic and ultra-sonic techniques being used advantageously for measuring moduli. The methods of vibrating systems can be classified into three groups, based on the vibration wavelength - dimension ratio of the specimen.

(i) For wavelengths much greater than the length of the specimen, the cross-sectional area rather than the mass per unit length is of prime importance (about 0.01 to 1 Hz). Under these conditions all portions of the fibre are subjected to the applied stress and are strained in unison in the same direction (as occurs at low extension rates in the Instron Tensile Tester).

(ii) If the wavelength is of the same order of magnitude as the specimen length, standing waves occur in the specimen which are controlled by the mass per unit length. The frequency at which standing waves occur is of the order 1 Hz to 1 kHz.

(iii) Finally, if the wavelength is small compared with the dimensions, elastic waves are propagated through the material. (This occurs at frequencies above approximately 10kHz).

Experiments conducted in category (i) are the most numerous and best explained. The literature

of these / .....

of these experiments is too great to discuss here. Many commercial instruments are available, these being mainly stress-strain recorders. The curves from the instruments can be used to determine the initial modulus, yield stress, breaking load, breaking extension and work of rupture. A good description of this type of instrument is given in a book by Meredeth and Hearle[18].

Experiments in the second category are of more significance to this thesis. Experiments were carried out by Ballou and Smith[19], who measured the frequency of vibration of a small mass attached to the lower end of a suspended fibre. The mass undergoes damped simple harmonic motion in the vertical plane and from the equation of motion, the modulus and damping factor can be determined.

Lotmar[20] seems to have been the first to have used standing waves in order to determine the velocity of sound in textile materials. By calculating the wavelength of the standing waves λ, the velocity can be found, knowing the frequency of oscillation f, since $c = f\lambda$; hence from the modulus velocity equation $E/\rho = c^2$ where ρ is the linear density of the material, the modulus E can be obtained. His method was relatively crude and consisted of exciting a specimen by longitudinal frictional contact applied manually, the note produced being matched with that of a standard specimen of known properties. Ballou and Silverman[21] refined this method by attaching the specimen to a driving source consisting of a steel bar and a Rochelle salt crystal, and plotting the

standing wave / .....

standing wave pattern in the specimen by means of a sensitive Rochelle salt crystal sensing probe. Measurements were made on rayon and nylon filament yarns and strips of cellulose film at 9.4 kHz. Hamburger[22] working along similar lines, determined the wavelength of standing waves by finding the length of the specimen at which the output wave was in phase with the input wave. Dunell and Dillon[23] and Tipton[24], excited specimens into resonant vibrations and determined the wavelength in the material. Tipton's results included sonic modulus measurements on worsted wool and mohair/wool blend yarns.

Weyland[25] measured dynamic moduli at about 1 kHz as a function of strain; obtaining results for wool. In principle, the dynamic elastic constant of the fibre is determined by measuring the resonant frequency of a cantilever spring which is loaded with a strained fibre - which then undergoes longitudinal vibrations. Joshi[26] suggested certain minor improvements to Weyland's technique.

Resonant vibrations of fibres mounted in the cantilever position have been measured by a number of workers. These include Lochner[14], Guthrie et al[15], Kärrholm and Schröder[17] and Lincoln[27]. Methods ranged from exciting the fibres mounted in front of a speaker, to excitation by means of an electro-mechanical transducer. There should be only a very small variation of diameter along the length of the fibre for this type of experiment in order for it to be

successful, / .....

successful, which is unfortunately, a serious limitation for wool fibres.

Transmitting stress pulses along the specimen and timing the interval between excitation at one end and reception at the other end of the specimen forms the basis of measurements in the third category. The method was used by Hamburger[22] as an alternative to his standing wave technique. Other workers were De Vries[28] and Fujino et al[29].

The above-mentioned workers were mainly concerned with applying a new technique of measurement of elastic constants. Later workers (such as Zorowski and Murayama[30]) using improved techniques, developed an interest in the theoretical aspects of wave propagation. They made an analytical and experimental study of dynamic moduli in continuous filament twisted yarns to establish how small amplitude strain waves are propagated. Charch and Mosely[31] worked on molecular structures as revealed by sonic observations in synthetic fibres. They used a frequency of 10 kHz and were mainly concerned in proving the usefulness of sonic moduli. Grover, Dillon and Suppiger[32], while determining variation of Young's modulus with fatigue, also noted that the modulus for stretching is a measure of molecular orientation. Morgan[33] developed a commercially available Modulus Uniformity Monitor which measures the acoustic velocity by means of a fixed frequency (5 kHz) standing wave technique. The most dramatic application of this instrument has been to pirn wound packages of filament nylon. Data have shown modulus peaks which occur regularly at the ends of pirns.

These modulus / .....

These modulus peaks are a source of length variations in knitted fabrics and a source of pirn taper barré. in dyed fabrics.

Wegener[34] has pointed out that the value obtained for the so-called "mechanical modulus" increases with increasing strain rate. At extremely high strain rates, the "mechanical modulus" equals the value of the sonic modulus (the elastic modulus at sonic frequencies). In viscoelastic materials the elastic component of the deformation is independent of the rate of strain, while the plastic component is not. At high strain rates and with such small stretch amplitudes as arise during the measurement of sonic modulus, high molecular weight polymers are for the most part deformed elastically. On the other hand, when measuring the mechanical modulus, the plastic component is involved. Basically then the mechanical modulus need not describe the same structural characteristics as the sonic modulus. (This point is more clearly illustrated when the theory is examined at a later stage.) Wegener's[34] results also show that the sonic modulus depends on the molecular structure of the fibre.

Apart from cantilever vibrations, all the above dynamic methods involve longitudinal excitation. The sonic measurements are also all longitudinal and few results on single wool filaments exist. Gelles[35] appears to be the only person who has obtained shear, longitudinal and torsional ultrasonic waves transmitted in thin films, fibres and fine wires. The techniques he used are suited for sample dimensions similar to those of single animal fibres, although limitations exist due to the high damping in fibres.

PART II

STATIC DETERMINATIONS OF YOUNG'S MODULUS

In an attempt to clarify differences between Young's modulus for static bending and static stretching, an instrument was built for the determination of static bending modulus, while an Instron tensile tester was used in determining the extension modulus. Measurements were conducted on mohair and kemp fibres, wool being excluded because of its high degree of crimpiness.

2.1 Apparatus

The apparatus (Figure 1) consited of a galvanometer G, with a small piece of a razor blade mounted on the end of its pointer, to provide a knife edge. Current passing through the coil deflected the needle - the torque produced being proportional to the current in the coil[36]. This torque was opposed by the restoring torque in the galvanometer restoring springs. By hanging different weights over the knife edge, the current required in each instance to restore the needle to its zero position (i.e. restoring torque of the springs equal to zero) was determined, and a calibration curve was drawn.

The galvanometer was mounted on a brass block A, which could be moved by means of screw B in a vertical plane along the two rods R_1 and R_2, R_2 being threaded. The fibre snippet to be tested was mounted in a fine glass capillary, which was held in clamp C by a small thumb screw. The clamp C was held firmly in place by another clamp D consisting of two parallel brass plates

and a / .....

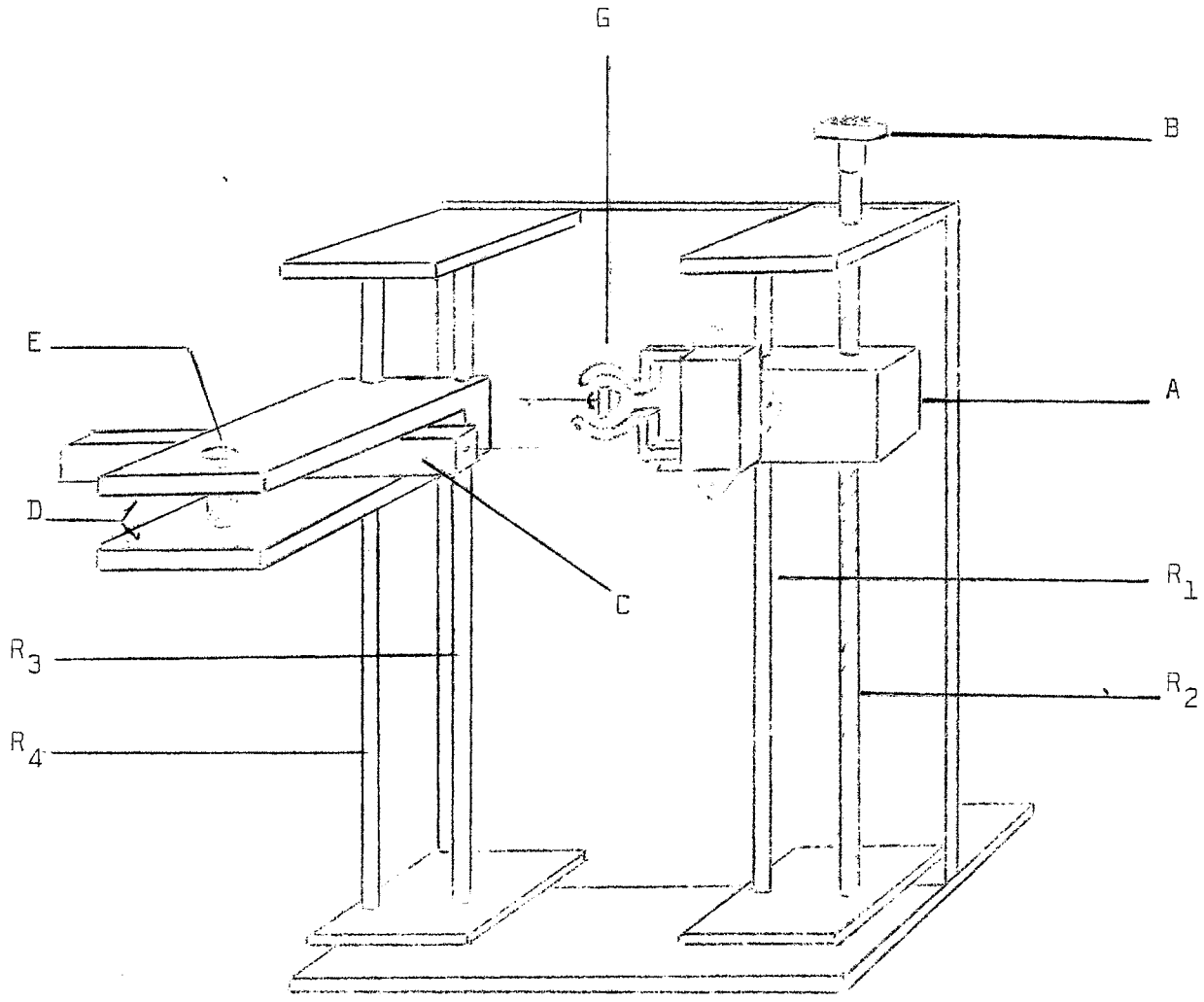

Figure 1.

G	-	Galvanometer
A	-	Galvanometer mount
R_1 R_3 R_4	-	Sliding Rods
R_2	-	Threaded Rod
B	-	Galvanometer positioning screw
E	-	Clamp securing screw
D	-	Sliding clamp
C	-	Capillary holder

and a securing screw E. Clamp C could move in a horizontal plane between the plates of D, thus facilitating alignment of the fibre under the knife edge. Clamp D could also be moved in a vertical plane along rods R_3 and R_4 and could be fixed in position by a locking screw.

The circuit providing the current consisted of a 3-v battery in series with two switch-in resistors and two series potentiometers for coarse and fine adjustment. The current was measured on a microammeter. The whole apparatus was made of brass to eliminate stray magnetic effects and was enclosed on three sides by an aluminium shield to eliminate air-current effects. Fibre deflections and lengths were measured by means of a travelling microscope capable of reading to 0.002 mm. A narrow beam of collimated light illuminated the knife edge at the point of contact with the fibre; temperature effects due to the light were then negligible.

2.2 Procedure

(a) General

Measurements were carried out in a conditioning room at 20°C and 65% RH. The fibres were conditioned for at least 24 hours before being subjected to measurement. Fibre diameters were measured on a Visopan projection microscope (Reichert) at about 100 places along their length. Fibres with a Coefficient of Variation (C. of V.) greater than 8% were rejected. Kemp, possessing a medulla and having an elliptical, cross section posed some problems. Diameter measurements had to be carried out with the fibre immersed in oil, rotated through 90°, and re-measured. By this method, the mean

major and / .....

major and minor axes were determined. Before the kemp fibres were stretched on the Instron, they had to be cleaned thoroughly and then conditioned in a standard atmopshere for at least 24 hours. Fibres to be bent were cemented in fine glass capillaries by means of "Cutex", care being taken for the fibre to emerge abruptly from the capillary tube.

Deflections were read on the travelling microscope for units or multiple units of current and the mean deflection calculated. Deflections were kept to less than 4% of the length of the snippet.

E_b for individual fibres were calculated from the formula[37] assuming the fibre weight to be negligible

$$E_b = \frac{gWl^3}{\gamma\ 3I} \qquad (1)$$

where W is the weight producing a deflection γ for a fibre of length l; and

g = acceleration of gravity

I = second moment of area of cross section of the fibre.

W = ik, where

i = current and k = slope of calibration curve.

For mohair, assuming a circular cross section of radius r, we have

$$E_b = \frac{4\ ikl^3}{3\ \pi\ r^4 \gamma} \qquad \text{since } I = \frac{\pi}{4} .r^4$$

OR

$$E_b = \frac{C\ l^3}{r^4\ \gamma} \qquad (2)$$

where / .....

where

$$C = \frac{4}{3}\,\frac{ikg}{\pi} = \frac{4}{3}\cdot\frac{kg}{\pi}$$

if γ is the deflection per unit of i.

For kemp, assuming an elliptical cross section, we have

$$I = \frac{1}{4}\pi\,(a_2b_2^{\,3} - a_1b_1^{\,3})$$

and from Equation 1,

$$E_b = \frac{l^3}{\gamma}\,\frac{C}{(a_2b_2^{\,3} - a_1b_1^{\,3})} \qquad (3)$$

where a_2 and b_2 are the outer major and minor axes, and a_1 and b_1 are the inner major and minor axes, respectively. Note that for an elliptical cross section, there are two neutral planes about which the bending can take place. Measurements of the bending modulus were measured in both these planes, and the result averaged.

(b) Comparison of E_b and E_s

Twenty mohair fibres of uniform diameter were bent on the apparatus at two different lengths l_1 and l_2. Each fibre was loaded and unloaded twice to obtain a good mean value for the deflection. The same fibre sections were then used for the determination of E_s by means of the Instron tensile tester at an extension rate of 0.05 cm/min and gauge length of 0.5 cm.

About 15 kemp fibres, having relatively small C.V. of diameter, were selected, bent, and stretched as described above. However, in determining E_s, the fibre snippets were too short to be clamped securely in the Instron tensile tester and it was necessary to glue

them into / .....

them into capillaries. Araldite cement was used and allowed to dry for 3 days. Lengths were measured on the travelling microscope before stretching. E_s values for mohair and kemp fibres were computed from the following formula.

$$E_s = \frac{\text{Stress}}{\text{Strain}} = \frac{m}{l'} \times \frac{glo}{A} \qquad (4)$$

where mg is the force producing an extension l' in a specimen of length lo and cross section area A.

(c) Sources of Error

The coefficient of variation of E_b for mohair was 3.3% with the major contribution being due to the measurement of γ. The use of the average value of diameter, instead of the expectation, leads to errors in most cases of about 1%. Extension rates and bending rates were considered to be high enough for creep effects to be neglected, and a more complete discussion of these and other errors is discussed in a previous report[38].

2.3 Results and discussion

The calibration curve of the galvanometer is shown in Figure 2; it is linear and reversible. The conversion factor for current to weight, i.e. the slope of the line, has a least-squares value[39] of 7.69 $\pm$ 0.09 x 10^{-5} g/micro/amp, with a C.V. of 1.2%.

A typical fibre deflection-applied force (or current) curve for mohair is given in Figure 3, showing a linear relationship and thus satisfying Equation 1. The graph of the deflection γ vs l^3 gave a straight line, as may be seen for the two kemp fibres illustrated in Figure 4. This also substantiates Equation 1. These results are similar to those obtained for mohair, as shown by the examples in Figure 5. The fact that one

of the / .....

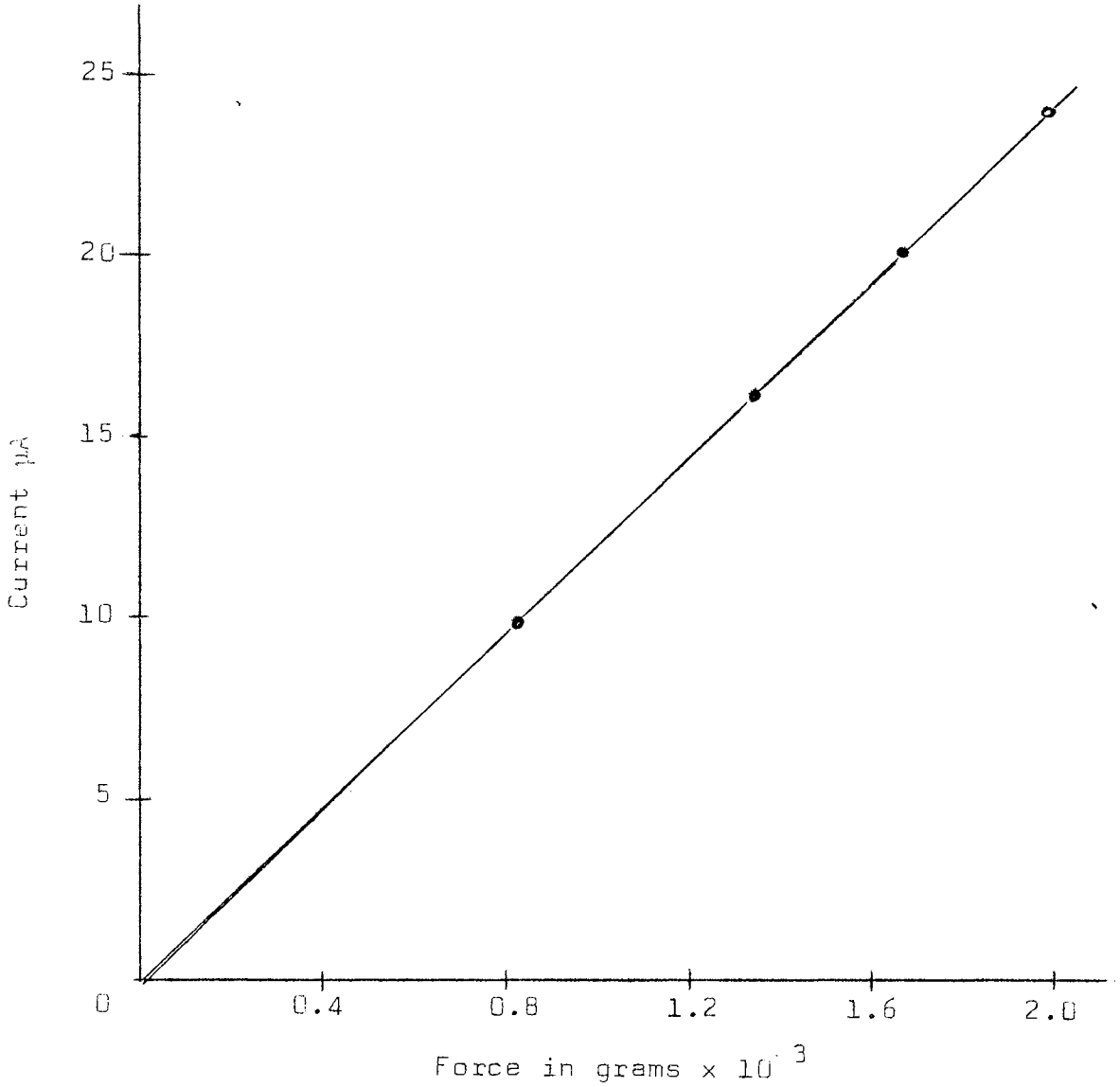

Figure 2. The relationship between galvanometer current and calibrating force.

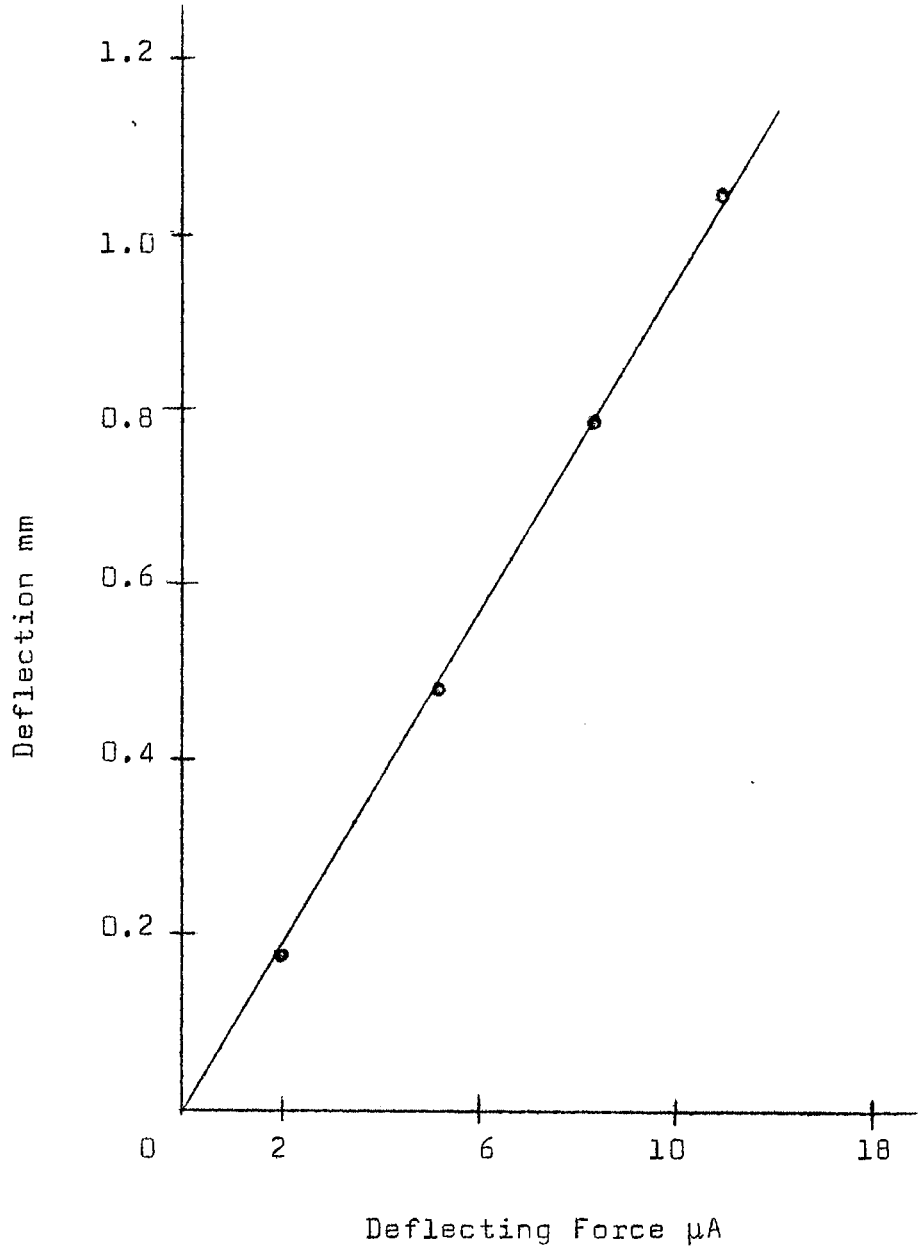

Figure 3. The relationship between applied deflecting force and deflection of mohair fibre M_1.

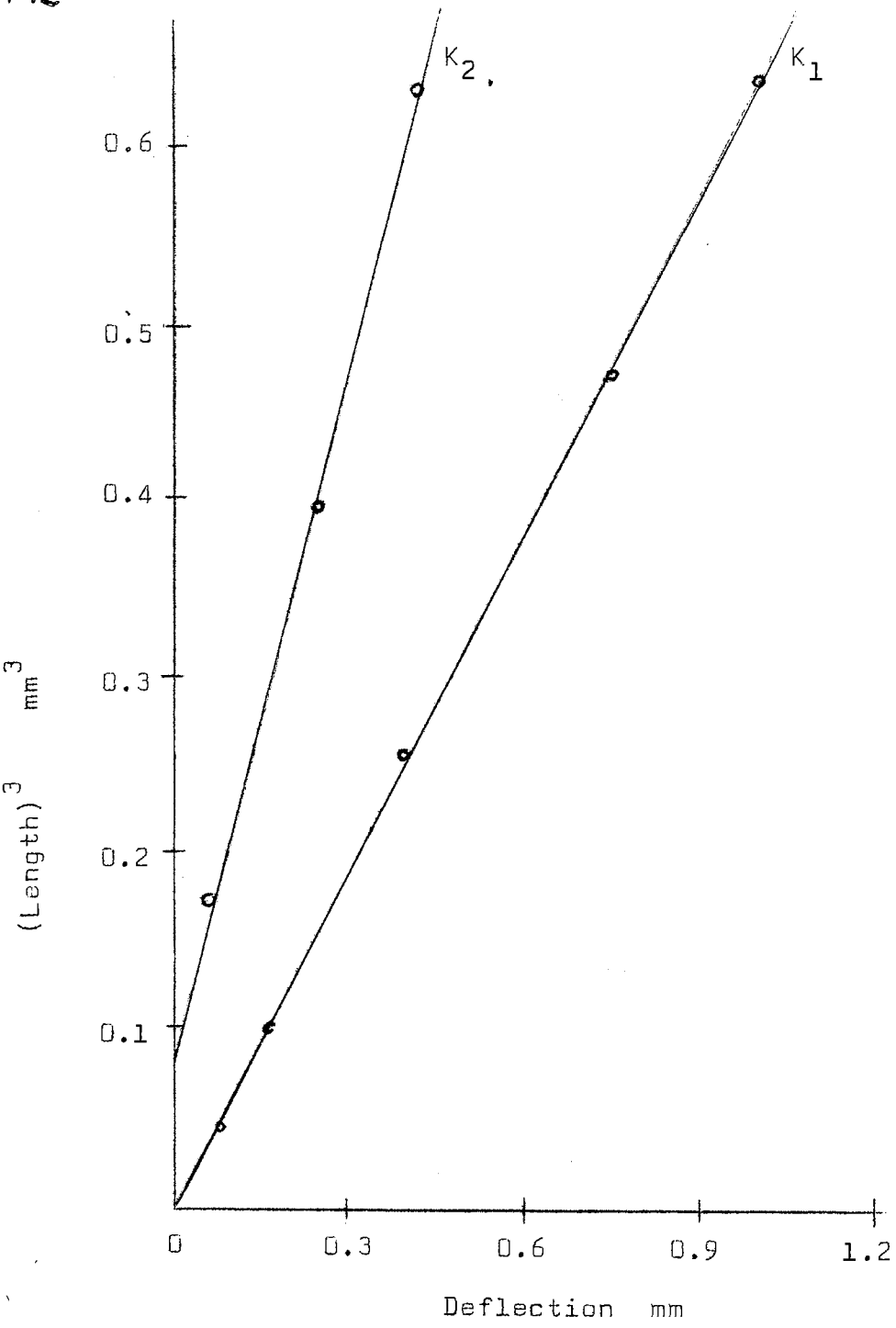

Figure 4. The relationship between (fibre length)^3 and deflection for two kemp fibres K_1 and K_2.

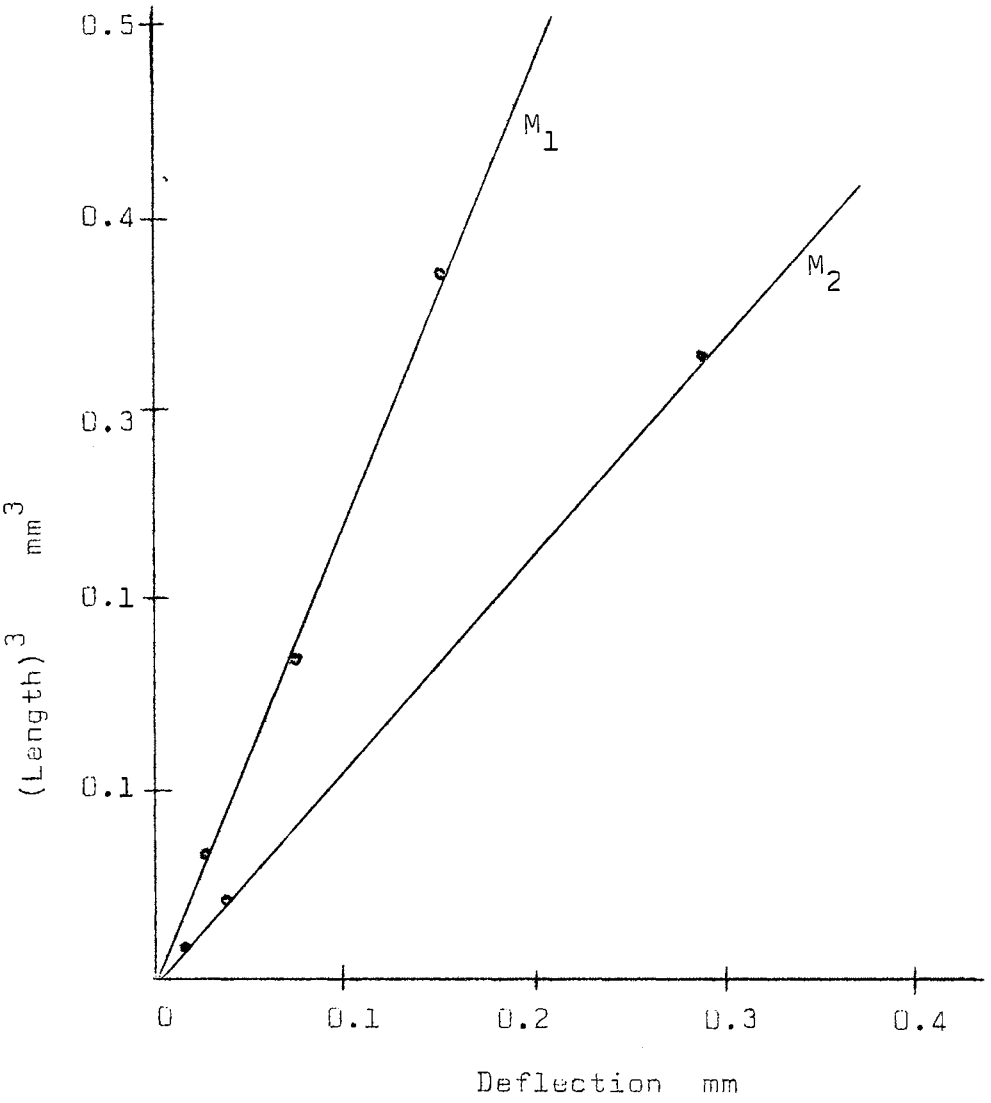

Figure 5. The relationship between (fibre length)^3 and deflection for two mohair fibres M_1 and M_2.

of the curves of kemp does not pass through the origin is probably due to the fibre not emerging abruptly from the capillary. The length measured would then possess a small error.

The results for mohair are given in Tables I and II while kemp results appear in Tables III and IV. There is a large fibre-to-fibre variation in E_b for kemp fibres, although the values do not vary significantly for a single fibre. The ratio l^3/γ is independent of the moment of inertia, although not completely independent of the radius, so that differences seem to be due to the elasticity of the fibre.

In Figure 6, E_b has been plotted vs E_s indicating a linear relationship with a regression coefficient of 0.35. The large scatter in the results of E_b can be ascribed to the fact that in bending, the fibre diameter near to the base of the cantilever will be more important than at the tip. Also, the calculation of E_b involves the third power of the length and the fourth power of the radius, so that errors in (l) and (r) will multiply. In contrast, calculation of E_s involves only the square of the radius and the first power of (l).

Although differences in E_b and E_s exist for individual mohair fibres, the sample means differ only slightly as can be seen by the following figures

$$\bar{E}_b = 4.09 \times 10^{10} \text{ dynes/cm}^2$$

and

$$\bar{E}_s = 3.47 \times 10^{10} \text{ dynes/cm}^2.$$

The difference between these means gave a t-value of 1.46 which is non-significant. This agrees with

Mitchell and / .....

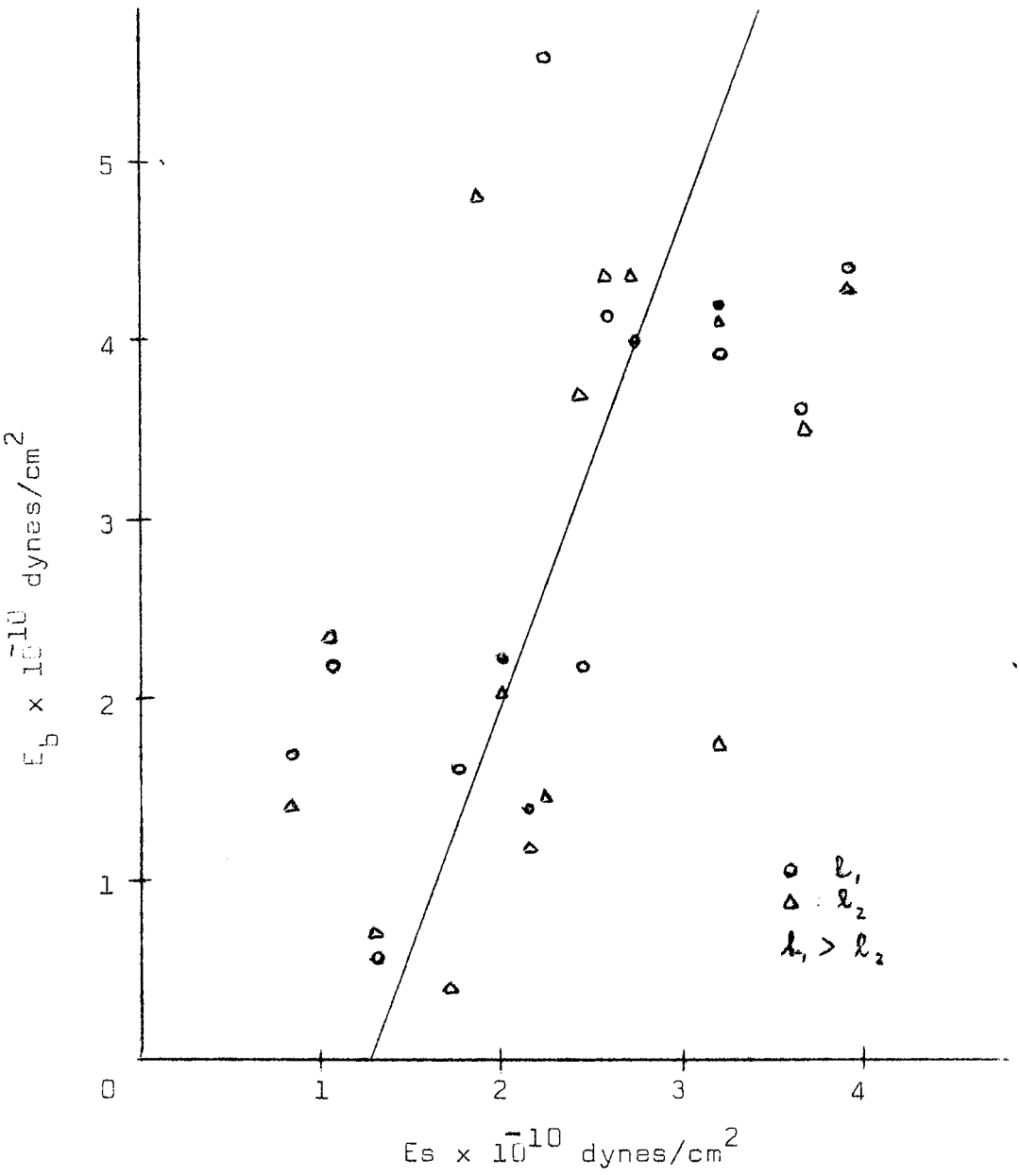

Figure 6. The correlation between Young's modulus for bending (E_b) and stretching (E_s) for mohair.

Mitchell and Feughelman's[12] finding, although their values for E_b are 50% smaller, probably, because their measurements were done in water which results in the well known breaking of hydrogen bonds so decreasing the "dry" value of E_b[18].

A poor negative correlation exists between E_b and the diameter as shown in Figure 7 and this effect becomes slightly more pronounced with E_s (Figure 8). The regression coefficients are 0.093 dynes/cm^2/micron and 0.095 dynes/cm^2/micron, respectively, but are non-significant. A similar negative correlation was found by Thorsen[40]. There appears to be no correlation between E_b and bending length l, a result which is to be expected.

Concerning kemp results, from a plot of l^3/γ vs $(a_2b^3_2 - a_1b^3_1)$ as shown in Figure 9, there appear to be two distinct types of fibre. The fibres on curve I (called Type I fibres) gave a mean value of E_b of 1.03 x 10^{10} dynes/cm^2 while those of curve II (Type II fibres) gave a mean value of 4.75 x 10^{10} dynes/cm^2.

A test for significance between the two means gave a t-value of 6.52 which is highly significant; hence, the above classification is a valid one. The most probable explanation for the above distinction must be sought in the presence or absence of a medulla.

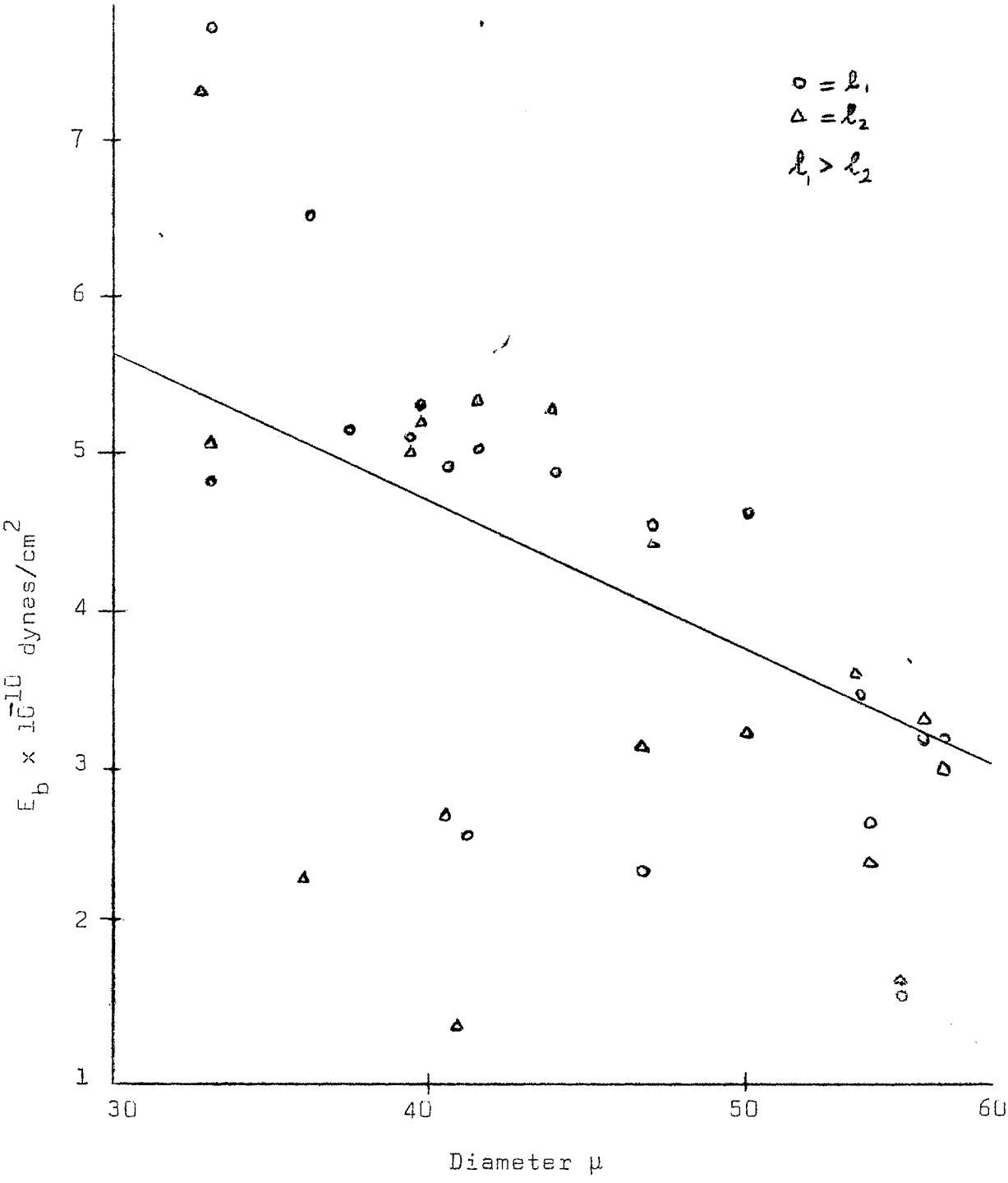

Figure 7. The correlation between Young's modulus for bending (E_b) and fibre diameter for mohair.

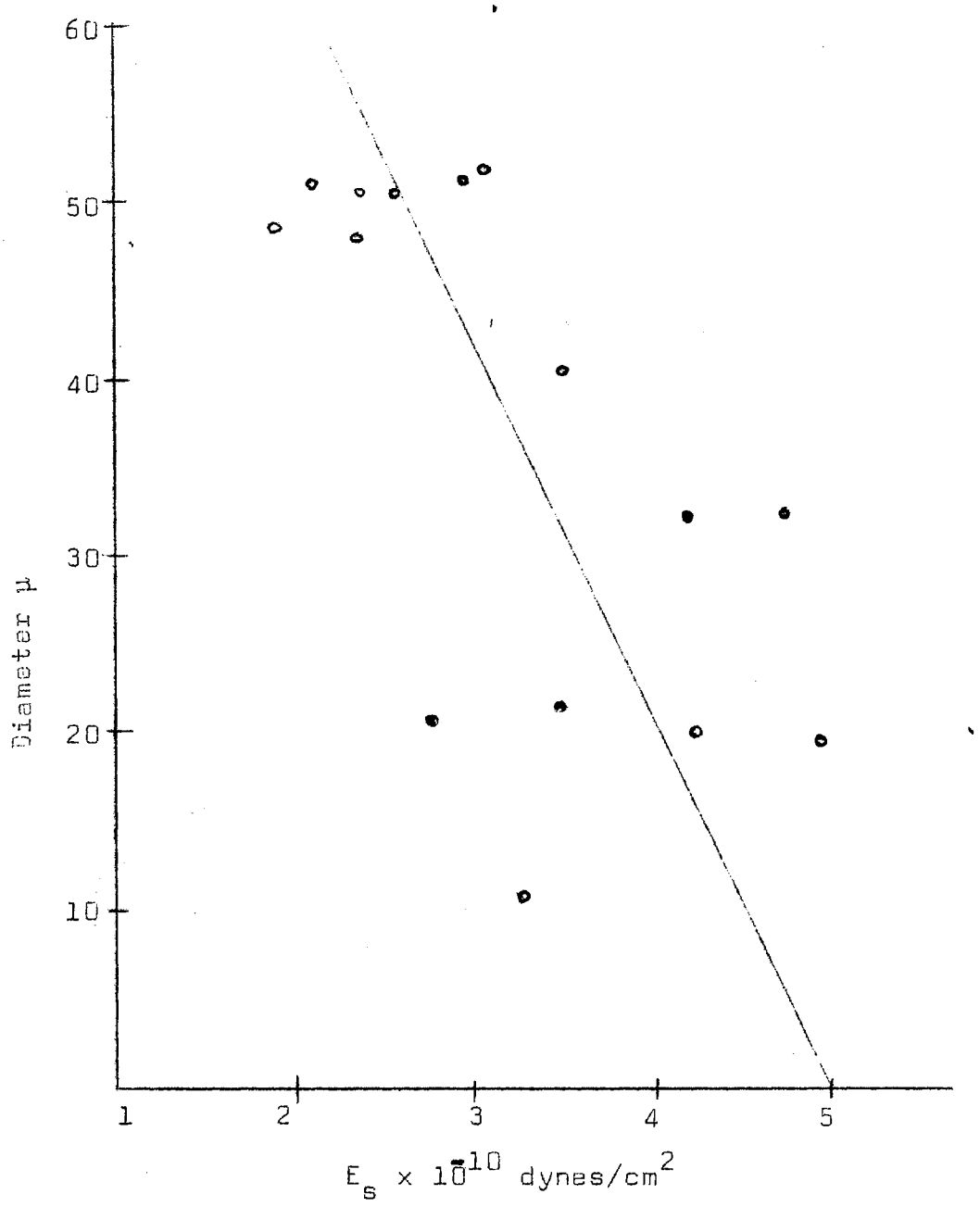

Figure 8. The correlation between Young's modulus for stretching (E_s) and fibre diameter.

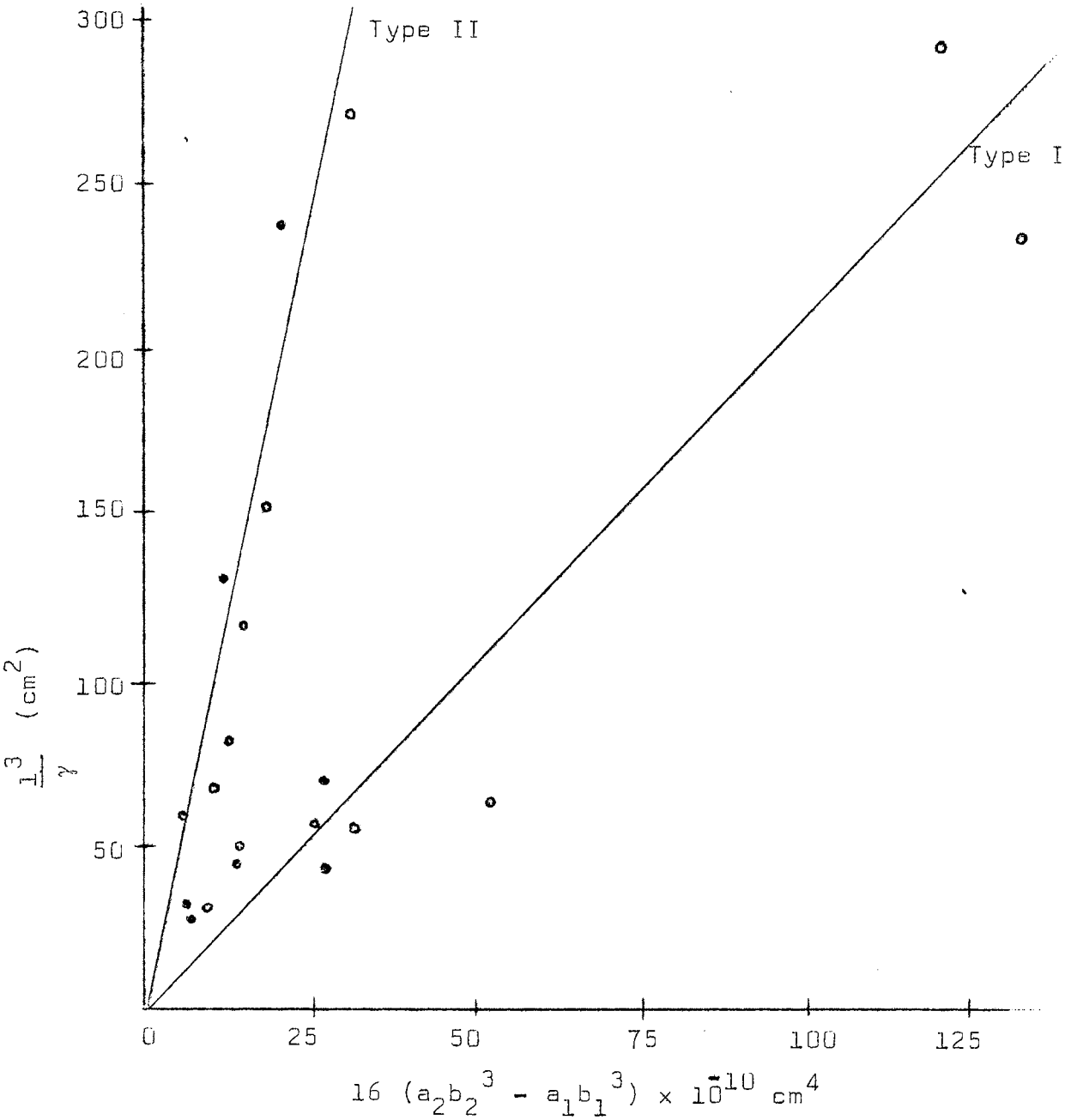

Figure 9. The relationship between deflection ratio ($\frac{l^3}{\gamma}$) and the moment of inertia for kemp.

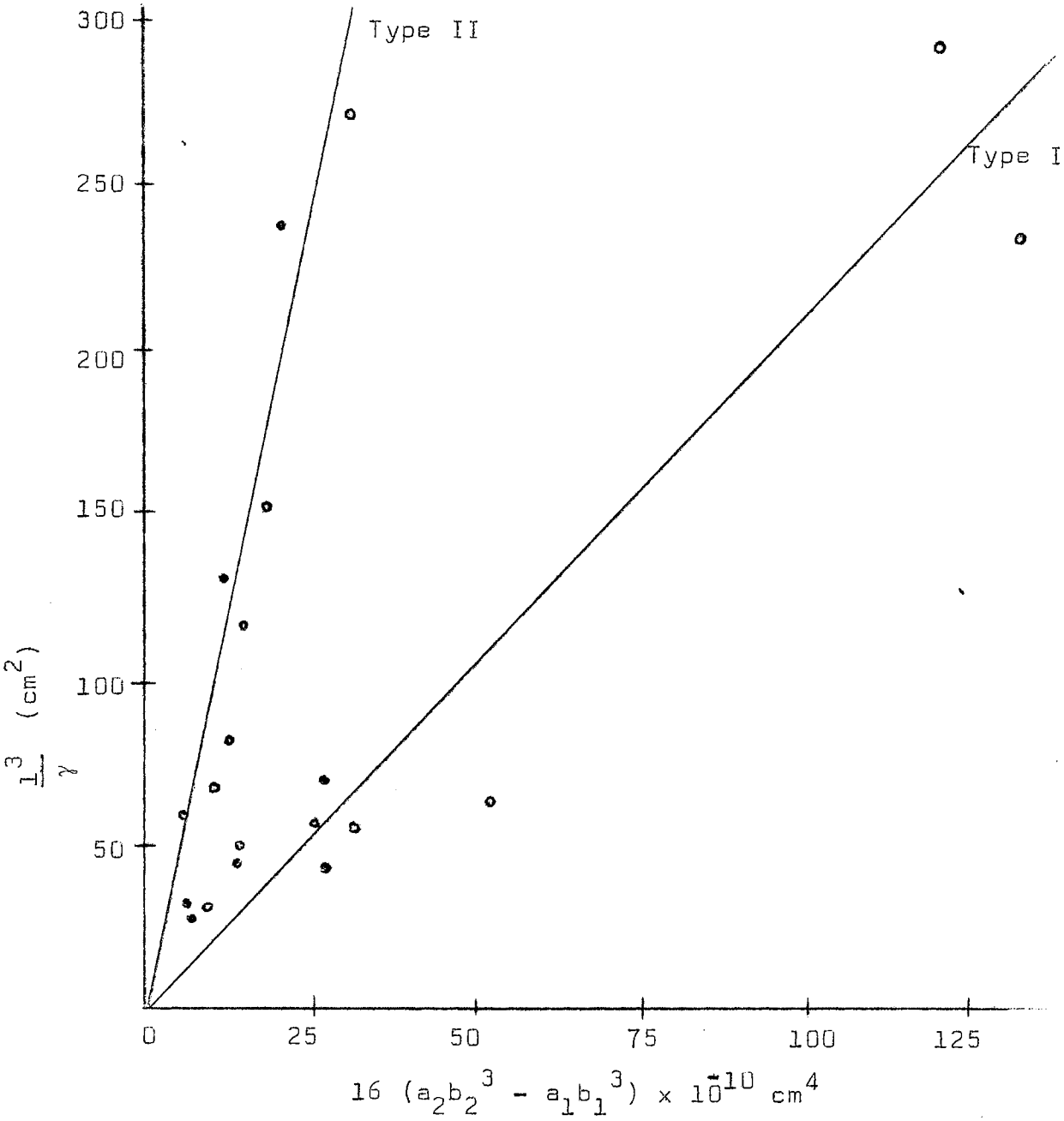

Figure 9. The relationship between deflection ratio ($\frac{l^3}{\gamma}$) and the moment of inertia for kemp.

TABLE I

Determination of the bending modulus of mohair fibres

Fibre No.	l, mm	γ, mm	l^3/γ	$E_b \times 10^{10}$ dynes/cm^2
a	12.435	0.7900	2.434	3.47
	9.702	0.3840	2.378	3.39
	7.137	0.1430	2.542	3.63
	5.450	0.0701	2.309	3.29
	3.914	0.0270	2.221	3.17
	1.990	0.0110	1.429	-
		Mean	2.377	3.39
b	8.975	0.7570	0.955	2.74
	6.884	0.2770	1.178	3.38
	5.016	0.1180	1.070	3.07
	3.251	0.0312	1.101	3.16
	1.844	0.0045	1.419	4.07
		Mean	1.084	3.29
c	7.444	0.4230	0.982	3.83
	5.095	0.1020	1.294	3.73
	2.874	0.0190	1.248	3.61
		Mean	1.175	3.72
d	7.691	0.3380	1.345	3.94
	5.434	0.1220	1.310	3.84
	3.916	0.0472	1.271	3.73
		Mean	1.309	3.67

TABLE II

Bending* and stretching moduli for mohair fibres

Fibre No.	Diameter μ	$E_b \times 10^{10}$ dynes/cm^2	$E_s \times 10^{10}$ dynes/cm^2
1	37.4	5.18	-
2	55.0	1.58	2.30
3	54.0	2.67 2.39	1.88
4	53.4	3.49 3.67	2.29
5	54.4	3.22 3.00	3.00
6	55.8	3.20 3.32	2.06
7	41.1	2.59 1.41	2.78
8	46.8	2.36 3.17	4.21
9	55.3	- -	2.54
10	55.8	7.05 5.82	2.93
11	41.5	5.06 5.33	3.59
12	50.0	3.15 4.66	3.49
13	39.4	5.14 5.10	4.25
14	33.2	7.76 5.08	5.09
15	47.4	4.54 4.47	4.71
16	36.1	4.54 2.32	3.27
17	44.4	4.92 5.32	3.72
18	40.6	4.94 2.70	4.19
19	39.6	5.31 5.22	4.95

* Bending moduli were determined at two different lengths for each fibre. The values of E_b refer to the two different lengths used.

TABLE III

Determinations of Young's modulus for kemp fibres

Fibre No.	l, mm	γ, mm	l^3/γ cm^2	$16(a_2b_2^3-a_1b_1^3)$	$E_b \times 10^{10}$ dynes/cm^2	
					Type I	Type II
1	3.186	0.0106	30.77	8.03($\times 10^{10}$cm^4)	-	1.96
2	3.831	0.0094	59.98	52.01	0.59	-
3	3.400	0.0030	132.87	9.92	-	6.85
4	3.533	0.0107	40.91	3.28	-	6.24
5	3.427	0.0027	151.13	17.26	-	4.48
6	4.845	0.0048	236.59	18.69	-	6.46
7	4.347	0.0033	252.05	144.97	0.89	-
8	3.669	0.0105	46.99	12.96	-	1.86
9	3.273	0.0125	28.16	5.55	-	2.59
10	4.105	0.0097	71.60	7.27	-	5.04
11	4.734	0.0103	103.30	9.09	-	5.66
12	3.751	0.0167	31.65	4.00	-	4.05
13	4.153	0.0120	59.67	4.86	-	6.26
14	4.083	0.0081	83.63	12.51	-	3.36
15	4.890	0.0101	115.77	12.48	-	4.64
16	4.390	0.0026	325.49	133.41	1.25	-
17	4.369	0.0154	54.07	30.11	0.92	-
18	5.767	0.0071	271.70	29.44	-	4.72
19	5.0166	0.0280	7.024	26.86	0.80	-
20	3.748	0.0086	61.22	4.83	-	5.55
21	2.704	0.0036	54.92	24.07	1.17	-
22	3.711	0.0020	255.6	25.60	-	5.12
23	3.807	0.0156	35.36	2.35	-	7.50
24	3.719	0.0131	39.27	26.96	0.79	-
25	3.764	0.0108	49.00	13.61	1.81	-
26	3.888	0.0092	64.11	10.40	-	3.08
				Mean	1.03	3.75

TABLE IV

Bending and stretching moduli for kemp

Fibre No.	$2a_2$	$2b_2$	$2a_1$	$2b_1$	$E_s \times 10^{10}$ dyn/cm^2	$E_b \times 10^{10}$ dyn/cm^2
1	57.86	52.72	28.70	24.96	-	1.96
2	103.32	92.32	82.64	70.76	1.05	0.59
3	58.11	-	34.92	-	-	6.85
4	52.39	41.14	28.86	23.33	1.17	6.24
5	66.70	65.40	36.04	33.85	1.03	4.48
6	71.64	67.00	41.81	40.88	1.31	6.46
7	120.46	119.96	89.69	88.88	0.70	0.89
8	96.93	54.77	74.63	34.13	0.69	1.86
9	49.56	-	26.69	-	-	2.59
10	54.03	51.82	23.14	22.11	1.59	5.04
11	60.35	55.59	36.53	32.71	-	5.66
12	67.74	40.44	43.89	22.15	1.76	4.05
13	56.11	45.17	26.57	22.63	1.93	6.26
14	91.03	58.58	69.22	43.73	1.39	3.36
15	76.20	56.61	42.28	31.70	1.50	4.64
16	120.20	112.39	85.45	75.81	0.76	1.25
17	81.19	80.79	60.07	59.57	1.20	0.92

In the development of the medulla, the cells may break down completely during keratinization of the rest of the fibre, leaving a completely hollow canal; this, however, is not always the case. In the case of wool, for instance, the medulla may be unbroken, interrupted, or fragmented[41]. The medulla may occupy as much as 90% of the fibre and, if it is unbroken (i.e., solid) it can be expected to contribute towards E_b, and for this sample, is in fact what is considered to occur for fibres of Type II. The medulla material, not being entirely compressible, offers some resistance to bending; γ is then smaller and E_b is larger than for a hollow fibre (i.e., interrupted medulla) of the same outer dimensions. The fibres on curve I and II (Figure 9) were microscopically examined and it appeared that Type II fibres have filled medullas, i.e., the medullas are packed with cells, whereas Type I fibres are virtually devoid of cells, i.e., almost hollow. It was observed, however, that the optical densities of the medullas varied in both types, indicating different cell densities in the medulla. Fibres with intermediate medulla densities lie at points between the curves (Figure 9). These only occur near the intersection of the curves, since, for large diameters, the medulla, if not solid, would have little effect on $1^3/\gamma$ because it is only influenced by filled medullas. Thus, for large diameters, semi-solid or hollow medullas would fall into Type I. (This may also account for curve II being better defined than curve I.) The occurrence of Type I fibre is much less common than Type II and is of the order of one to five for this sample.

A plot of / .....

A plot of E_b for Type II fibres vs E_s (Figure 10) gave an approximately linear relationship, with a correlation coefficient of 0.517. E_b was always larger than E_s, which is not true for mohair. There is no significant difference between E_b of Type I and E_s. Also, there is no significant difference between the stretching moduli of Types I and II. This tends to agree with the above theory that in a solid medulla type of fibre, the material in the medulla offers resistance to compression but not to extension yielding higher results for bending moduli than their hollow or semi-hollow counterparts. Experiments carried out simultaneously at this Institute by Hunter (unpublished at the time of writing) have shown that the presence of material in the medulla does not contribute significantly towards the breaking strength of the fibre but the medulla has a dielectric constant comparable with that of the rest of the fibre. Results from Part IV of this thesis (see 4.4(vi)) also indicate that the above argument may apply. Kemp seems to be a composite material and appropriate theory, although not applied here, may be very fruitful. The medulla, it seems, plays no part in stretching; hence, E_s for Type I and II are similar. It is apparent that the values of E_b of Type II fibres cannot strictly be compared with mohair, since to a large extent they are influenced by the medulla, and, consequently, are not isotropic.

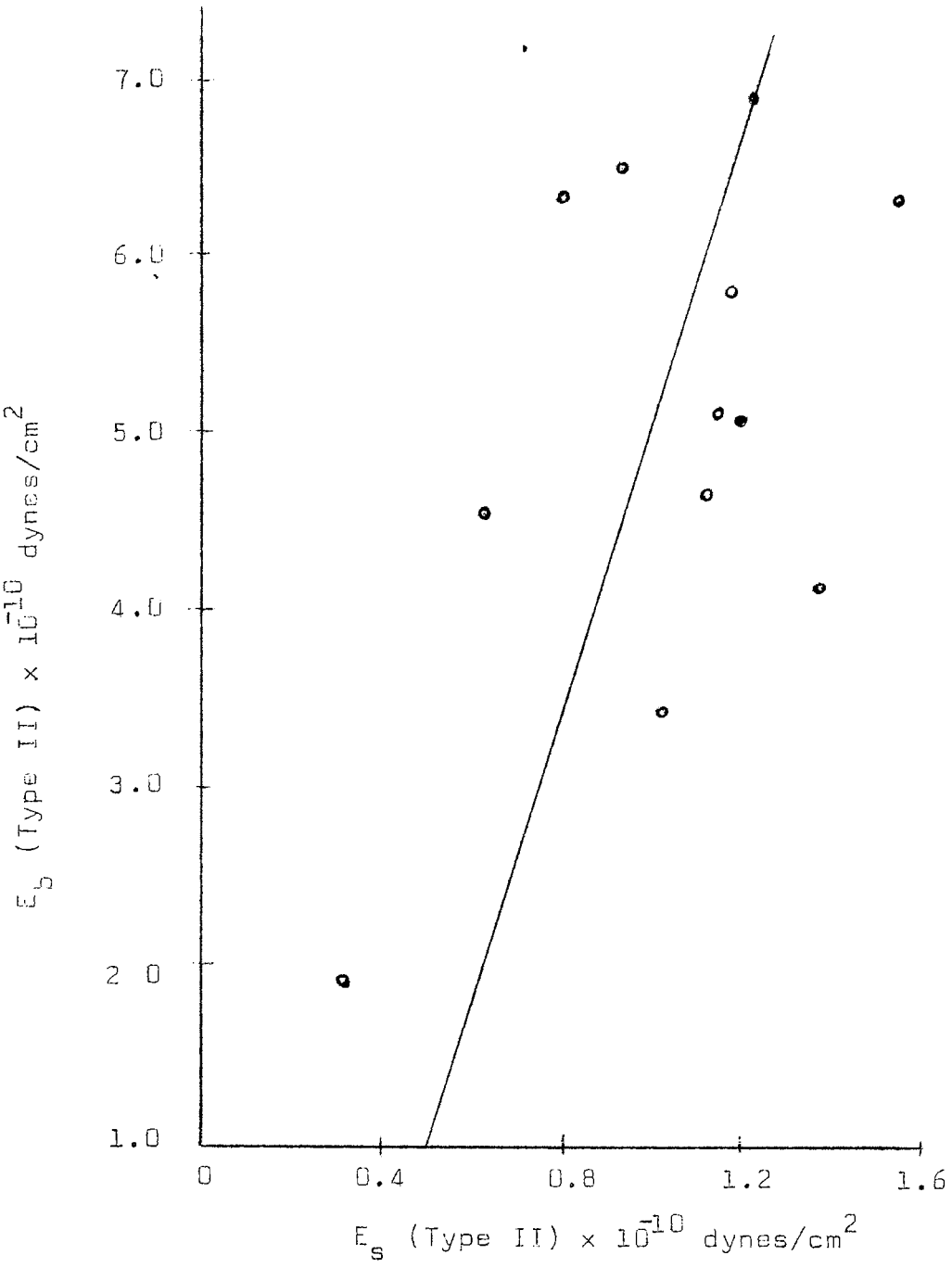

Figure 10. The correlation between Young's modulus for bending (E_b) and stretching (E_s) for the fibres of Type II.

PART III

THEORY RELEVANT TO THE PROPAGATION OF ULTRASONIC PULSES IN ELASTIC WAVEGUIDES

3.1 Introduction

Explanation of the transmission of mechanical vibration from source to receiver through a material requires the concept of an acoustic wave. If one of the particles of a medium is displaced from its equilibrium position, the elastic forces acting on it from the other particles will tend to restore it to its original position. The neighbouring particles themselves are displaced from their equilibrium state and by virtue of the inertia of the medium, continue to oscillate about their original position even after the wave has passed. When the frequency of the oscillating particle of the medium lies within the audible range of the human ear, the elastic waves are perceived as a sound while ultrasonic oscillations are distinguished from elastic sound waves only by their higher frequency. The classical relationship holds for the sound propagation velocity (c), the wavelength (Λ), and the frequency (f) such that

$$\Lambda = \frac{c}{f}$$

The upper limit of the frequencies for ultrasonic oscillation is of the order of 10^8 to 10^9 Hz and is followed by the hypersonic range which extends to frequencies of the order of 10^{13} Hz. The wavelength of the upper limit of ultrasonic oscillation approaches the wavelengths of light since a frequency of 10^8 Hz in

air will / .....

air will have a wavelength of order of 30×10^{-5} cm. This is comparable to the wavelength of electromagnetic oscillations perceived by the human eye as light which have wavelengths between the limits (4 to 8) $\times 10^{-5}$ cm. Ultrasonic waves are, therefore, in many respects similar to light waves - and the laws of geometric optics, such as the laws of reflection and refraction, can be applied to ultrasonic waves.

Ultrasonic waves may be propagated in all types of elastic media; the form of the wave propagated, however, depends on the elastic properties of the medium. Fluids for example resist a change of volume (but not a change of shape) and possess volume elasticity or bulk elasticity. Unbounded liquids and gases therefore are capable neither of generating nor maintaining shear stresses or forces. Compressional stresses can be propagated in liquids and gases and the propagation of the deformation takes place in the direction of the wave front i.e. the particle motions are in a direction perpendicular to the wave front. Such waves are longitudinal waves. Solids, on the other hand, resist a change of shape as well as a change of volume and possess rigidity or shear elasticity. In solids which have been elastically deformed both volume deformation stresses and shear stresses arise and besides longitudinal waves, transverse waves are propagated. The deformations associated with a transverse wave are propagated in a direction perpendicular to the direction of propagation. In a purely transverse wave compressions and rarefactions of the medium do not occur. In solids surface waves

can also / .....

can also be propagated but these are not important in this thesis. A theoretical treatment of the types of wave generated in solid media, is given at a later stage.

3.2 The behaviour of a macromolecular fibre during sonic excitation

According to Wegener[34] the rate at which a sonic wave will be transmitted from one atom to another depends on the nature of the bond energies, the spacial disposition of the atoms and the direction of the atomic vibration superimposed by the sonic excitation. The direction of the vibrations superimposed on the atom by the sonic vibration and the direction of propagation of the applied sonic wave need not coincide. If the direction of propagation of the applied sonic vibration coincides with the direction of atomic vibration between adjacent atoms in a chain molecule, i.e. if the transmission of the sonic excitation is caused by intermittent changes in the space between the atoms, a comparatively high rate of propagation of the applied energy will result with the rate increasing as the bond energy increases. Atoms in a chain molecule are, however, not in linear arrays but are staggered and thus the transmission of the sonic energy will take place with intermittent changes of the valence angle. The smaller the angle the slower will be the rate of transmission of the energy applied. Hence, stretching the chain molecules

with the / .....

with the consequent distortion of the valence angles, will increase the velocity of the wave. The rate of sonic transmission along a chain molecule depends, therefore, on the rigidity of the atomic bonds.

The various chains in a molecule are linked by secondary valencies across which applied sonic energy can be transmitted by superposition, but these bonds are considerably weaker than atomic bonds. Consequently, the sound is transmitted through the secondary valencies at a lower velocity than through the atomic bonds. On account of the numerous cross-linkages of the chain molecules, these component parts are prevented from vibrating freely. Various conditions of excitation with differing directions of propagation become superimposed one on the other. To illustrate this consider an element of yarn being excited by sound, the excitation travelling first of all along the affected chain molecules, and is transferred from one chain molecule to another at the point of linkage between the chain molecules. Compared with the atomic linkages the secondary valencies, slow down the transmission of sound. Transference of the energy applied through the secondary valencies, is necessary in order to transmit sound from one chain molecule to another. The rate of transmission in the direction of the yarn axis depends, therefore, in

the first / .....

the first place on the speed at which the sound can travel through a secondary valence bond on to another chain molecule, in other words on the bond energy at the point of linkage, and in the second place on the frequency with which such linkages occur. Using these principles Nosor and Osmin[42] have developed an acoustic method of determining the molecular orientation in fibres. From the above, it should be clear that a closer look at the molecular structure of wool, as in the next section, is required. It will be necessary to discuss briefly the structural nature of wool and its viscoelastic nature in order to obtain a clear understanding of this complicated system. It should be noted, that substitution of certain molecules in the protein structure gives rise to new methods of studying molecular structure. Wegener[34] seems to have been the only one who has applied ultra-sonics to this type of investigation - which is untouched at frequencies as high as 1 MHz in the textile field. It has been shown by Mason[43], using frequencies from 200 Hz to 20 kHz that sonic and ultrasonic measurements of elastic moduli are useful in investigating the structure of fibrous proteins.

3.3 The structure of protein fibres, with particular reference to wool

Proteins are formed by the polymerization of amino-acids (with the general formula, NH_2-CHR-COOH) by means of peptide links (CO-NH) to give long-chain molecules with the general formula[44]:

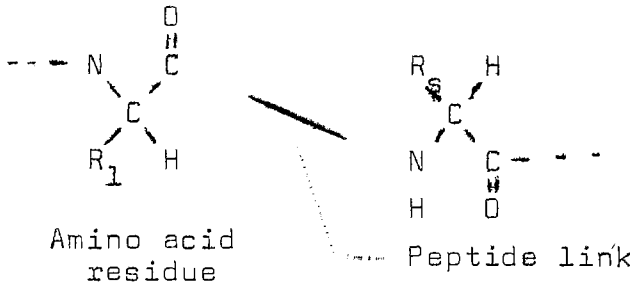

In natural / .....

In natural proteins at least twenty different amino acid side-groups (R_1 R_2 ....,) are found. It is the variation in the order and amount of these groups that determine the properties of the material and give rise to the large number of natural proteins which occur in animal and plant life.

There are various sorts of cross-links which can form between neighbouring protein molecules:

(a) Hydrogen bonds can be formed between the -NH - and -CO- groups, linking neighbouring main chains together:

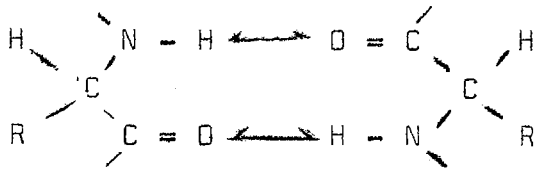

(b) Hydrogen bonds may form between hydroxyl groups present in the side-chains.

(c) Since there are both acidic and basic side-chains, salt bonds may form between them, holding the side-chains together by electrovalent forces.

(d) The cystine linkage, derived from a double amino-acid, will form a covalent cross-link between adjacent chains. Where this occurs, it really turns the many chain molecules into a single network molecule. The linkage is:-

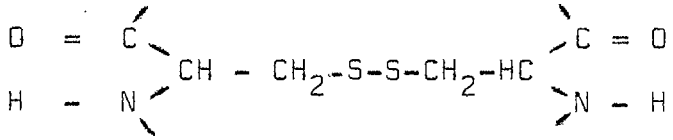

All these cross-links play an important part in determining the form of the protein. For example, single long-chain molecules may fold up into a compact ball, held together by internal cross-links; these are known as globular proteins. Alternately, the molecules may be more or less extended, and linked to their neighbours; these are

the fibrous / .....

the fibrous proteins, the most important of which from a textile point of view are silk, wool and mohair.

Keratin, a principal constituent of wool, is a complex protein with a large number of side-groups of all types occurring in appreciable proportions. Many of these contain active groups so that side-chain linkages are important. Evidence from x-ray diffraction[44] photographs show that two quite different crystal structures occur in keratin. There is the so called α-keratin structure, on the other hand if wool is stretched (it can be extended 50% in water, or a maximum of 100% in steam) there is a gradual and reversible transformation to another form known as β-keratin. The macro structure of a wool fibre is, in itself, a complex structure and is illustrated in Figures 11(a) and 11(b).

Although it has been well-known for some time that the α-helices in a keratin fibre unfold on extension of the fibre, the stability of the α-helices, their mechanical interrelationship, and the rôle of the disulphide bond in this stabilisation and possible "destabilisation" as in the case of setting treatments, is only now becoming clearer.

Recent work has emphasized the co-operative nature of the unfolding of α-helices in a keratin fibre and the important rôle of sulphydryl-disulphide interchange in modifying the properties of a fibre.

The unfolding of α-helices during the extension of wool fibres has been investigated by a technique known as the theory of rate processes[45]. This has shown that on extending the fibre the α-helices can only unfold into opened-out structures in a co-operative manner, that is,

a unit consisting / .....

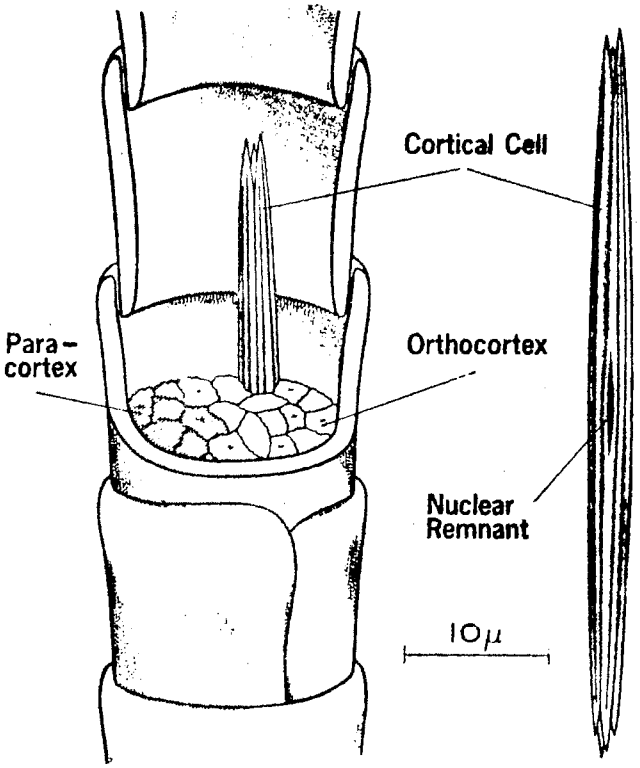

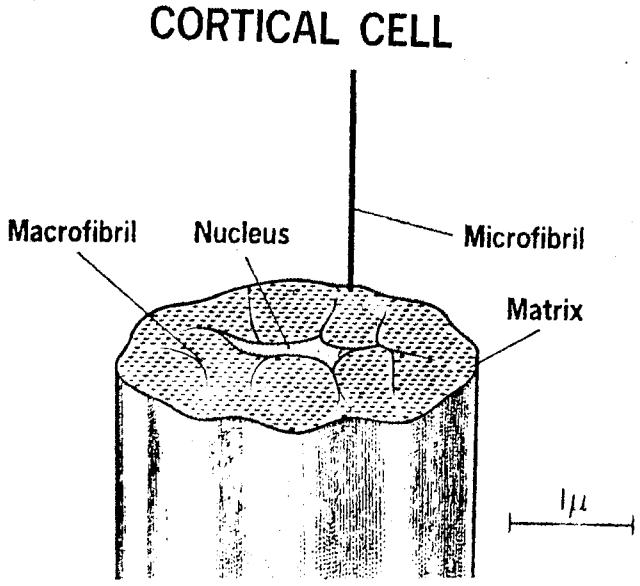

Figure 11(a). The structure of a wool fibre.
(Reproduce from the Textile Journal of Australia, Jan. 20, 1962)

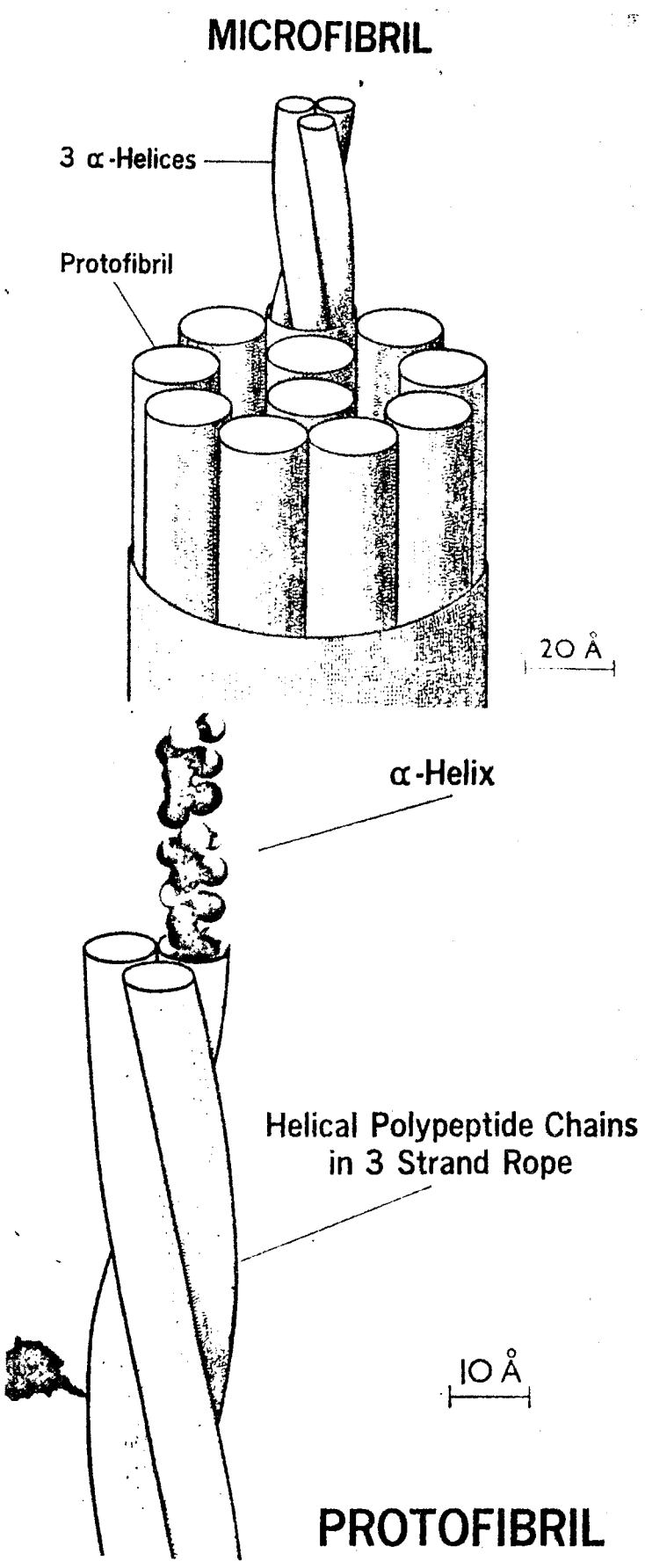

Figure 11(b). The structure of a wool fibre.

a unit consisting of a group of α-helices must open simultaneously rather than one helix at a time. In addition studies of recovery and setting have indicated that these α-helical units are partially stabilised by disulphide bonds. Thus, when the helices are unfolded during extension of a fibre, the "memory" which directs the structure back to its original unextended state is mainly provided by these disulphide bonds. Sulphydryl-disulphide inter-change, while the helices are unfolding, may interpose new cross-links, which sterically hinder the reformation of the original crystalline structure and may stabilise the β-crystallines found in the extended states. This has important consequences in permanent setting of wool.

The mechanical properties of wool and mohair are closely related to the molecular structure of the cortical cells which form the bulk of the keratin fibres. At practically the molecular level, these cells consist of long cylindrical units known as fibrils, and micro-fibrils which are approximately 80 Å diameter and are aligned parallel to the fibre direction with a centre to centre distance of about 100 Å. The material between the micro-fibrils is an amorphous sulphur-rich material called the matrix. In water the matrix becomes swollen and mechanically weakened, whilst the micro-fibrils are relatively unaffected. As a result the torsional modulus of a fibre in water decreases much more than in longitudinal extension.

By converting the disulphide groups to thiol in the keratin molecule, a decrease in stiffness is observed[46].

Studies of / .....

Studies of such phenomena reveal the mechanism of permanent setting, for example, and has led to the development of theoretical models which are useful in predicting and explaining mechanical properties. Feughelman and Watt[47] have classified the methods of chemical modification of wool into two categories. These are:

(a) The introduction of a suitable molecule into the keratin structure, which by its presence reduces the volume of loosely bound water, in the fibre. This can be achieved, for instance, by the introduction of ninhydrin which has the effect of increasing the internal viscosity of the keratin structure by reducing the amount of loosely bound water.

(b) Introduction of cross-links between polypeptide chains in the wool fibres. This can be achieved by combining formaldehyde with the structure and is verified by the marked reduction in swelling in formic acid, the mechanical effects being opposite in nature to those brought about by ninhydrin. Oku et al[48] have also found differences in the mechanical properties in wool as a result of chemically modifying the fibre by formalization which decreases the cystine content of wool with corresponding changes in mechanical properties.

3.4 The viscoelastic nature of keratin

The classical theory of elasticity deals with mechanical properties of perfectly elastic solids, for which stress is always directly proportional to strain;

i.e. $\tau = Ee$ / .....

i.e. $\tau = Ee$ where τ is the stress, e is the strain and E the proportionality constant, in this case Young's modulus. The theory of hydrodynamics on the other hand deals with properties of perfectly viscous liquids, for which, in accordance with Newton's law, the stress is independent of the strain but directly proportional to rate of strain; i.e. $\tau = \mu \frac{\delta e}{\delta t}$ where μ is the proportionality constant or the shear modulus, but independent of the strain itself. These categories are idealizations, however, any real solid shows deviations from Hooke's law under certain conditions, and any real liquid would show deviations from Newtonian flow if subjected to sufficiently precise measurements.

There are two important types of deviations. Firstly, the strain (in a solid) or the rate of strain (in a liquid) may not be directly proportional to the stress but may depend on the stress in a more complicated manner. Such stress anomalies are familiar when the elastic limit is exceeded for a solid. Secondly, the stress may depend simultaneously on the strain and the rate of strain. Such time anomalies evidently reflect a behaviour which combines liquid-like and solid-like characteristics, and they are therefore called viscoelastic. Both stress and time anomalies may coexist. If only the latter are present, we have <u>linear</u> viscoelastic behaviour.

The viscoelastic boundaries of keratin are difficult to define and Mason[43] has shown that although α-keratin is typically half crystalline and has a much more complex structure than ordinary polymers, there are indications

that a / .....

that a substantial component of this structure may be treated as an amorphous polymer. A slow extension of an α-keratin fibre in water reveals it to be very stiff with a Young's modulus greater than 10^{10} dynes/cm^2. In a comparably slow lateral compression, the same fibre is some 100 times softer. The relatively low time-dependent shear modulus evidently reflects the viscoelastic character of the non-crystalline keratin found between the orientated helices. In extreme cases, where crystalline keratin has been melted by heat treatment it showed "rubber-like" qualities.

During static and quasi-static tests (creep and stress relaxation, etc.) the viscous losses accompanying these viscoelastic deformations are negligible and the model has consequently been assumed to be purely elastic. During dynamic modulus measurements, however, the stresses and strains usually vary sinusoidally with time. If viscous losses accompany the deformation, then the stress is out of phase with the strain. If the viscoelastic behaviour is linear, the stress can be decomposed vectorially into two components, one in phase with the strain and the other 90° out of phase with the strain; when these are divided by the strain, the modulus is separated into an in-phase (real) and an out of phase (imaginary) component. Thus the modulus of a viscoelastic material is given by

$$E^* = E + i\omega\mu \qquad (5)$$

where E is Young's modulus and μ the modulus of the viscous phase of the material, i.e. the shear modulus. The simplest type of stress wave propagation in a

viscoelastic solid / .....

viscoelastic solid, is that of an infinite train of longitudinal sinusoidal waves along a slender rod or filament, the specimen being sufficiently long for reflection from the opposite end to be neglected. (This is the arrangement used by Ballou and Silverman[21], Ballou and Smith[19], Nolle[49], Hiller and Kolsky[50], and Hiller[51].) If, for this case, at the angular frequency w, the particle displacement at the driving end of the filament is taken to be

$$A \sin wt,$$

then, at a distance x along the rod, the particle displacement will be given by

$$A \sin w\left(t - \frac{x}{c}\right) \exp.\ (-\alpha x)$$

where α is the attenuation coefficient of the material and c the phase velocity. The constants α and c may, under these conditions, be related to the viscoelastic properties measured quasi-statically, and for a linear viscoelastic solid, when α is not too large,

$$c^2 = \frac{E^*}{\rho} \text{ and } \alpha = \frac{w}{2c} \tan \delta \qquad (6)$$

where ρ is the density of the material, and tan δ is the loss factor which is equal to the ratio of imaginary to the real part of the complex modulus, i.e. tan $\delta = E/\mu$. For viscoelastic materials E* increases with increasing frequency whereas tan δ can either increase or decrease. Tan δ never decreases more rapidly than $\frac{w}{c}$ however, so that α always increases. At high frequencies, therefore, waves are propagated with higher phase velocity and attenuated more rapidly with distance than waves of lower frequency.

In real / .....

In real viscoelastic solids the manner in which the mechanical properties vary with frequency depends on the various microscopic and molecular relaxation processes, and in general no simple relations exist for the dependence of α and c on the frequency. In order to treat the problem of wave propagation analytically a number of simple models has been constructed. The stress relaxation for these materials is asuumed to be similar to that of the mechanical models which are composed of perfectly elastic springs, and dash-pots, which observe linear viscoelasticity. The simplest models are the well known Maxwell and Voigt models. The wave equation for plane wave in a viscoelastic material is given by (for a Voigt model)

$$E \frac{\partial^2 \xi}{\partial x^2} + \mu \frac{\partial^3 \xi}{\partial t \partial x^2} = \rho \frac{\partial^2 \xi}{\partial t^2} \qquad (7)$$

where displacement has the solution

$$\xi = A \exp.- (\alpha + \frac{iw}{c}) \exp. (iwt)$$

Nolle[49] has shown that by considering real and imaginary terms

$$E = \rho c^2 \quad \frac{1-\frac{\delta}{4\pi^2}}{(1 + \frac{\delta^2}{4\pi^2})^2} \qquad (8)$$

where $\delta = \alpha \Lambda$, Λ being the wave length. If δ is much smaller than 2π, equation 8 reduces to

$$E = \rho c^2.$$

It is important then, to determine the value of δ when wave propagation measurements are undertaken in a material. (It is shown at a later stage that for keratin, δ is sufficiently small for the latter equation to be used in

the determination / .....

the determination of E.)

The equations given above, assume certain simplifying conditions and it should be noted that in real solids, it is not possible to displace a section of the medium in one direction without causing displacements in the other directions (the ratio of the change in diameter to the change in length is known as Poisson's ratio σ). Where the medium has finite boundaries the lateral components of a wave generated in it will be reflected from side to side and the medium behaves as an elastic waveguide, so that the classical theories of elastic wave propagation do not give a complete description of the phenomenon, and more sophisticated theory is necessary.

3.5 General theory of elasticity:

To describe the force acting on a small element of area of a cube in a material nine components of stress are required:

Three perpendicular to the faces of a cube and six tangential to the faces of the cube, (See Appendix II). By the Onsager reciprocity relation only 6 are independent. If the general form of Hooke's law is assumed, i.e. each of the six components of stress is a linear function of six components of strain, then there are 36 elastic constants describing the elastic behaviour of the body. As the symmetry of the material increases, the number of constants decreases, until in an isotropic material only four constants, of which two are independent, are usually considered. These are Young's modulus E, Poisson's ratio σ, shear modulus μ, and the bulk modulus k.

It is rare for fibres to be isotropic and the simplest

assumption which / .....

assumption which is likely to hold reasonably well for many fibres is that there is no difference in properties between different directions at right angles to the fibre axis, although these are different from the constants for longitudinal deformation. Under these conditions, which are called orthotropic or transversely isotropic, the number of constants may be reduced to seven, i.e. two Young's moduli E_L, E_T two shear moduli μ_{LT} and μ_{TT} and three Poisson's ratios σ_{LT}, σ_{TL} and σ_{TT} (See Figure 12), where the subscripts L and T refer to the longitudinal and transversal axes. Of these, E_L is the modulus measured in tensile or bending tests and μ_{LT} the shear modulus involved in torsional rigidity. The others have been neglected, experimentally partly because their technological importance is less obvious but also because they are more difficult to measure. In fact, real fibres are unlikely to satisfy the conditions of homogeneity and perfect elasticity, but nevertheless, the above system will be a reasonable approximation. Few measurements of the elastic constants of fibres other than E_L and μ_{LT} have been made. Bankey and Slen[52] found values between 0.42 and 0.63 for σ_{LT} wool at various levels of extension and Ferrous[53] has reported values between -0.2 and +0.5 for nylon at various humidities.

With a knowledge of the elastic constants in a fibre the following pages give a theoretical explanation of the production of different types of waves which are possible in solids. Only those sections of the theory applicable to the special sample shape used here, the cylinder, will be given. Other information can be gained from the original text by Redwood[54].

3.6 The general / .....

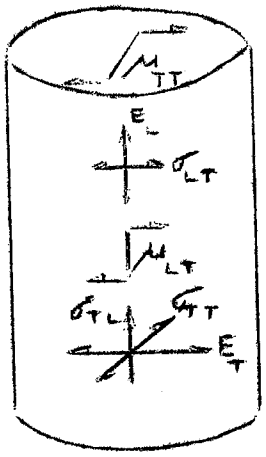

Figure 12. The elastic constants of a transversely isotropic fibre.

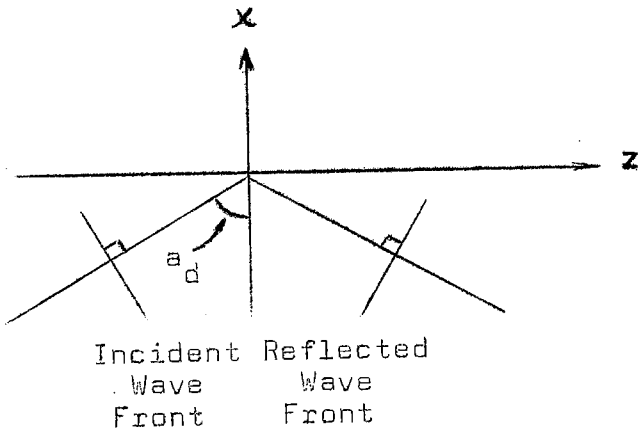

Figure 13. Reflection of a plane dilatational wave at a fluid/vacuum interface.

3.6 The general wave equation for isotropic solids

The derivation of the general wave equation for unbounded media is given in Appendix II and only the most important results are quoted here. The potential functions ϕ and $\bar{\psi}$ will satisfy the wave equation if they are solutions of

$$\nabla^2 \phi = \frac{1}{c_d^2} \frac{\partial^2 \phi}{\partial t^2} \qquad (9)$$

$$\nabla^2 \psi_i = \frac{1}{c_t^2} \frac{\partial^2 \psi}{\partial t^2} \quad i = x, y, z \qquad (10)$$

where $c_d^2 = \frac{\lambda+2\mu}{\rho}$ and $c_t^2 = \frac{\mu}{\rho}$ (11)

and λ and μ are the Lamē constants and ρ is the density of the material.

The Equations 9 and 10 indicate that two types of disturbance may be propagated in an elastic solid. One type of wave represented by the potential function ϕ travels with velocity C_d and involves no rotation. This type of wave is described as "longitudinal", "compressional", "dilatational" or "irrotational". The suffix "d" is used here to refer to the term "dilatational".

The other type of wave, corresponding to the vector potential function $\bar{\psi}$ is called "transverse", "shear", "equivolumental", "rotational" or "distortional". The suffix "t" is used to denote "transverse". In fluids only one velocity of propagation is possible since the shear modulus μ is zero. This has important consequences when discussing liquid coupling methods. / .....

methods.

3.7 Reflection and refraction of waves at an interface

It is necessary to discuss briefly the effects of a simple boundary before solving Equations 9 and 10, since these determine the type and mode of wave propagation.

Solid vacuum interface:

(i) Reflection of a dilatational wave

We consider the reflection of a plane wave at a plane interface separating solid and vacuum as illustrated in Figure 13. The boundary conditions, which must be satisfied, are that stresses both normal and parallel to the boundary surface must be zero, i.e.

at $x = o$ $\tau_{xx} = \tau_{xy} = \tau_{xz} = 0$

(See Appendix II.)

Equations 9 and 10 must be solved. Substituting equations of the form given in Equation A14 and A15 for the potential functions ϕ and $\bar{\psi}$; gives two differential equations which when boundary conditions are applied, show that the first equation cannot be satisfied by ϕ alone and it is necessary for ψ_y to be finite also, because there is also a transverse wave with motion in the xz - plane. Boundary conditions can be satisfied only if the dilatational incident coefficient, and reflection coefficient

and the / .....

and the transverse reflection coefficients are finite. This means that a plane dilatational wave incident on a solid/vacuum interface produces both a reflected dilatational wave and a reflected transverse wave.

By analogy with optics it can be shown that the angle of incidence and reflection of the dilatational waves are equal and the angle of reflection of the transverse wave a_t is related to a_d by

$$\frac{\text{Sin } a_d}{C_d} = \frac{\text{Sin } a_t}{C_t} \qquad (12)$$

A proof of this can be found in Kolsky[55].

(ii) The reflection of a transverse wave

The analysis of the reflection of a transverse wave at a boundary is similar to that of a dilatational wave. When considering the reflection of a plane transverse wave, there are two problems to be dealt with, for transverse waves may be polarized in the y-direction ("Shear horizontal" or S.H.) or in the z.-direction (S.V.). Any other polarization may be synthesized from a combination of these two.

It can be shown that a plane transverse wave, the displacement of which wholly in the y-direction, is reflected

without phase change or loss in amplitude. For a S.V. wave, however, it is not possible to satisfy the boundary conditions at all angles of incidence with a reflected transverse wave alone, and a dilatational wave is also generated. (A more detailed analysis of the above can be found in Redwood[54].)

3.8 Continuous waves in fluid waveguides:

The analysis of the simplest type of waveguide will illustrate most of the remaining concepts which are important in mechanical waveguides. As an example the fluid plate will be used, although cylinders are of prime interest. The plate, however, is more simply understood and illustrates the same phenomena as the cylinder but the solutions involve sine and cosine functions which are more easily handled than the Bessel Functions for cylinders. Application of the technique of analysis to a solid cylinder is given in Appendix III. The difference in analysis between the plate and cylinder lies mainly in the boundary conditions applied.

The fluid plate with free boundaries.

Consider a plate with boundaries at $x = a$ and $x = -a$ as in the adjacent figure.

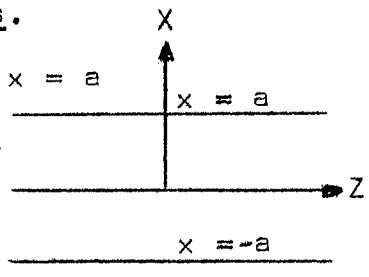

We must find solutions for the Equation 9 which satisfy the boundary conditions $(p)_{x=\pm a} = 0$ where p is the pressure. Introducing a time factor e^{iwt}, and assuming no

variation in / .....

variation in the y-direction, Equation 9 may be written

$$\frac{\partial^2 \phi}{\partial x^2} + \frac{\partial^2 \phi}{\partial z^2} = - \frac{w^2}{c_d^2} \phi \qquad (13)$$

For a complete solution the potential is put equal to the product of two functions X(x) and Z(z) which are independent of z and x respectively. This merely separates ϕ into two components with one parameter each, a well-known technique in solving differential equations. This gives two equations:

$$\frac{\partial^2 X}{\partial x^2} + k_d^2 X = 0 \qquad (14)$$

$$\frac{\partial^2 Z}{\partial z^2} + \left(\left(\frac{w}{c_d}\right)^2 - k_d^2\right) Z = 0 \qquad (15)$$

The solution of the first equation is a combination of $\sin k_d x$ and $\cos k_d x$ while for the second $\exp(-ik_o z)$ is chosen to represent waves travelling in the positive z-direction.

Here $$k_o^2 = \left(\frac{w}{c_d}\right)^2 - k_d^2 \qquad (16)$$

Combining the various parts of the solution and inserting constants we have the solution:

$$\phi = A\begin{Bmatrix}\text{Sin}\\ \text{Cos}\end{Bmatrix} k_d x \exp(-ik_o z)\exp iwt. \qquad (17)$$

Boundary conditions require that:

$$[p]_{x = \pm a} = \left[\frac{\partial^2 \eta}{\partial t^2}\right]_{x = \pm a} = 0 \qquad (18)$$

So if / .....

So if we choose the sine terms in the solution, $\sin k_d a = o$, while if we choose the cosine terms in the solution, $\cos k_d a = o$

This means that

$$k_d a = \frac{m\pi}{2} \qquad m = 1,2,3... \qquad (19)$$

If we separate these into sine and cosine solutions

$$k_d a = \frac{m\pi}{2} \qquad m \text{ even} \qquad (20)$$

for sine solutions and

$$k_d a = \frac{m\pi}{2} \qquad m \text{ odd.} \qquad (21)$$

for cosine solutions.

This means that only certain forms of waves can be propagated. Each value of m describes a "mode" of propagation. Those modes for which m is even are called asymmetric modes while for m odd we have symmetric modes.

Some important features of these modes are listed below:-

(i) Each mode may be thought of as a synthesis of plane waves reflecting at the boundaries, and travelling along the guide in a zigzag path. The sinusoidal distribution of pressure over a cross-section is the "interference pattern" formed by these waves as they cross one another.

(ii) ko depends / .....

(ii) k_o depends on the value of m hence it is written as k'_{or} instead of k_o. The full solutions are

Asymmetric modes m even

$$\phi = A \sin \left(\frac{m\pi}{2a}\right) e^{-ik'_o z} e^{iwt} \qquad (22)$$

Symmetric modes, m odd

$$\phi = A \cos \left(\frac{m\pi}{2a}\right) e^{-ik'_o z} e^{iwt} \qquad (23)$$

Designation of the modes is similar to the convention used in electromagnetic wave guides. The first term in the brackets corresponds to the variation in the x-direction the second to that in the y-direction - which is zero in this case because there is no dependence on y. Thus, the modes are called the (m, o) modes.

(iii) Phase velocity Each mode has a characteristic pressure distribution as shown in Figure 14 and a characteristic phase velocity C_p given by

$$C_p = \frac{w}{k'_o} = \frac{C_d}{\sin a_d} \qquad (24)$$

Since k_d is a constant for any particular mode we may write

$$k_d^2 = w^2 \left(\frac{1}{c_d^2} - \frac{1}{C_p^2}\right)$$

or

$$C_p = \frac{C_d}{\left[1 - \left(k_d \frac{Cd}{w}\right)^2\right]^{\frac{1}{2}}} \qquad (25)$$

(iv) Cut-off / .....

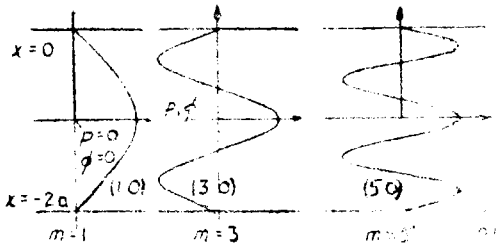

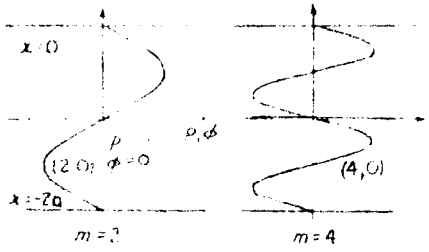

Figure 14. Pressures and potentials for modes in a fluid plate with free boundaries.

(a) Symmetrical modes.

(b) Asymmetrical modes.

(iv) Cut-off frequencies and evanescent modes

The cut-off frequencies of modes (f_{co}) are important. For any mode C_p is infinite when

$$\frac{k_d C_d}{w} = 1$$

or

$$f_{co} = \frac{k_d C_d}{2\pi} \qquad (26)$$

Below this frequency k'_o is imaginary and negative and the wave is attenuated in the z-direction, according to the term $e^{-ik'_o z}$. The mode is then described as "evanescent" and there is no transmission of energy along the waveguide.

(v) Simultaneous excitation of several modes

If the waveguide is excited by a source producing a pressure distribution identical with that corresponding to one of the modes as given by ϕ in Equation 17, then that mode alone will be excited. Whether it will be propagated unattenuated or is evanescent, depends on the frequency of excitation.

If the source of excitation of the waveguide is not the same function as any one of the distribution corresponding to the modes of Equation 17, which is usually the case in practice, then several modes will be excited simultaneously. If the source of waveguide excitation produces a constant pressure over

the cross-section/....

the cross-section, for example, an infinite number of symmetrical modes will be excited, since an infinite series of sine waves is needed to synthesize the constant amplitude function. Of this infinite number of modes, the majority will be evanescent. At high frequencies, many non-evanescent modes may be excited, but as the frequency is reduced, the number diminishes until at frequencies below the cut-off frequency of the (3,0) mode, only one symmetrical mode can carry energy. Below the cut-off of this mode (1,0) all modes are evanescent.

3.9 Continuous wave in a solid cylinder

(i) Longitudinal Modes

The derivation of the wave equation for a solid cylinder is given in Appendix III. The characteristic equation is more complicated and solutions of this equation are usually expressed graphically. The most useful method is a plot of the phase velocity as a function of frequency, or the inverse of the wavelength. From the value of C_p at any frequency, k_o may be found and then k_d and k_t from equations A31 and A32 respectively - which in turn allow the displacements to be calculated. The group velocities may be obtained from the

slope of / .....

slope of the curve of phase velocity versus frequency through $C_g = \frac{dw}{dk_o}$. Bancroft[56] has presented most comprehensive calculations of phase velocity as a function of frequency and his curves are reproduced in Figure 15 where $C_g = \frac{w}{C_p}$.

One cannot use the same nomenclature for these modes as was used for the fluid, since the number of cycles of the displacement function across a cross-section depends on frequency. The system of suffixes adopted here is the same as that used by Redwood[54], i.e. naming modes, the L (1,m) or L(2,m) mode. The first suffix indicates whether the mode is symmetrical or asymmetrical, through the number 1 and 2 respectively. The second number indicates the order of the mode. L(1,1) is a symmetrical mode with no cut-off frequency, L(1,2) is a symmetrical mode with lowest cut-off frequency of the series of symmetrical modes, L(1,3) that with next lowest cut-off and so on. Other symbols are, however, in use in the literature.

Bancroft's calculations refer only to "Young's modulus" mode L(1,1). It can be seen that at low frequencies in fact as frequency approaches zero, C_p approaches $(\frac{E}{\rho})^{\frac{1}{2}}$, hence the name for this mode.

Davies[57] has / .....

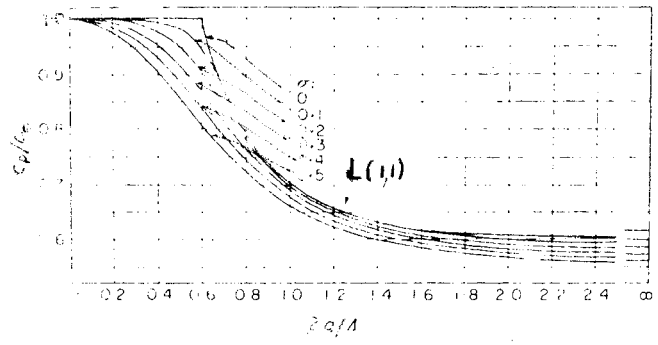

Figure 15. $\frac{C_p}{C_o}$ as a function of $\frac{2a}{\Lambda}$ and σ for the L(1,1) mode.

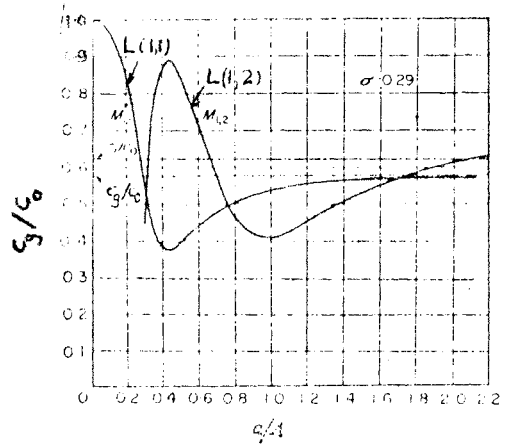

Figure 16. $\frac{C_g}{C_o}$ vs $\frac{a}{\Lambda}$ for the L(1,1) and L(1,2) mode for σ = 0.29.

Davies[57] has plotted $\frac{a}{\Lambda}$ vs $\frac{C_g}{C_o}$ for L(1,1) mode as reproduced in Figure 16.

From this it can be seen that for the L(1,1) mode when $\frac{a}{\Lambda}$ approaches 0, $\frac{C_g}{C_p}$ approaches unity. In our case we have for f = 0.5 Mhz, assuming a velocity of the order of 2×10^5 cm/sec, that $\frac{a}{\Lambda}$ is about 10^{-3}. For an extremely thick fibre, say a = 100 μ the ratio is 4×10^{-3} and it can be taken that $\frac{C_g}{C_o} = 1$. That is, we assume the group velocity at low frequencies to be given by

$$C_g^2 = \frac{E}{\rho}.$$

(ii) Torsional Modes

Again the derivation of the wave equation for the special case when $u_r = 0$, and $u_z = 0$ and that u_θ is finite and independent of θ is given in Appendix IV, and leads to the torsional modes of propagation in a solid isotropic cylinder, designated T(0), T(1) etc.

Equation A42 represents a non-dispersive wave since Cp = C_t at all frequencies. The other modes, the characteristics of which may be obtained from A43 are dispersive and have cut-off frequencies given by $k_o = 0$,

$$\frac{w_{co}}{C_t} = k_t$$

which in / .....

which in our case is

$$w_{co} = 2\pi f_{co}$$

$$f_{co} = \frac{\mu^{\frac{1}{2}}}{2\pi\rho^{\frac{1}{2}}} k_t . \qquad (27)$$

So that, provided we operate in the frequency range below f_{co}, only the fundamental Torsional mode, T(0) mode, will be propagated. This mode requires a special sort of excitation, with the amplitude of the displacement proportional to the radius, but such an excitation is not practicable. Even if the excitation takes some other form, the remaining modes will be evanescent if the frequency and radius are adjusted so that the waveguide is operating below cut-off frequency of the second mode. This, of course, is useful in fibres with high damping since all the energy will be carried by one mode and not divided, making transmission more likely.

(iii) Shear Waves

According to Gelles[58], shear waves through cylinders for which $\frac{a}{\Lambda}$ is less than 1 have not yet been discussed in the open literature, and the author has not yet come across any publications. McSkimin[59] has studied the case of $\frac{a}{\Lambda}$ much greater than 1. For our case this would require a frequency of at least 200 MHz, which, if course, is impossible with the apparatus described in Part IV.

For this / .....

For this reason the theory of shear waves is not discussed here. Values of λ can be obtained from longitudinal velocity measurements, while torsional velocity measurements for an isotropic medium will yield the same velocity for shear modes and torsional modes, yielding the same value for the modulus. The problem of including a viscous term in the above theory in order to extend it to viscoelastic materials will not be included here.

The theory given above, applies to continuous waves in the particular waveguide. The use of a short square pulse generally necessitates complex analysis, such as Fourier analysis to describe the shape of the pulse mathematically. Redwood[54] has shown that for a pulse modulated carrier wave, under certain conditions, continuous wave analysis can be used to describe the pulse shape mathematically. He ascribes a "bandwidth figure", defined by the first zero of a Fourier spectrum of the pulse (since the most important Fourier components lie within the first zero). If this bandwidth figure is only a small fraction of the carrier wave frequency, the frequency spectrum of the pulse only occupies a relatively narrow bandwidth, and continuous wave theory can be used to predict the

appearance of / .....

appearance of the pulse. The relative bandwidth can be assessed by the number of cycles of the carrier inside the modulating envelope. When this is large, say 100 or more, continuous wave theory can be used. When the number of cycles is less than say 10, other analytical methods must be used. This analysis can often be justified, and simplifies matters to a large extent should pulse shape be of importance.

The theory given in this section, should be sufficient to understand the advantages and limitations involved in waveguide analysis as applied to the animal fibres used here.

PART IV'

TECHNIQUES OF TRANSMITTING SHORT ULTRASONIC PULSES THROUGH FIBRES

4.1 Introduction

For the propagation of pulses through animal fibres a wave train of pre-determined carrier frequency fo = 1 MHz, or alternatively 0.5 MHz, and pulse width up to about 20 μs was used. For accurate pulse propagation measurement, the pulse length is required to be much smaller than the time of transmission. This then sets a limit on the frequency used which is further restricted by the fact that according to McSkimin[59] the radius to wavelength ratio, $\frac{a}{\lambda}$, must be less than 0.1, if excitation of high-order or spurious modes is to be avoided. Assume a pulse in a wool fibre with an average diameter of 30 μ, say, to have a velocity of 2×10^5 cm/sec (Calculated from $C^2 = \frac{E}{\rho} = \frac{5 \times 10^{10}}{1.31}$), then for $\lambda \sim 10a = 300 \times 10^{-4}$ cm, and the frequency $f = \frac{c}{\lambda} = \frac{2 \times 10^5}{300 \times 10^{-4}} = 6.6$ MHz. Thus as long as the frequency is less than about 7 MHz radius to wavelength ratio will be less than 0.1. However, if the attenuation in the fibre is very high, short fibre lengths must be used, which limits the pulse length. For a fibre 3 mm long the time a pulse travelling at 2×10^5 cm/sec takes to traverse it is approximately 1 μs. By using pulse delay techniques, however, this can be extended and a pulse width of 10 μs can be safely used. A carrier frequency must be used which is high enough to allow about 10 cycles (see page 55) of carrier frequency into a pulse width of about 10 μs but it must not be too

high since / .....

high since attenuation increases with frequency. The frequency chosen was 0.5 MHz which satisfies these requirements. Furthermore, $\frac{a}{\Lambda}$ is small enough for the longitudinal velocities and torsional velocity to be equal to C_d and C_t, respectively, so that

$$C_d^2 = \frac{\lambda + 2\mu}{\rho} \tag{28}$$

and

$$C_t^2 = \frac{\mu}{\rho} \tag{29}$$

Substituting these equations into Equation A3 of Appendix III yields

$$C_d^2 = \frac{E}{\rho} \frac{1-\sigma}{(1+\sigma)(1-2\sigma)} \tag{30}$$

Only under certain circumstances, however, particularly when the radius to wavelength ratio approaches zero, does the equation reduce to the classical equation

$$C_d^2 = \frac{E}{\rho} \tag{31}$$

In the classical derivation of this equation, it is assumed that plane transverse sections of the specimen remain plane during the passage of the stress pulse. The longitudinal expansions and contractions of a section will result in similar lateral movements, so that Poisson's ratio cannot be neglected. This effect only becomes important, however, when the wavelength is of the same order of magnitude as the specimen diameter. Equation 31 is assumed to hold true for the experiments described in this thesis.

Rearrangement of Equation 30 provides a relationship which is suitable for fitting of linear regression

lines to / .....

lines to the data, i.e.

$$C_d^2 = mf(\sigma)\ E+b \qquad (32)$$

where

m = constant of proportionality and conversion factor of units

$mf(\sigma)$ = slope of the straight line,

and b = Y axis intercept at E = 0.

This equation is useful for the study of non-ideal materials which are not homogeneous or isotropic as has been assumed in the original theoretical derivation of Equation 30.

4.2 The apparatus

A block diagram of the link-up is given in Figure 17 and consists of a pulse generator, a specimen and transducer holder, a wide band-width amplifier (Arenburg L.F.A. 5501) and a Tektronix, model 555 dual beam oscilloscope (Photograph 1). Two of these items will be discussed in detail, i.e. the pulse generator and sample-transducer holder, since both were built at SAWTRI.

The pulse generator

The pulse generator[60] was designed by Arenburg and produces a pulse packet of high voltage sine waves which are variable in pulse length and delay. This generator was chosen because, due to the high acoustic damping expected in keratin fibres, a high source of energy for the transducers was necessary in order to overcome the energy loss in transmission. For the same reason it was necessary to use short fibres, and lengths

of 2 to 5 mm / .....

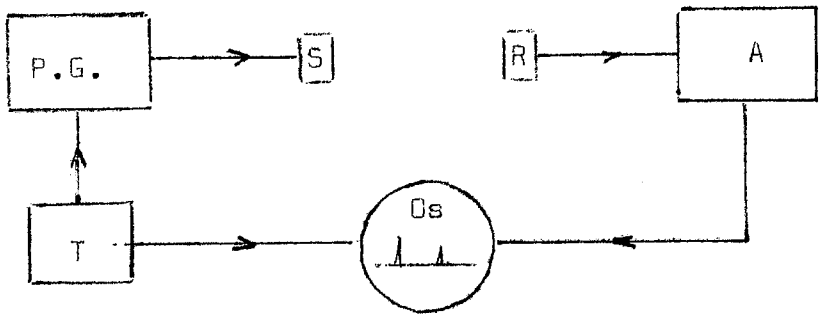

Figure 17. Experimental System

P.G. - Pulse Generator
S - Sender Transducer
R - Receiver Transducer
A - Amplifier and Detector
Os - Oscilloscope
T - Time Delay and Trigger

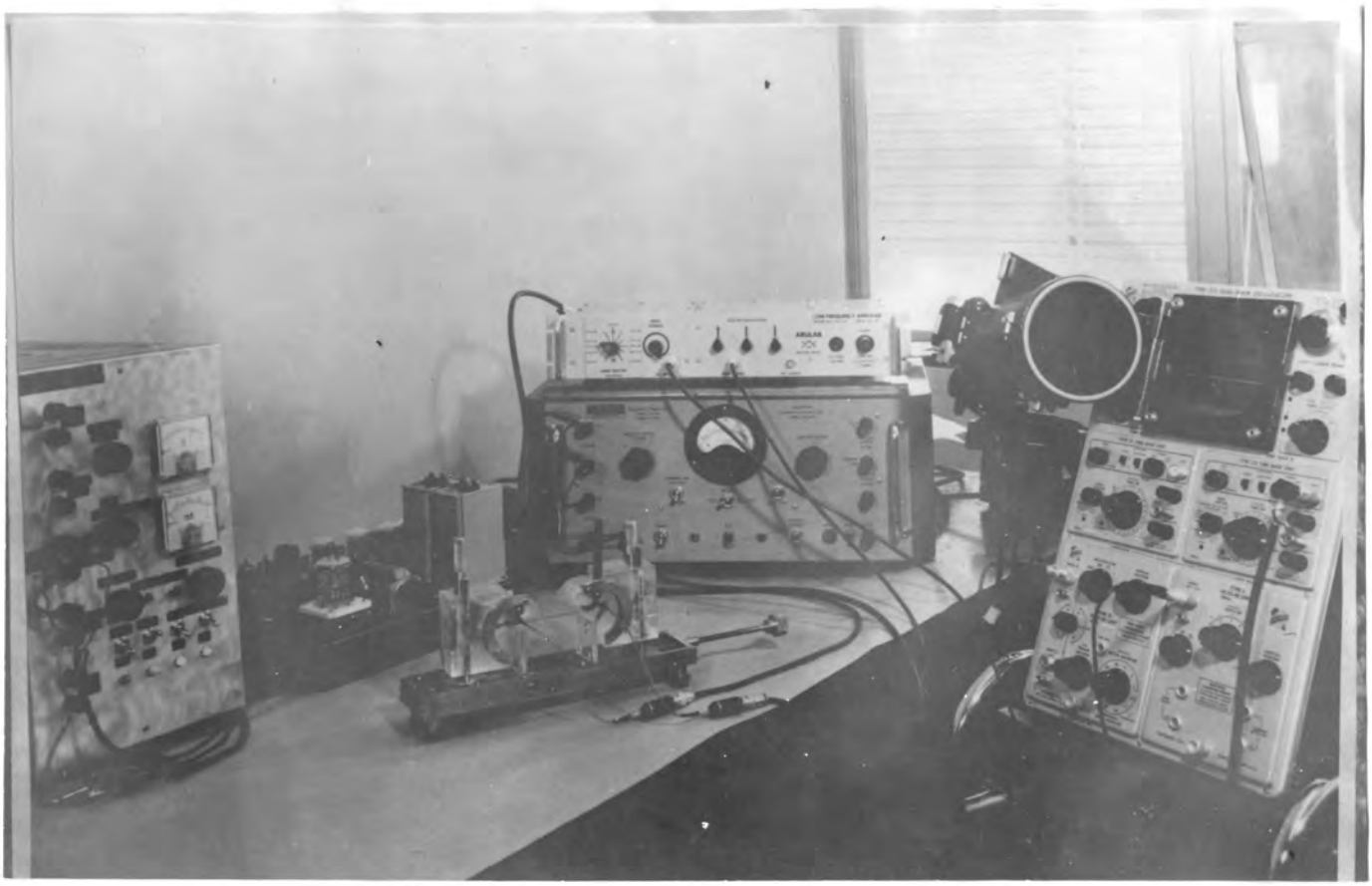

Photograph 1(a) : The apparatus.

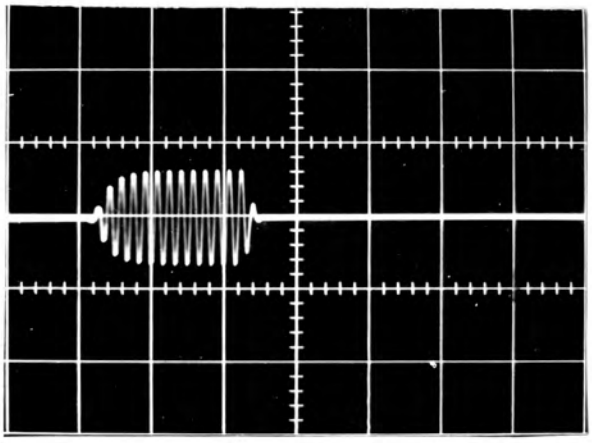

Photograph 1(b) : The pulse packet.
Time scale: 10 μs/cm.

of 2 to 5 mm were anticipated, which as pointed out, limits the pulse length used. The Arenburg pulse generator has a suitable pulse length adjustment, and can be operated at sufficiently high voltages. (500 V to 1 Kv.) A circuit diagram is given in Figure 18.

The crucial element here is V8, a tetrode oscillator connected with tank coil L1 and condenser C3 in a push-pull arrangement. The output is taken from L1 via a step-down transformer which supplies a high voltage oscillation to the transducer. The inductance of the secondary winding was found to be very critical since if it was too large oscillations would cease due to overloading. The grids of V8 are normally cut off by the large positive bias on the cathodes, put there by the network R1, R2, R3 and C1 and C2. Full-plate voltage is available from the positive H.V. supply via the centre-tapped primary of L1, the screen grids are grounded and no current flows, so that no tendency exists for oscillations. At a predetermined time a large positive pulse is applied to both the screen and control grids and oscillations begin immediately. The grid resistors R4 and R5 together with their condensers quickly cause the control grids to reach a fixed, class C, operating condition and within a cycle or two the pulse packet oscillations have stabilized. The damping diode V9 would short out these oscillations if it were not reverse biased by the same large positive pulse which is present on the screen grids. At the end of the predetermined pulse width, the activating pulse is removed, the screen voltage drops to zero, the grid bias attains a large negative value (with respect to the cathode which has a

high positive / .....

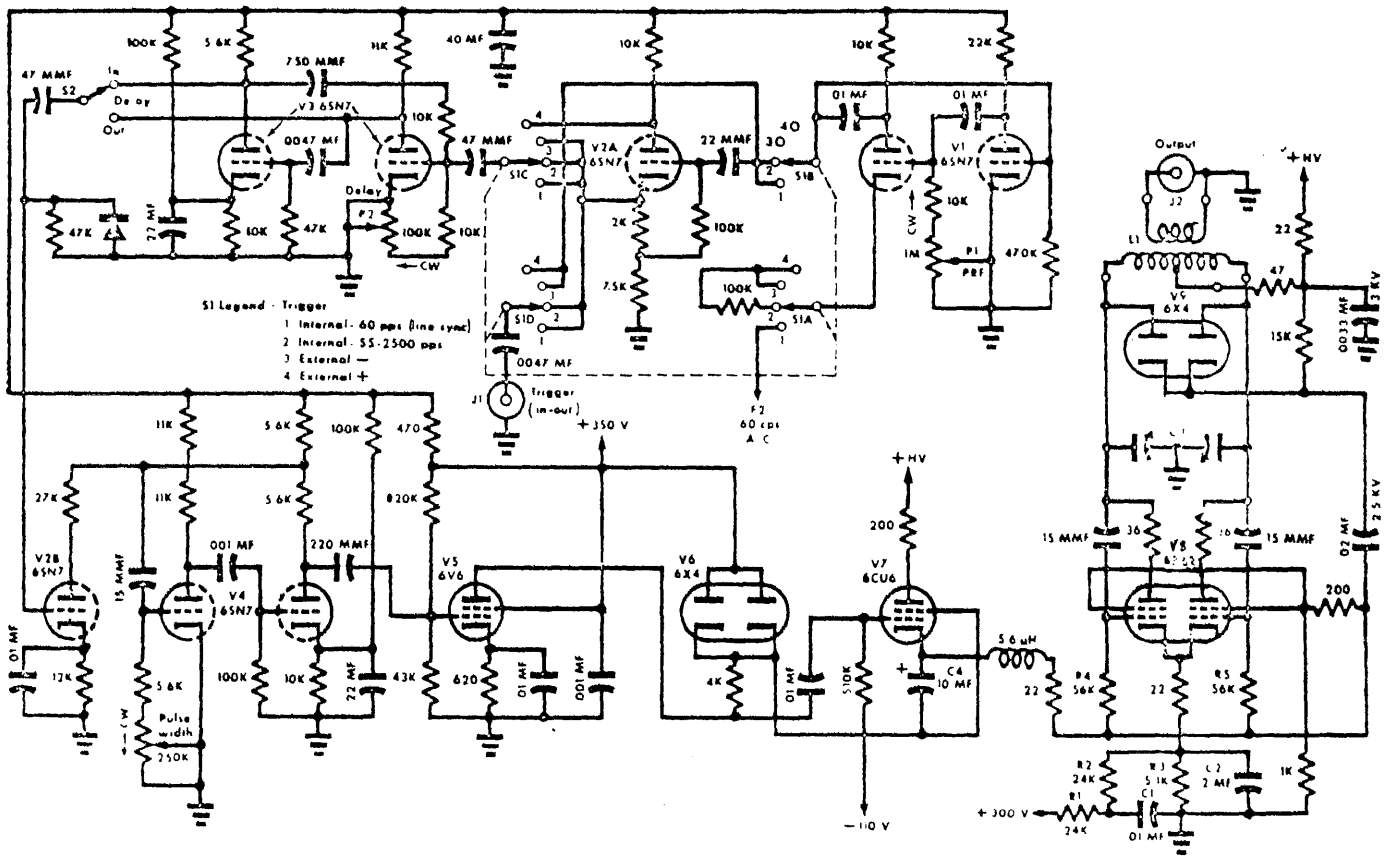

Figure 18. The circuit diagram of the Arenburg pulse generator.

high positive value with respect to ground), and the oscillations cease almost immediately. The tank circuit, however, would continue to ring if the damping diode V9 did not short it out, at this instant, so as to terminate the oscillations abruptly. The pulse packet developed by this oscillator is shown in Photograph 1(a).

The control circuitry is more conventional. VI is a free-running, square wave multivibrator, the frequency of which is controlled by PI. The negative going edges of each square wave are differentiated to provide negative spikes which then pass through the cathode follower V2A and drive the monostable multivibrator V3. Each differentiated pulse causes a square pulse output from V3, the width of which is adjusted by P2, the delay control. Between V2A and V3 is a connector, J1, from which a synchronizing trigger is taken. The rear edge of the adjustable pulse from V3 is applied to V2B. Since it is the rear edge that is used as a trigger and since the pulse width is adjustable, V3 acts as a delay generator, delaying the start of the oscillations from V8 in proportion to the setting of P2. After amplification in V2B, the delayed trigger activates the monostable multivibrator V4 of which the output pulse width is adjusted by the "Pulse Width" potentiometer, as was done in the case of V3. Instead of differentiating this pulse to get a trigger, as was done with the output from V3, the whole pulse is applied to the V5 amplifier which feeds the cathode follower V7 to give the positive pulse on the screen and control grids of V8 starting oscillations. The undifferentiated pulse from V4 is eventually applied

to V8 and /.....

to V8 and consequently the width of the pulse packet of oscillations from LI is controlled by the setting of the "Pulse Width" potentiometer controlling the output pulse width V4. The Arenburg pulse oscillator is a most useful device, giving a sharply defined oscillation group with controlled delay and width for driving piezoelectric and other transducers.

The power supply was designed and built at SAWTRI and supplied 600 volts to the oscillator circuit.

The Sample and Transducer Holder

Details of the sample and transducer holder which was built on lines suggested by Gelles and Bombhard[61], are shown in Photograph 2. Two vertical perspex supports hold the sample or delay plates. The top edge of the support is rounded with a small radius of curvature (about 0.2 mm) to minimize the tendency to shear the sample when a plastic contact with the transducer is used. One of the transducer supports can be displaced in a horizontal direction, by means of a long feed screw to accommodate samples of different length and to alter coupling between sample and transducer. Both can be rotated about a vertical axis to adjust for parallelism at the supports, and both can be moved in a vertical plane by means of the brass screw adjustors. The transducer holders slide on two vertical brass rods on either side of the screw adjustor. Variation in the vertical plane of the coupling angle between transducer and sample is achieved by rotation of the cylindrical perspex segment by means of an arm attached to it.

The spacing between the sample support and transducer

support is / .....

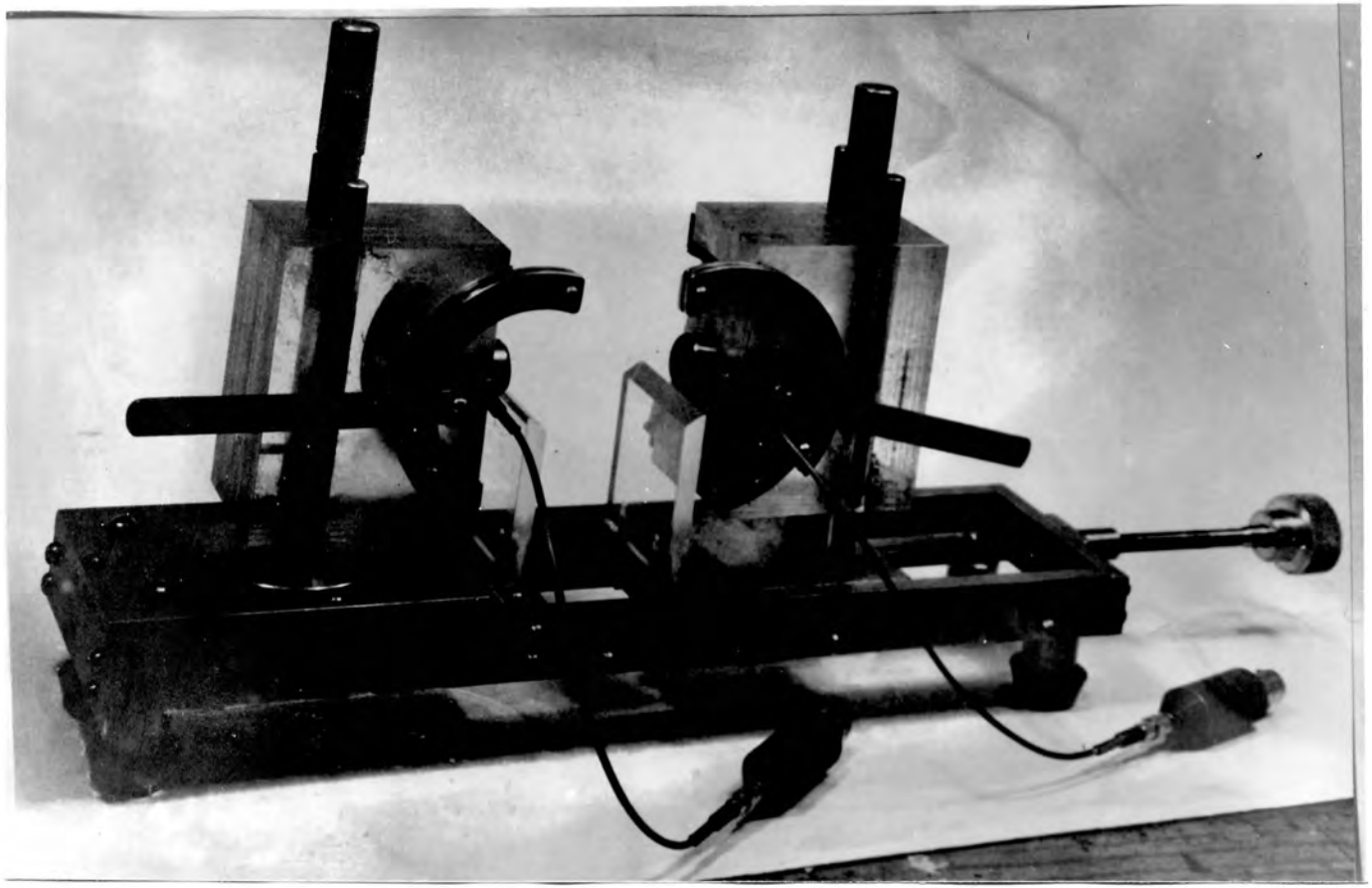

Photograph 2 : The sample and transducer holder.

support is such that the transducer rotation axis coincides with the knife edge of the sample support, that is, the sample support edge is at the centre of the circle, on the circumference of which the perspex segment rotates. This allows the transducer angle to be varied without breaking the sample-transducer contact. The transducers press-fit into the perspex hemi-cylinders.

The transducers used were 1 MHz X- cut and Y-cut quartz (obtained from Standard Telephones and Cables, Boksburg) and 0.5 MHz P.Z.T.-transducers (obtained from Branson Instrument Company, Connecticut U.S.A.). For compressional wave generation the X-cut quartz or the P.Z.T.-5 transducers were employed, while Y-cut quartz and P.Z.T.-4 shear wave transducers were used for shear and torsional wave generation. Both X-cut and Y-cut quartz transducers had high Q's and were damped by fixing hard rubber to their edges and sometimes loading their rear faces with plasticine. They were not as efficient as the P.Z.T.'s, although they exhibited good mode purity, i.e. they did not tend to excite spurious modes. The P.Z.T.'s on the other hand, were more robust, efficient and completely screened, and were consequently used most of the time.

Recording of the results was achieved by means of a Robot Royal 24 camera attached to the oscilloscope.

4.3 Experimental procedure and related results

All experiments described in this part of the thesis were conducted at 20°C and 68% R.H.

Generally, the procedure followed corresponds to that advocated by Gelles[35] who transmitted ultrasonic

pulses at / .....

pulses at 10 MHz through films, foils, fine wires, whiskers, etc. He did not give any results for visco-elastic materials, and most of his samples were good acoustic conductors. No other attempts have been noted in which frequencies above 5 kHz have been used in determining elastic moduli in single fibres.

The sample-transducer holder used here, utilizes three configurations generally used in the generation of the various modes of wave propagation in a sample. These three configurations A, B and C are illustrated in Figure 19.

CONFIGURATION A ($\theta = 90^{o}$)

This configuration is used with compressional transducers (P.Z.T.-5) to propagate the lowest order longitudinal mode, L (0,1), in the sample. Minimum loss of energy is incurred with this configuration when using rigid samples. According to Gelles[35], the total loss from electrical input to electrical output (exclusive of sample attenuation) is generally about 50 dB.

CONFIGURATION B (θ about 45^{o})

This configuration is used with compressional transducers to produce the L (0,1) mode and the T(0) mode (lowest order torsional mode) in the sample. Non-brittle samples are bent around the perspex supporting edges and taped into position. (The taping of the sample ends forms an absorbent termination which helps to eliminate echoes originating from the sample end reflection in good acoustic conductors).

The over-all loss from electrical input to electrical output (exclusive of sample attenuation) is generally about 56 d B.

CONFIGURATION C / .....

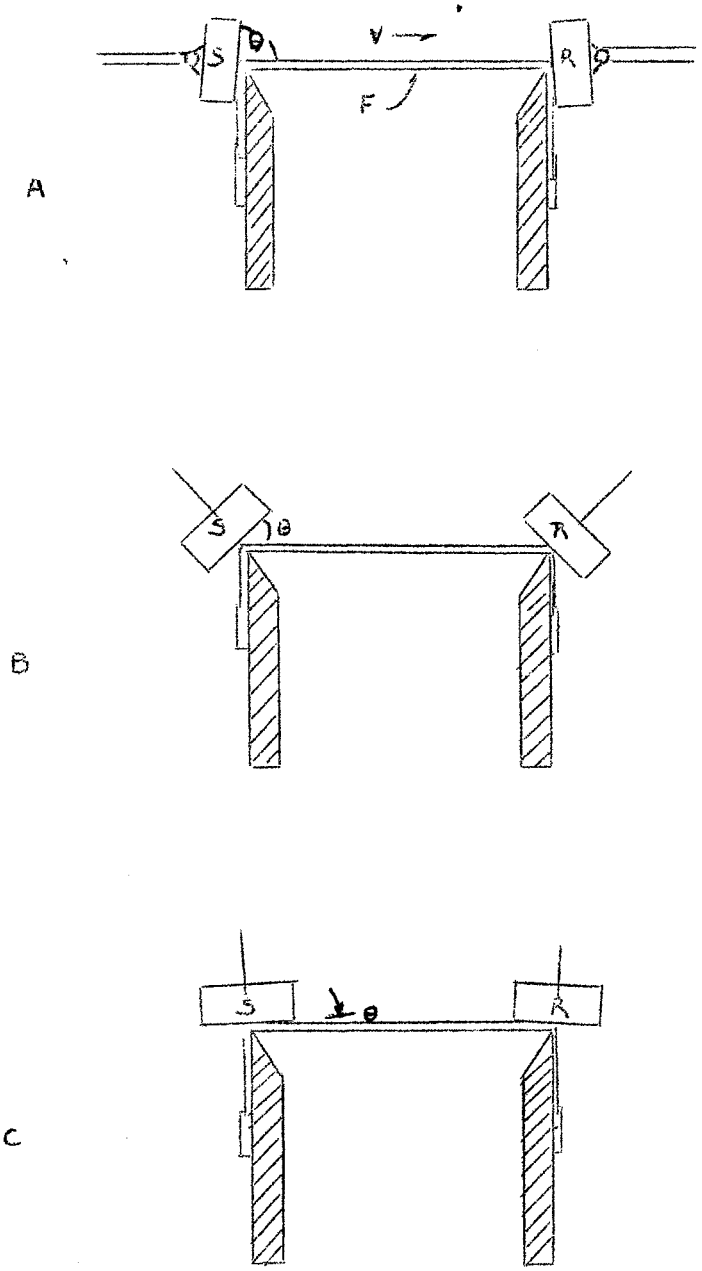

Figure 19. Side views of three transducer configurations used to propagate ultrasonic pulses through thin samples.

V : Group velocity.
θ : Transducer coupling angle.
F : Fibre.
S : Sender.
R : Receiver.

Polarization of shear transducers - normal to page.

CONFIGURATION C (θ about 2^{o})

This configuration is used with shear wave trans-ducers to propagate the T(0) mode in cylindrical samples. The total electrical loss in this case is generally about 60 d.B. . It should be noted that P.Z.T. transducers do not exhibit good mode purity and, in particular in configuration B, simultaneous excitation of the L(01) and T(0) (and other fundamental modes) is often possible. One can, therefore, calculate both Λ and μ from a single experimental arrangement. This is well illustrated by Gelles[61] whose photographs are reproduced in Figure 20 for a copper wire of 4.40 cm length and 75 μ diameter. Figure 20(A) illustrates the good mode purity of a Y-cut quartz transducer, in which only T(0) mode is excited. On replacing the Y-cut quartz transducer with a shear polarised transducer, as shown in Figure 20(B), there is a 15 d.B. gain in signal level, but additional modes are excited and some dispersion is evident. This dispersion is moderate for the L(01) mode, slight for the flexural, F(1,1), mode and negligible for the T(0) mode. Suppression of one or more of these modes can be effected by altering the transducer coupling angle or the contact pressure.

It is essential, where rigid samples are used, to adopt some means of efficiently coupling the ultrasonic energy from the transducer to the specimen, and is usually a viscous liquid such as glycerine. The use of liquid coupling agents however, limits the type of wave that can be generated since liquids have no shear modulus. In the case of keratins the fibres are sufficiently elastic to be bent over the sample support knife edges and the

transducer pressed / .....

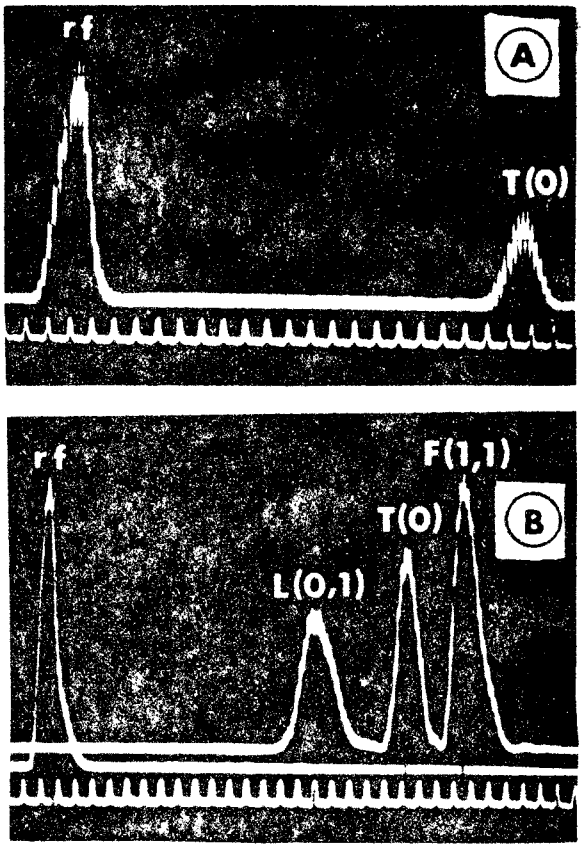

Figure 20. Results by Gelles for fine copper wire. Time marks at bottom indicate 1 μs intervals. Note that the separation of the pulses is only 4-5 μs. Y-cut transducers were used in A, while P.Z.T.-4 transducers were used in B.

transducer pressed against the fibre to make a plastic contact.

Initial attempts to obtain wave propagation in keratin fibres were unsuccessful when using both a pressure contact (plastic) or liquid coupling agents between the transducers and the sample so that the delay plate technique was then adopted as described below. Satisfactory results were obtained when good acoustic conductors such as glass and fine copper wire were used both with the P.Z.T. and quartz transducers. The pulses produced in a specimen of glass 4.74 cm in length and 0.030 cm in diameter using P.Z.T. transducers for example, are shown in Photographs 3 and 4. The uppermost trace in each photograph is the pulse packet supplied to the transmitter.

Assuming that the decrease in amplitude of successive echoes in Photograph 3(a) for example, is exponential, an estimate of the acoustic damping factor α can be calculated from the equation

$$Y_n = Y_o \exp(-\alpha \Lambda)$$

where the successive amplitudes of the echoes are labelled Y_o to Y_n and Λ is the distance between successive pulses (wavelength). The damping is more commonly expressed as the log decrement δ, and is the product of α and Λ. A value of δ of 3.1×10^{-3} was obtained, which agrees favourably with a value of 9.5×10^{-3} quoted by Kolsky[55] for soft glass. (The specimen used here was not soda-glass and this probably accounts for the difference between the results.)

The quartz transducers were not very satisfactory for pulse propagation measurements since they were

susceptable to / .....

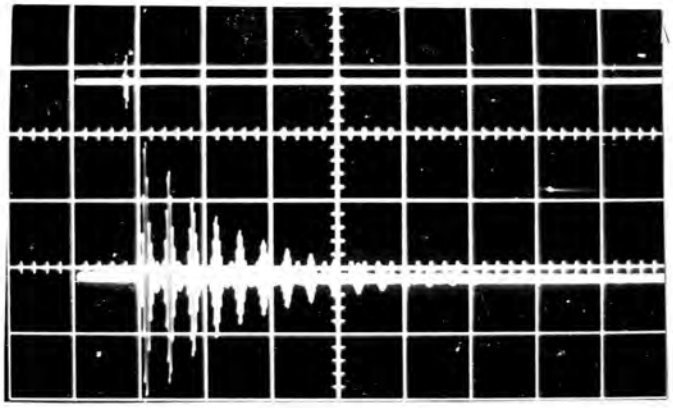

Photograph 3(a) : The R.F. output of a short pulse in a glass specimen
1 = 4.74 cm and
a = 0.030 cm.
Time scale : 1 cm = 50 μs.

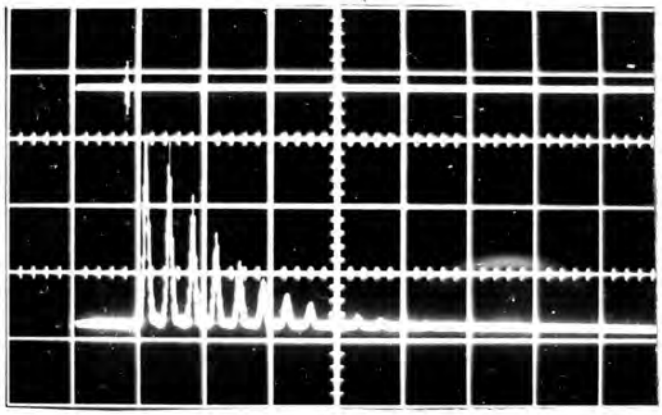

Photograph 3(b) : The video output of the above pulse. The upper trace in both cases is a display of the input pulse. Voltage of upper and lower trace are not on the same scale.

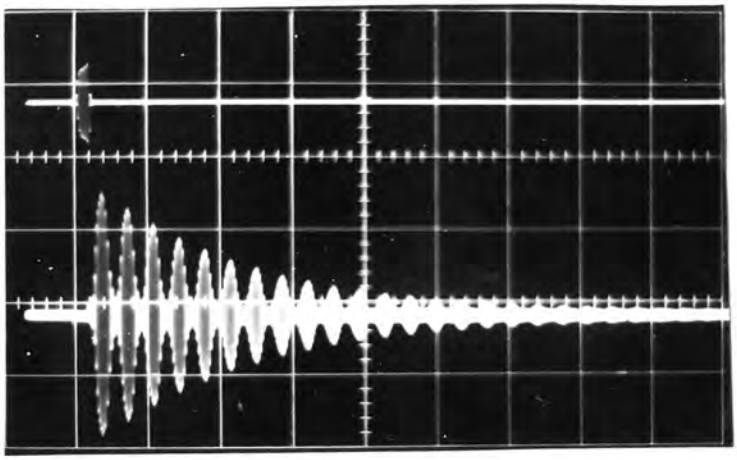

Photograph 4(a) : The R.F. pulse of specimen of photograph 3(a) and (b) with a longer input pulse.
Time scale : 1 cm = 50 µs.

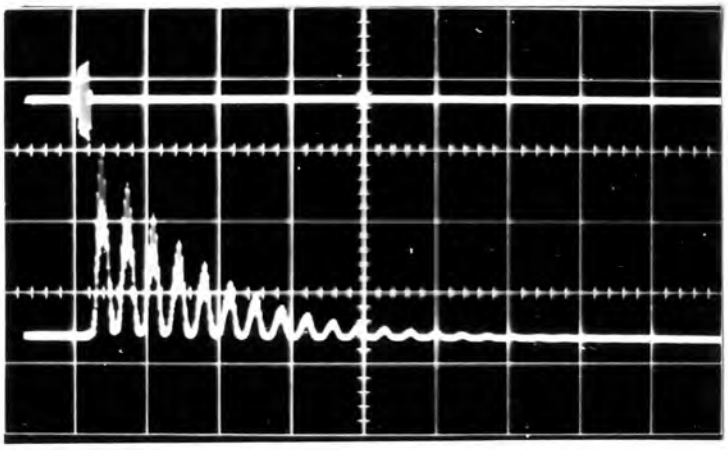

Photograph 4(b) : The Video output of 4(a).

susceptible to ringing once the excitation pulse had been switched off. The ringing effect could be eliminated by damping the crystals and was accomplished by fixing pieces of hard rubber to the sides and back of the crystal. The transducer efficiency, however, was then drastically reduced and the signal to noise ratio became too small for this type of transducer to be useful. The P.Z.T. transducers were, therefore, subsequently used for all measurements. The ringing effect in the quartz transducers is demonstrated in Photograph 5.

Another method, the delay plate method used by Gelles[35] for very short samples (of the order of a few millimeters) was then used to propagate pulses in keratin fibres since the plastic coupling method was unsuccessful. If no propagation was previously obtained because of the high damping of the ultrasonic energy in keratin, then by this method, it was hoped fibre damping would be of minor importance because of the short keratin ultrasonic path length involved. Briefly, the delay plates consisted of two identical glass plates, (approximately the size of microscope slides) separated from each other by a few millimeters and bonded together by means of hard rubber struts to form a rigid planar assembly. The pulse is then conducted from the sender through the first delay plate, through the fibre which bridges the gap between the plates, and is picked up via the second delay plate, by the receiver. Coupling between the transducers and delay plates was achieved by means of glycerine, while fibre to delay plate coupling was by means of an adhesive, water or glycerine.

Photograph 6(a) / .....

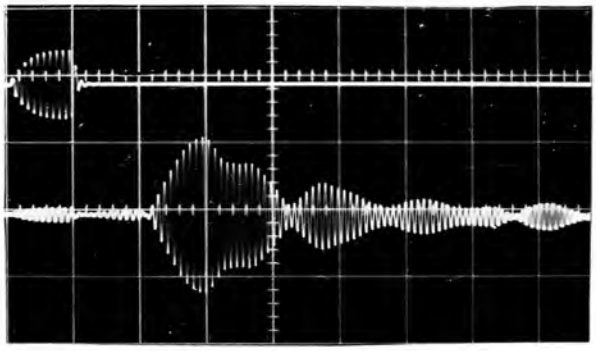

Photograph 5 : The R.F. pulse received after transmission through a thin glass rod with Y-cut Quartz as receiver. The high Q of the Quartz transducer causes the ringing effect after the main pulse has passed.

Time scale : 1 cm = 10 μs.

Photograph 6(a) displays the pulse transmitted across a 2 mm air gap (without a fibre bridging the gap) while in Photograph 6(b) a typical pulse conducted through mohair fibre is depicted. Similar results were obtained for kemp fibres but attempts with wool fibres were unsuccessful. Although the pulse conducted through air could serve as an ideal reference velocity, results were very difficult to interpret, and the exact velocity of the pulse could not be found. It was impossible to identify any modes or to separate them. Consequently, this approach was abandoned. It became apparent that the main problem to be dealt with was not the relatively high damping of the ultrasonic pulses in the keratin fibres, but the loss of energy in 'injecting' the pulse into the fibres.

The obvious solution to the problem of coupling the fibre to the transducer was to fix the fibre directly to the face of the transducer; a method which was tedious and damaged the transducer face, so that the only alternative was to fix small hooks to the transducer face, over which the fibre could be suspended. Good fibre-transducer contact could thus be established. Two discs, about the same diameter as the transducer faces, were cut from thin brass shimming, and a small wire hook soldered in the centre of each. The assembly was then cemented to the transducer face with Eastman 90 adhesive. The hook assembly was kept as light as possible, in order not to load the transducer excessively. In fact, no observable difference was seen in the transducer performance. With this assembly, the fibre with small weighted clamps on its ends, was merely suspended over the hooks when taking measurements. The

arrangement functioned / .....

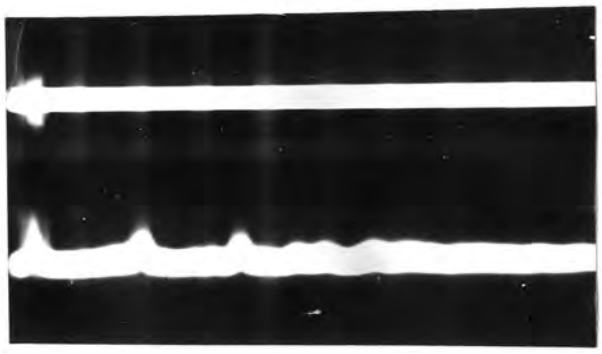

Air pulse

Photograph 6(a) : Propagation of pulse across air gap of delay plates.

Time scale : 1 cm = 50 μs.

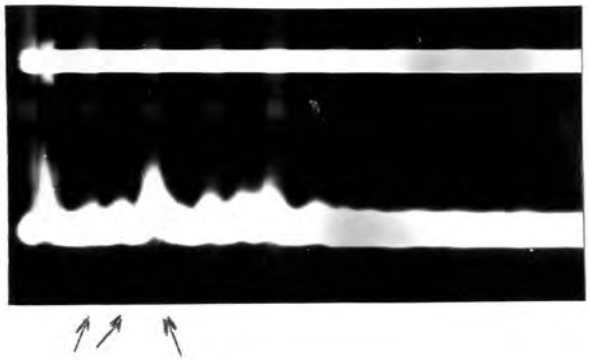

Mohair Air

Photograph 6(b) : Air gap in the delay plates bridged by a mohair fibre.

Time scale : 1 cm = 50 μs.

arrangement functioned very well and good large amplitude pulses were obtained. Thus relatively lower amplification could be used, and consequently noise and jitter created fewer problems.

Damping Measurements

With this hook suspension method, the fibre length could be varied without upsetting the coupling to the transducer. A method devised by Nolle[49] and discussed in paragraph 3.4 to determine the damping factor α in highly damped materials at a particular frequency was investigated. From Equation 6, if the log. decrement δ is very much less than 2π, then damping factor α can be neglected in the calculation of Young's modulus. However, a simple plot of amplitude versus length of fibre did not give a simple exponential decay of amplitude. Instead, a standing wave pattern was obtained as shown in Figures 21 and 22 for mohair and coarse wool fibres respectively. Therefore the method adopted to determine the attenuation was that according to Ballou and Smith[19]. By means of a plot of pick-up voltage V versus the distance x of the pick-up from the transmitter, the maximum and minimum pick-up voltage envelopes were found. The peaks decay exponentially and they[19] have deduced an analytical expression for the relationship between α and the received voltage envelopes in terms of tanh $(\beta + \alpha x)$, i.e.

$$\frac{V \text{ min}}{V \text{ max}} = \tanh (\beta + \alpha x) \qquad (33)$$

where β is the constant real part of the exponent of the reflection coefficient. In order to calculate α from Equation 33 a plot of arg. tanh $\frac{V \text{ min}}{V \text{ max}}$ versus distance x, was drawn for mohair, yielding a straight line as shown

in Figure 21./ .....

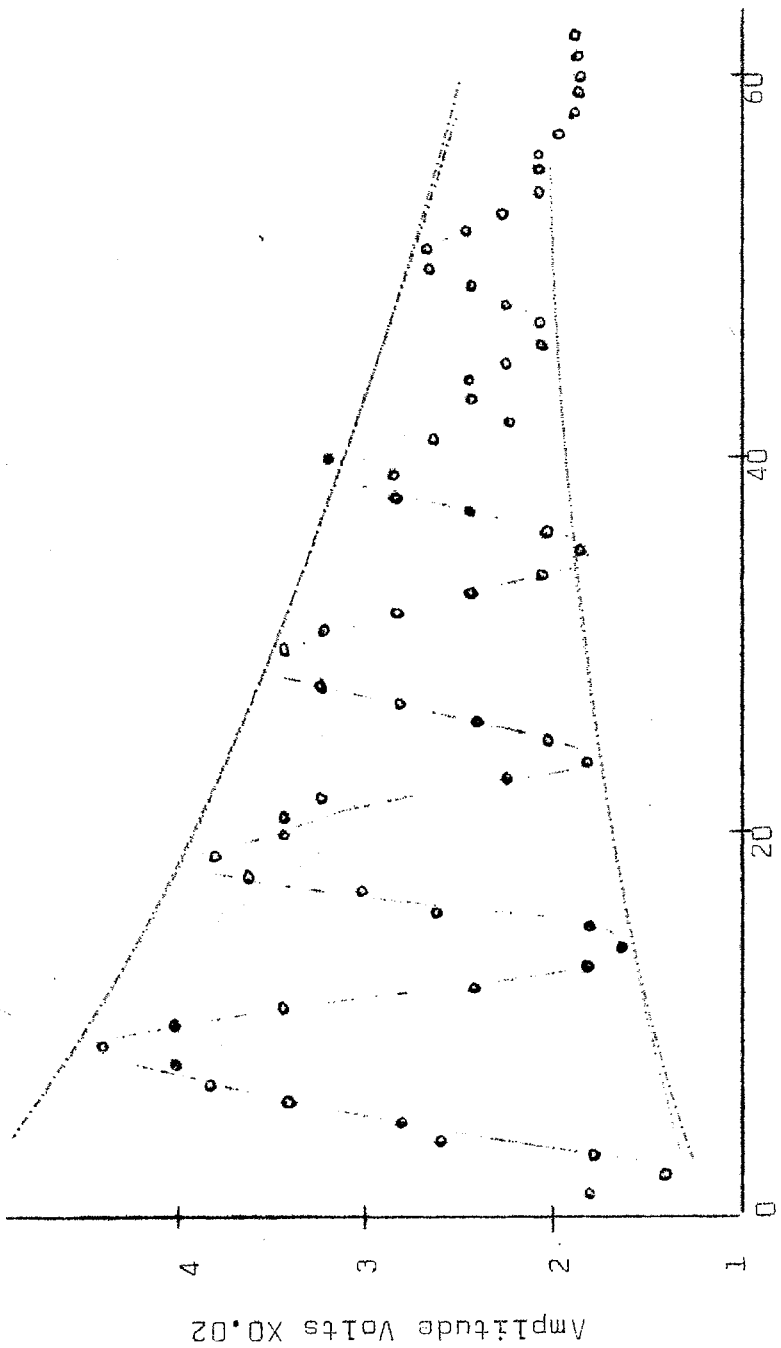

Figure 21. The standing wave pattern for a mohair fibre.

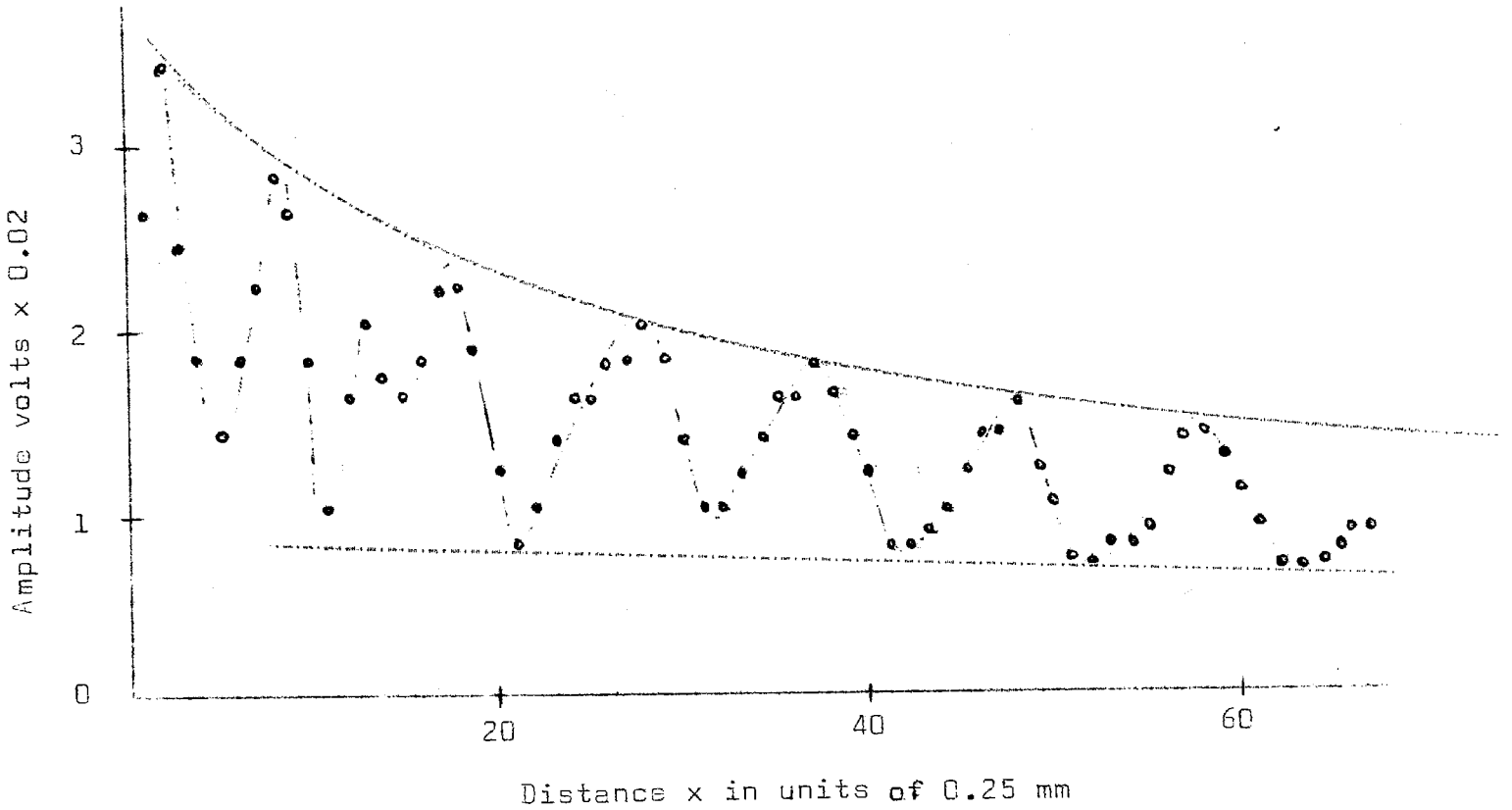

Figure 22. The standing wave pattern for a coarse wool fibre (Interference with the air transmitted pulse occurs for the first few mm)

in Figure 23. Thus α is the slope and was found for the mohair fibre to be

$$\alpha = 0.013 \text{ nepers/cm}$$

or

$$\delta = 0.0033 \text{ nepers.}$$

Because δ is much smaller than 2π we are justified in neglecting α in calculations of E.

The value obtained for α is not very accurate since amplitudes cannot be determined by better than (0.004) volts/cm on the oscilloscope due to a jittery trace. Nevertheless it does serve as a rough estimate in establishing the magnitude of δ.

A good example of pulse propagation in mohair is given in Photograph 7(a). The fibre was suspended over the hooks under slight tension but was not fixed to them by an adhesive. The first pulse is conducted in the sample while the second large pulse is that transmitted directly through air, and the others are probably secondary modes or shear modes conducted through the fibre. Using a different length of the same fibre the results displayed in Photographs 7(b) and 7(c) were obtained. Similar results were obtained with mohair and other fibres and some results are given in Table V. (In all photographs, the input or transmitter pulse (upper trace) is coupled electromagnetically to the receiver and is shown directly below it on the lower trace.)

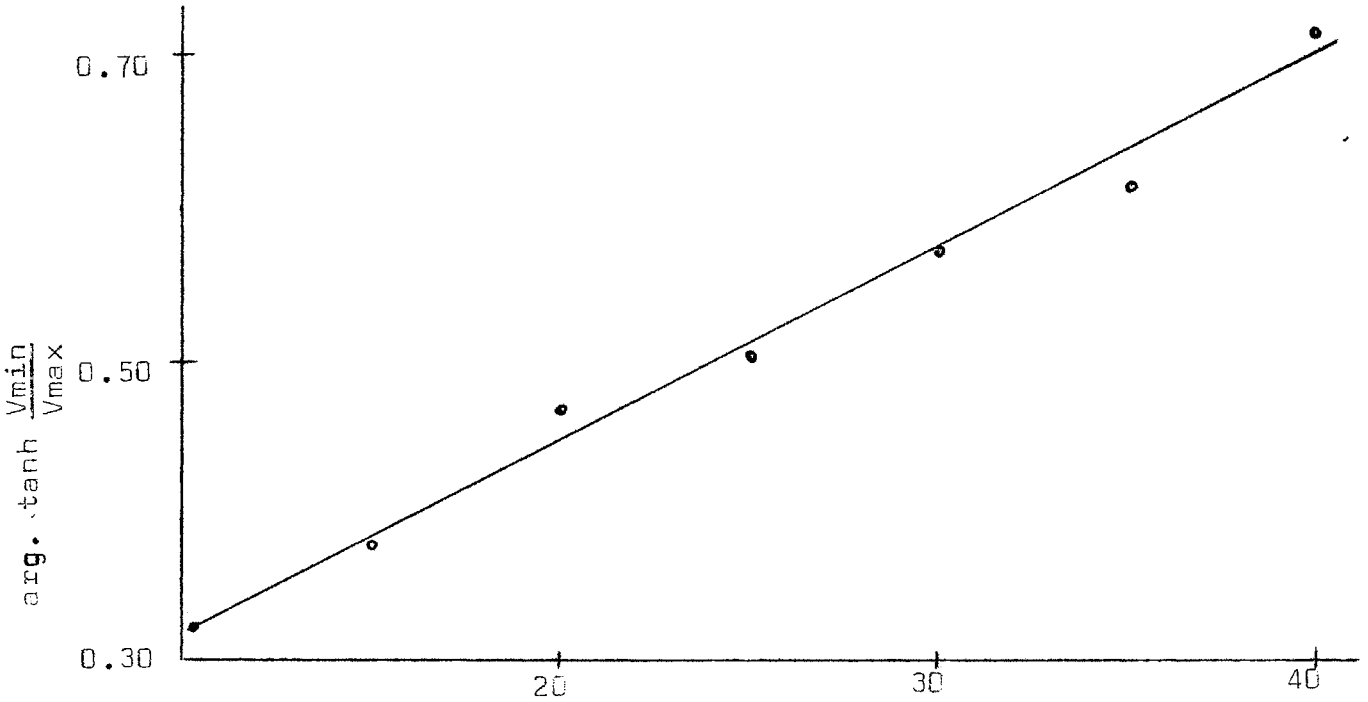

Figure 23. Determination of the attenuation factor α from the standing wave pattern for mohair.

(a)

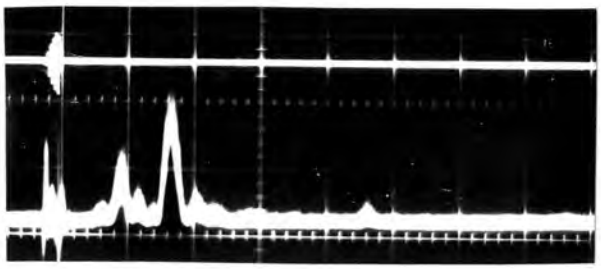

(b)

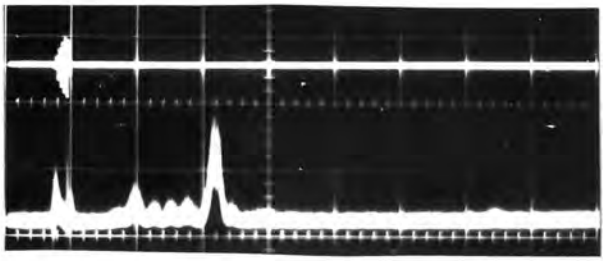

(c)

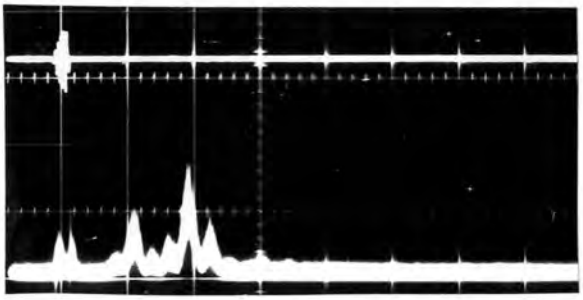

Photograph 7 : This sequence illustrates the pulse pattern received in mohair by the hook method, as sample length is increased. The 1st pulse is that conducted through the specimen while the 2nd pulse is conducted through the air between the transducer faces and the 3rd pulse is an echo of the 2nd pulse.

Time scale : 1 cm = 50 μs.

TABLE V

Velocity determinations with hooks fixed to transducers

Sample		V-from Equation 34	V-from Equation 35
Nylon		1.28 x 10^5 cm/sec	1.25 x 10^5 cm/sec
Kemp		0.38 " "	0.48 " "
Kemp stretch 30%		0.59 " "	0.67 " "
Coarse wool		0.61 " "	0.51 " "
Mohair M-1			
l = 1.94 cm	1st Pulse	0.76 " "	0.92 " "
	2nd Pulse	-	-
	3rd Pulse	0.48 " "	0.63 " "
	4th Pulse	0.35 " "	0.38 " "
	Air Pulse	0.032 " "	-
l = 3.39 cm	1st Pulse	0.75 " "	0.70 " "
	2nd Pulse	0.56 " "	0.53 " "
	3rd Pulse	0.45 " "	0.44 " "
	4th Pulse	0.39 " "	0.39 " "
	Air Pulse	0.032 " "	- " "
l = 3.48 cm	1st Pulse	0.77 " "	0.68 " "
	2nd Pulse	0.63 " "	0.58 " "
	3rd Pulse	0.50 " "	0.46 " "
	4th Pulse	0.44 " "	0.41 " "
	Air Pulse	0.032 " "	- " "

The velocities of pulses measured under these conditions are subject to a small error since their transit time measurement, includes a circuit time delay factor, t_o. This delay arises by virtue of the fact that a certain finite time is spent by the electrical pulse excited in the receiver transducer in being amplified and fed to the plates of the oscilloscope. The delay was estimated by plotting the time taken for the pulse conducted directly between transducer faces through the air, as a function of the distance between the transducer faces, and extrapolating to obtain the zero-intercept time delay (see Figure 24). A regression analysis yielded a t_o value of 4 μs for the P.Z.T.-4 transducers, while a value of t_o of 12 μs was obtained for the P.Z.T.-5 transducers. The true velocity of the pulse through the fibre is then

$$v = \frac{l_s}{t - t_o} \qquad (34)$$

where t is the time interval between transmitted and received signals read on the oscilloscope, and l_s is the sample length. The slope of the line in Figure 24 is the velocity of the pulse in air. The velocity obtained from tables[62] having been corrected for temperature and humidity was taken to be 3.44×10^4 cm/sec. This agrees within 2% with the results obtained for the P.Z.T.-4 and P.Z.T.-5 transducers. The velocity of the pulse in air serves as a good reference.

Suppose the pulse transit time in the reference medium is

$$t_r - t_o = \frac{l_r}{V_r}$$

where l_r / .....

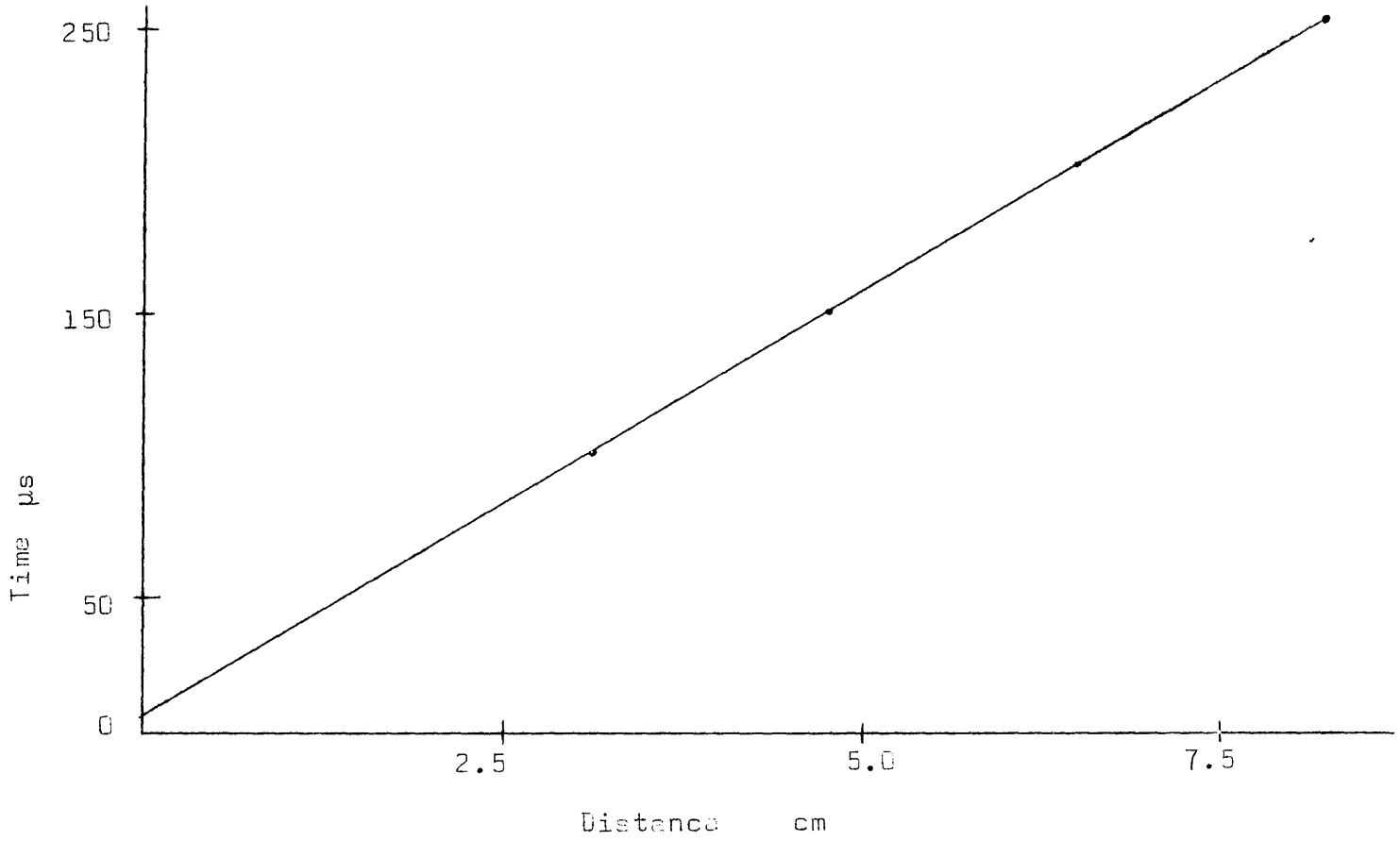

Figure 24. Determination of time delay t_o, introduced by the circuit, using the P.Z.T.-4 transducers.

where l_r is the distance between the transducer faces, and V_r the velocity of the pulse in the reference medium. The corresponding equation for the velocity of a pulse through a sample is

$$t_s - t_o = \frac{l_s}{V_s}$$

The difference in time between these two when $l_s = l_r$ is given by

$$t = \frac{l_s}{V_s - V_r}$$

OR

$$Vs = \frac{l_s}{\frac{l_s}{V_r} - \delta t} \qquad (35)$$

and is independent of the zero time intercept delay.

There is a fair correlation between the individual velocities as calculated from Equations 34 and 35 in Table V. This type of suspension leads to the generation of spurious modes, and it was difficult to reproduce any particular pulse pattern in any one fibre.

As a modification of the above coupling technique, thin flat rectangular pieces of brass, approximately 2 mm wide, were soldered to the thin circular brass shims, which were then fixed to the transducer faces by means of Eastman 90 adhesive. These flat pieces of brass were fixed in the plane of the transducer face and extended a few millimeters beyond its circumference. The ends of the brass extensions were tapered to form smooth polished knife edges. The fibres were suspended over the perspex

supports and / .....

supports and tensioned either by weights attached to their ends, or by taping the ends to the supports. The transducers were brought into contact with the fibres as indicated below.

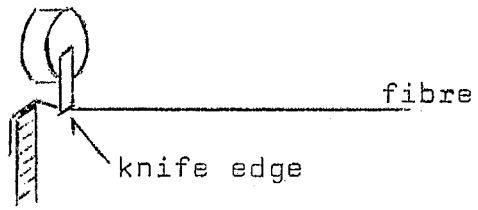

The contact angle θ, could thus be varied and it was found that most of the spurious modes observed with the hook coupling method could be eliminated. A typical signal received is given in Photograph 8, in which the first two pulses are transmitted through the fibre, while the third is that propagated through the air. Amplitudes too, were at least ten times greater than previously observed. With this type of coupling it was found that usually only one pulse was transmitted through the fibre using the P.Z.T.-4 transducers, while usually at least two pulses were observed when the P.Z.T.-5 transducers were used. Spurious modes were sometimes generated but were of lower amplitude and did not cause complications. Table VI gives some results obtained with both pairs of transducers. Where possible, if the sample was not severed when adjusting the transducer coupling, velocities were calculated on the same fibre using both the P.Z.T.-4 and P.Z.T.-5 transducers. Measurements were carried out on the same fibre, but at different lengths, and, are indicated by (b), (c), (d) etc. for the particular fibre. The t_o corrections of 4 μs and

12 μs for / .....

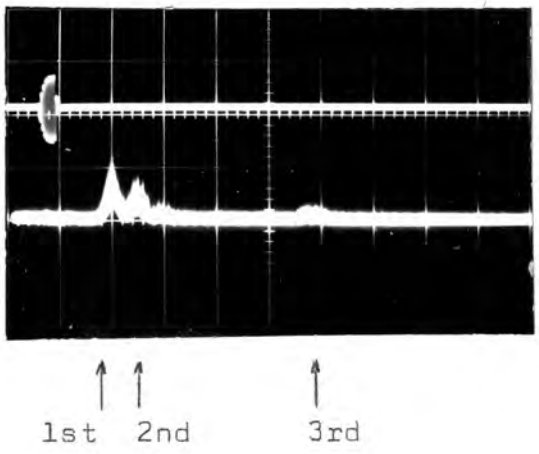

Photograph 8 : Knife edge coupling on a mohair specimen. The first and second pulses received are conducted through the fibre, while the third is that directly transmitted by the air between the two transducers.

Time scale : 1 cm = 50 μs.

12 μs for the P.Z.T.-4 and P.Z.T.-5 transducers respectively were applied, and included in Table VI. In most cases, the amplitude of the air conducted pulse was too small to be detected so that the use of Equation 35 to calculate velocity could not be employed. The highest velocity pulse in each case was tentatively termed the "L(0,1)" or "Longitudinal" mode velocity, while the next highest was termed the "T(0)" or 'torsional' mode velocity. Results marked with an asterisk indicate that both T(0) and L(0,1) mode velocities were determined with the same transducer, viz. the P.Z.T.-5 transducers. Comparison of the uncorrected values of velocity of the "longitudinal" mode, (as determined with the P.Z.T.-5 transducer) with the uncorrected velocity of the "torsional" mode (obtained with the P.Z.T.-4 transducers), indicates that the "longitudinal" mode has the same velocity as that of the "torsional" mode. For example, mohair fibre (1) has an uncorrected longitudinal velocity of 1.48×10^5 cm/sec when measured by means of the P.Z.T.-5 transducer. Using the same fibre and the P.Z.T.-4 transducer, the so-called 'torsional' velocity is given in 1(a) as 1.49×10^5 cm/sec. The "torsional" mode as measured with the P.Z.T.-5 transducer (and marked with an asterisk) is 0.99×10^5 cm/sec. Other examples are fibres 7 and 7(a), 8 and 8(a) etc. This means that the P.Z.T.-4 and P.Z.T.-5 transducers were in fact generating the same mode, which was thought to be the longitudinal mode, while the second pulse observed with the P.Z.T.-5 transducers was either the torsional mode or a second order longitudinal. In view of the discussion at the beginning of Part IV, it was

assumed that / .....

assumed that this was the T(0) mode, and was again, tentatively termed accordingly. Further comparison of the "longitudinal" and "torsional" mode velocities, excited by the same transducers indicate a fairly consistant velocity difference of about 0.3×10^5 cm/sec for the two modes. Conversion of these velocities to moduli values (by squaring the velocity and dividing by the density) provided in Figure 25, gives values which are comparable with Young's modulus and shear modulus for keratin[63].

Further conclusions from Table VI are that mohair fibre 1(d) has a velocity which is almost the mean of fibre (b) and (c). It was found that the velocity of the pulse depended on the position of the knife edge on the fibre, and a position could be found at which both these pulses could be simultaneously excited. Photographs 9(a) to (c) illustrate the sequence, while Photograph (d) shows the simultaneous excitation. The pulse patterns for the three different fibre types is shown in Photographs 10, 11 and 12.

TABLE VI

Velocity determinations using knife edge method

Sample Fibre	No.	Longitudinal velocity x 10^5 cm/sec. (obtained by P.Z.T.-5 transducer) Uncorrected	Corrected	Torsional velocity x 10^5 cm/sec. Uncorrected	Corrected
Wool	1			1.19	1.32
	2	1.54	1.67	1.25*	1.67*
	3	-	-	0.94	1.04
	4	0.78	1.07	0.49*	0.59*
	5	0.89	1.17	0.58*	0.69*
	6	1.16	1.66	-	-
	7	0.91	1.19	0.60*	0.71*
	7(a)	-	-	1.09	1.23
	8	0.95	1.21	0.78*	1.02*
	8(a)	-	-	1.08	1.18
	9	1.01	1.30	0.86*	1.05*
	9(a)	-	-	1.17	1.28
Mohair	1	1.48	1.98	0.99*	1.19*
	1(a)	-	-	1.49	1.65
	1(b)	-	-	1.15	1.25
	1(c)	-	-	1.35	1.49
	1(d)	-	-	1.26	1.39
	2	-	-	1.39	1.50
	2 repeat	-	-	1.52	1.63
	3	1.12	1.48	0.77*	1.08*
	4	1.15	1.44	0.188*	1.03
	4(a)	-	-	1.29	1.40
	4(b)	-	-	1.40	1.52
	4(c)	-	-	1.22	1.33
	4(d)	-	-	1.38	1.52
	4(e)	-	-	1.46	1.58
	5	1.40	1.82	1.04*	1.25
Kemp		-	-	0.97	1.07
		0.97	1.33	0.69*	0.84*
				0.65*	0.80*
Nylon	1	0.9	1.1	0.7*	0.9*
	1(a)	-	-	1.1	1.2
	1(b)	0.9	1.2	0.8*	0.9*
		-	-	1.1	1.2

Velocities marked with an asterisk indicate that the P.Z.T.-5 transducer was used to generate the so-called "torsional mode".

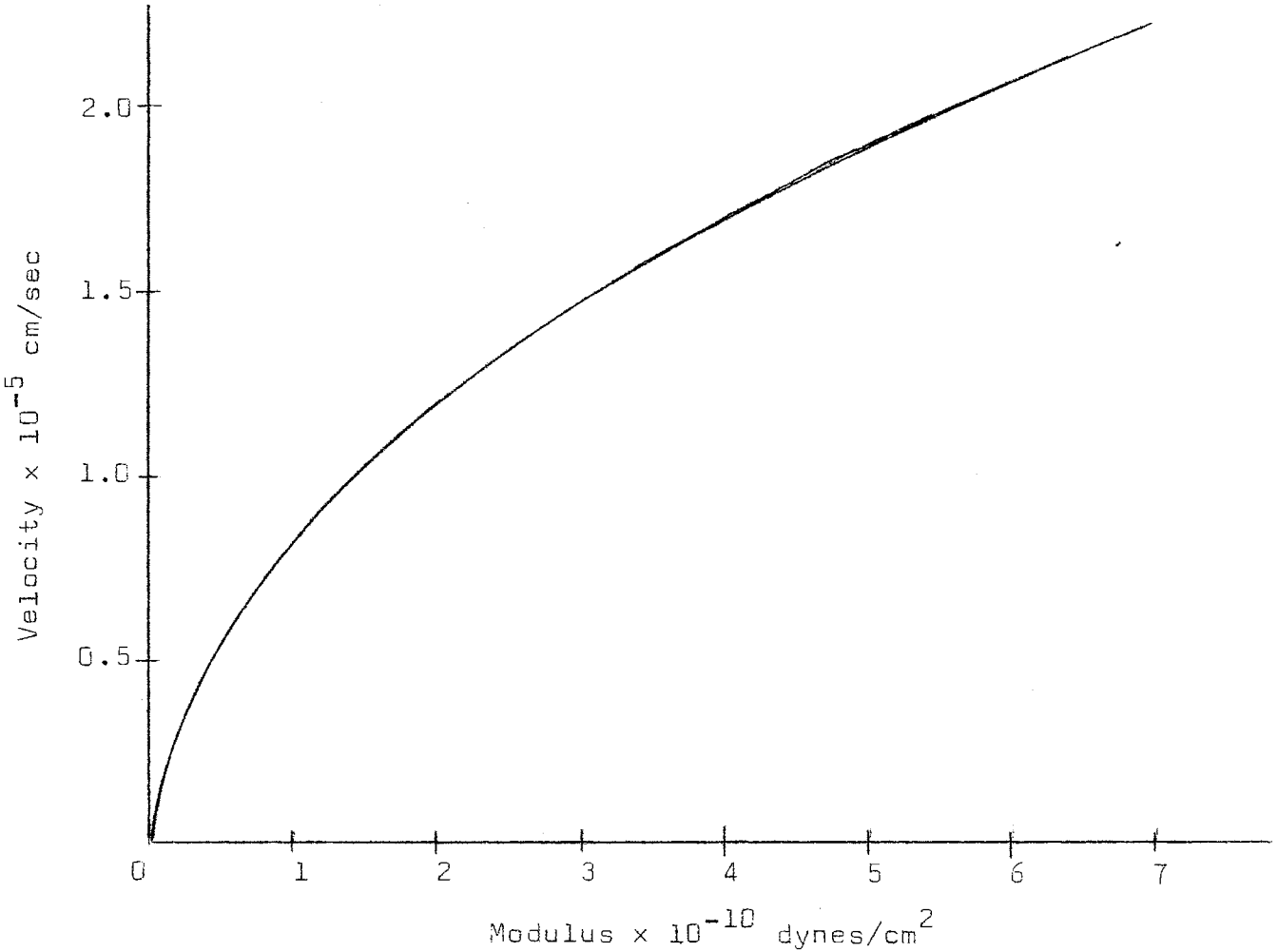

Figure 25. Theoretical relationship between velocity of pulse through a fibre and the corresponding modulus of the fibre.

(a)

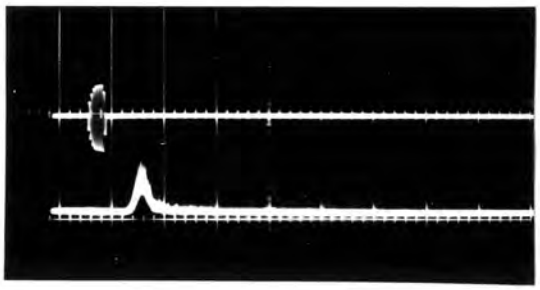

(b)

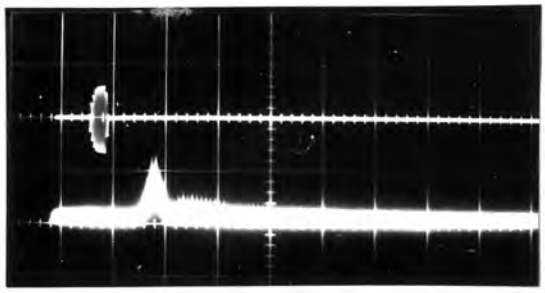

(c)

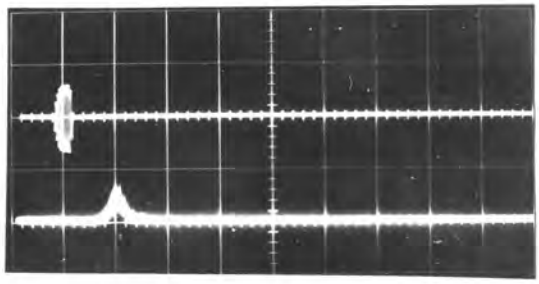

(d)

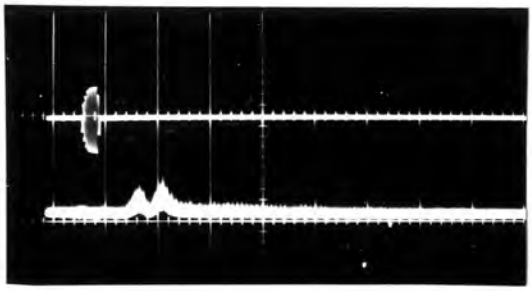

Photograph 9 : Variations in position of the knife edge on the fibre yields slightly different velocities as illustrated in the sequence of photograph (a) to (c). The pulse shown in photograph (b) has the mean velocity of that shown in (a) and (c). Simultaneous excitation of (a) and (c) is shown in photograph (d).

Time scale : 1 cm = 20 μs.

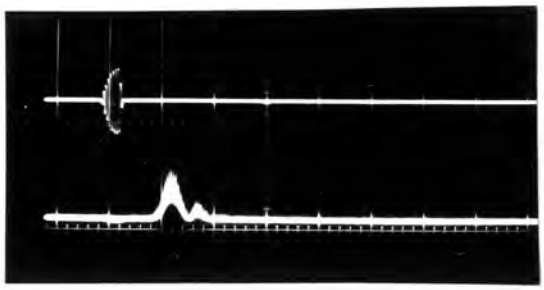

Photograph 10 : A secondary mode excited in a mohair sample of length 6.50 cm with knife edge coupling and longitudinal transducers.

Time scale : 1 cm = 20 μs.

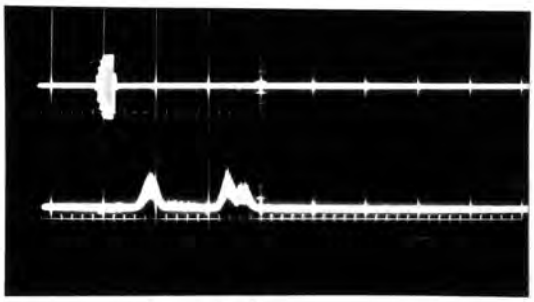

Photograph 11 : A kemp fibre produces the pulse shown here using shear wave transducers. The second pulse is that conducted through air, while the third appears to be an echo of the first fibre conducted pulse.

Time scale : 1 cm = 20 μs.

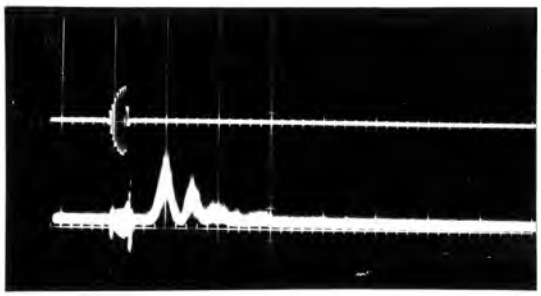

Photograph 12 : The pattern obtained with a wool fibre using longitudinal wave transducers. This is similar to that depicted in photograph 10 for mohair.

Time scale : 1 cm = 20 μs.

Prior to this it had not yet been possible to excite or distinguish the L(0,1), T(0) and F(1,1) modes excited either individually or simultaneously in a specimen. It was felt, however, that this could be accomplished provided a method was employed in which the coupling angle could be effectively varied. This again suggests the method used by Gelles[35], viz. plastic contact between transducer and specimen when the latter is bent over the sample support and taped into position, a method which, without refinement to the existing apparatus was unpractical for diameters less than about 30 μ. Amplitudes with knife edge coupling were very large which indicated that coupling losses were relatively small so that losses with the plastic coupling method as initially attempted, must have been excessive, and means to reduce these losses were then employed.

By fixing thin discs, cut from brass shimming, to the transducer faces and polishing the surfaces as much as possible, contact could be made with the specimen without interference from the pedestals, thus reducing contact losses. The straight edge of the sample supports were altered so that they had finer, highly polished knife edges, and were slightly convex so that contact with the transducer face was localised to one small area. With the aid of an eyeglass the transducer could be lowered into gentle contact with the sample. Shearing of the sample which in this arrangement became more probable, created some problems but improvements to the manipulating system could not be immediately brought about and the "crude" existing system had to suffice.

Using a single strand of unravelled Litz wire the results obtained by Gelles[61] shown in Figure 20 could be reproduced as depicted in Photograph 13. A shear

transducer was / .....

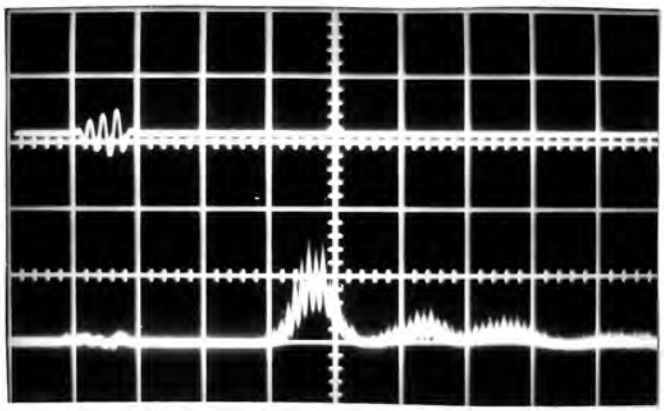

Photograph 13 : The L(0,1), T(0,1) and F(1,1) modes excited in a fine copper wire specimen of length 9.80 cms, using plastic coupling of the shear wave transducers. Note the short pulse length necessary.

Time scale : 1 cm = 10 μs.

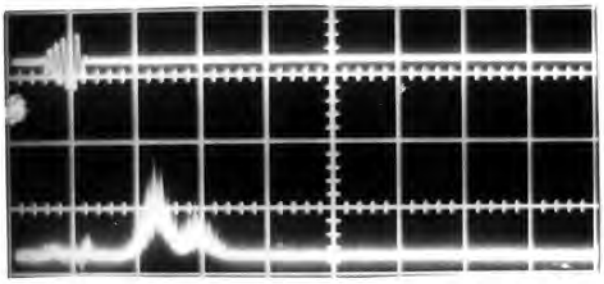

Photograph 14 : Most probably the L(0,1) and T(0) modes excited in a mohair sample with longitudinal wave transducers at a coupling angle θ of about 90^{0}.

Time scale : 1 cm = 10 μs.

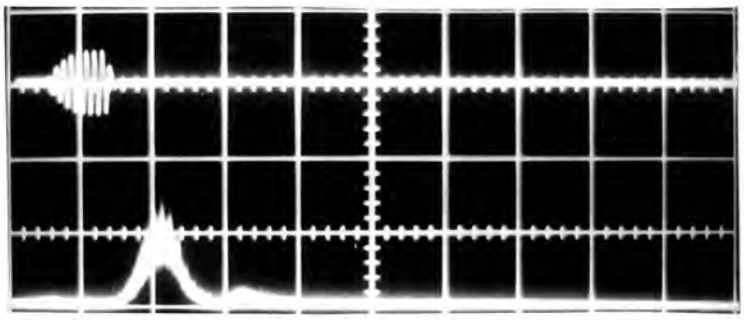

Photograph 15 : The echo observed when long specimens are used.

Time scale : 1 cm = 20 μs.

transducer was used at an angle of about zero degrees. In most cases it was difficult to excite all three modes simultaneously, as one mode, usually the L(0,1) or T(0) dominated. Similar results were obtained with the P.Z.T.-5 transducers at angles between 45^{o} and 90^{o}, the results of which are tabulated in Table VII. The reason that this technique had not been successful previously was due mainly to the fact that the transducer faces were relatively soft and uneven. On pressing the transducer into contact with the fibre, it was impossible to avoid contact between the sample support and the transducer and energy losses were too great. The hard polished brass surface, in conjunction with the curved knife edge, made clean contact between specimen and transducer possible, and the problem was to a large extent overcome.

TABLE VII

The velocities of the L(01), T(0) and F(11) modes in a single strand of unravelled Litz wire

Transducers	Trial Number	$C_{L(01)} \times 10^5$ cm/sec	$C_{T(0)} \times 10^5$ cm/sec	$C_{F(11)} \times 10^5$ cm/sec
P.Z.T.-4's	1	2.70	-	-
	2	-	2.32	1.79
	3	-	2.21	1.77
	4	2.97	2.39	2.04
P.Z.T.-5's	1	-	-	1.85
	2	-	2.16	1.75
	3	2.57	2.16	-
	4	2.58	2.17	1.78
Gelles' Results		2.96	2.21	1.90

The velocities for the respective pulses calculated from Gelles'[61] results are also included in Table VII. Note however that no t_o correction was applied to any calculations in the table. The variation in the calculated value of the velocity was due mainly to the error involved in measuring the sample length. Different tensions were inadvertently applied during each measurement consequently the lengths measured are subject to a small error. Agreement with Gelles'[61] results is good, especially in fourth P.Z.T.-4 transducer case. Pulse lengths varied from 4 μS to 8 μs and sample lengths up to about 10 cms were used.

Upon substituting a mohair fibre for the copper wire specimen pulses were obtained of which a typical example is given in Photograph 14 for the P.Z.T.-5 transducers. A secondary mode or echo was sometimes observed, an example of which is given in Photograph 15 (note that the time scale is different from Photograph 14. Judging from the velocity, this second pulse was most probably an echo, which in most fibres was not observed for either type of transducer for nearly all configurations (from $\theta = 0^o$ to $\theta = 90^o$). By using both P.Z.T.-4 and P.Z.T.-5 transducers on the same fibre specimen, the results given in Table VIII were obtained. Diameters of the samples were also measured as described in Part II. During measurements on one particular fibre, it was found that two exceptionally large amplitude pulses were received, and on microscopically examining the fibre, it was found to be highly medullated. A second fibre in the group was found to produce three pulses - and on examination it was found to be split into a number of parts. Thus certain gross structural differences were indicated by the odd pulse patterns for these particular

fibres. From / .....

fibres. From Table VIII it will be noted that the results obtained with the P.Z.T.-4 transducer are slightly greater than those obtained with the P.Z.T.-5 transducers. It has since been found that this difference in velocity obtained is due to there being a different value of t_o for each transducer for this type of coupling. This value of t_o, is different from that obtained when using knife edge or hook coupling and accounts for the velocities here being different from those obtained in Table VI.

A plot of velocity against radius for some of the fibres in Table VIII as shown in Figure 26 reveals a fairly positive correlation and this could account for the general scatter of velocities obtained for a particular sample, since the thicker fibres would tend to yield higher velocities.

The procedure for the above-mentioned results, was to lower the transducer gently into contact with the specimen with the face of the transducer at an angle of about 45^{o} to the specimen and then adjust both the pressure and this angle to give a maximum amplitude of the received signal, the pulse width being set at maximum - viz. about 18-20 μ secs. Shortening of the pulse length had no apparent effect other than to reduce the amplitude of the received signal. The time separation of the L(01) and T(0) modes in the fibre, if they existed, may be less than the pulse width (in the case of Litz wire, these were separated by about 10 μ secs for about a 10 cm sample length). Shorter pulse lengths were then employed and consequently shorter fibre lengths were necessary, i.e. from 3 cms to 5 cms in order to make up for the attenuation of the received pulse. With extremely delicate coupling the pulse pattern depicted in Photograph 16 was obtained.

TABLE VIII.

Velocity measurements on the same fibre with both P.Z.T.-4 and P.Z.T.-5 transducers

Fibre No.	P.Z.T.-5 transducer velocity X 10^5 cm/sec	P.Z.T.-4 transducer velocity X 10^5 cm/sec	Mean Radius
1	1.31	1.24	21.1
2	1.15	1.12	21.6
3	1.41	1.47	28.3
4	1.31	1.47	17.5
5	1.25	1.62	-
6	1.21	1.48	20.7
7	1.34	1.58	24.6
8	1.28	1.65	27.6
9	1.16	1.46	16.8
10	1.46	1.46	25.6
11	1.48	1.54	28.5
12	1.33	1.25	25.3
13	1.23	1.23	(medullated)
14	1.23	1.37	20.9
15	1.34	1.61	(split)
16	1.37	1.64	28.17
17	1.39	1.47	24.18
18	1.33	1.51	-
Average	1.31	1.45	

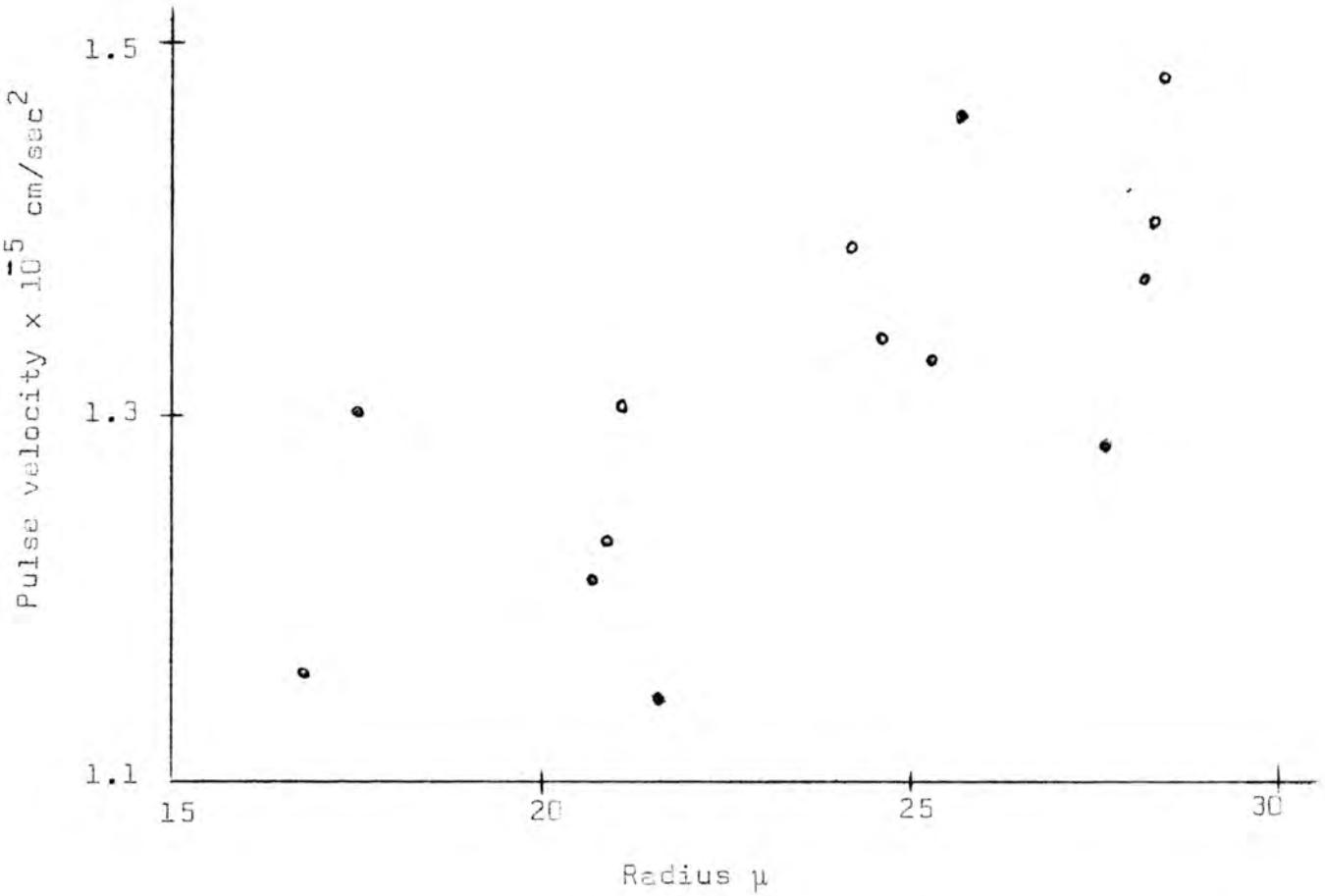

Figure 26. The correlation between pulse velocity in a fibre, and radius of the fibre for mohair.

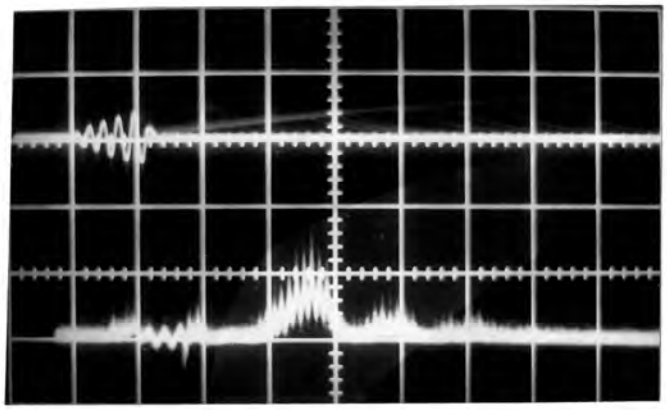

Photograph 16 : Most probably the L(0,1), T(0) and F(1,1) modes excited in a mohair fibre of length 3.03 cms by longitudinal transducers at a coupling angle of about 90^{o}.

Time scale : 1 cm = 10 μs.

With most fibres two pulses were visible, which would merge into one of considerably greater amplitude if the pulse length were too long. These, it was assumed, were actually the L(01), T(0) and F(11) modes being produced in the specimen. The single pulses observed in the previous results, were therefore most probably a superimposition of the L(01) and T(0) modes. Once they had been separated, the higher velocity component was generally more easily excited on its own by adjusting the coupling.

Again a number of mohair fibres from the same group were examined with each type of transducer. Young's modulus for stretching, E_s and fibre diameter were computed as described in Part II. The velocities, and their respective moduli, were calculated and tabulated with E_s and diameter in Table IX. The moduli calculated from the velocities of the two modes are accepted to be E and μ and are tabulated as such, although the validity of the modes have yet to be conclusively proved. The values of E and μ appear to be of the same order of magnitude as those obtained by other workers at lower frequencies[63].

Correlations of $C_L^2\rho$ and $C_T^2\rho$ versus E_s are given in Figures 27 and 28 whilst those for $C_L^2\rho$ and $C_T^2\rho$ versus radius are shown in Figures 29 and 30 respectively. These latter plots, indicate a positive correlation as previously found. The correlation between ultrasonic modulus and stretching modulus, as indicated in the former graphs is poor. This poor correlation can be partially accounted for by errors introduced in both moduli measurements. Length measurements during ultrasonic

TABLE IX

Pulse velocity, ultrasonic moduli, stretching moduli and radii for mohair fibres

Fibre No.	$C_L X10^5$ cm/sec	$C_T X10^5$ cm/sec	$E = C_L^2 \rho$ $X10^{10}$ dynes/cm^2	$\mu = C_T^2 \rho$ $X10^{10}$ dynes/cm^2	Radius $X\ 10^{-4}$ cm	E_s $X10^{10}$ dynes/cm^2
1	1.65	1.15	3.57	1.73	23.16	4.13
2	1.37	1.02	2.44	1.36	31.58	3.41
3	1.44	1.09	2.71	1.55	24.44	4.53
4	1.38	0.96	2.50	1.26	24.88	4.02
5	1.47	0.98	2.84	1.28	21.86	4.72
6	1.55	1.01	3.16	1.41	23.22	4.83
7	1.52	0.88	2.96	1.02	30.96	3.36
8	1.26	0.89	2.86	1.03	21.57	4.18
9	1.24	-	2.02	-	25.74	3.79
10	1.41	0.90	2.62	1.06	-	-
11	1.26 1.16	0.88 0.79	2.06 1.75	1.02 0.83	24.47	2.36
12	1.30	0.86	2.22	0.97	19.33	4.54
13	1.23	0.94	2.15	1.16	19.73	3.51
14	1.36	0.92	2.40	1.13	-	-
15	1.36	0.88	2.40	1.02	26.17	3.42
16	1.35	0.85	2.36	0.94	23.70	2.77
17	1.45	1.04	2.76	1.41	28.58	3.00
18	1.28	0.88	2.14	1.01	22.17	4.88
19	1.41	0.92	2.62	1.11	18.75	4.72
20						

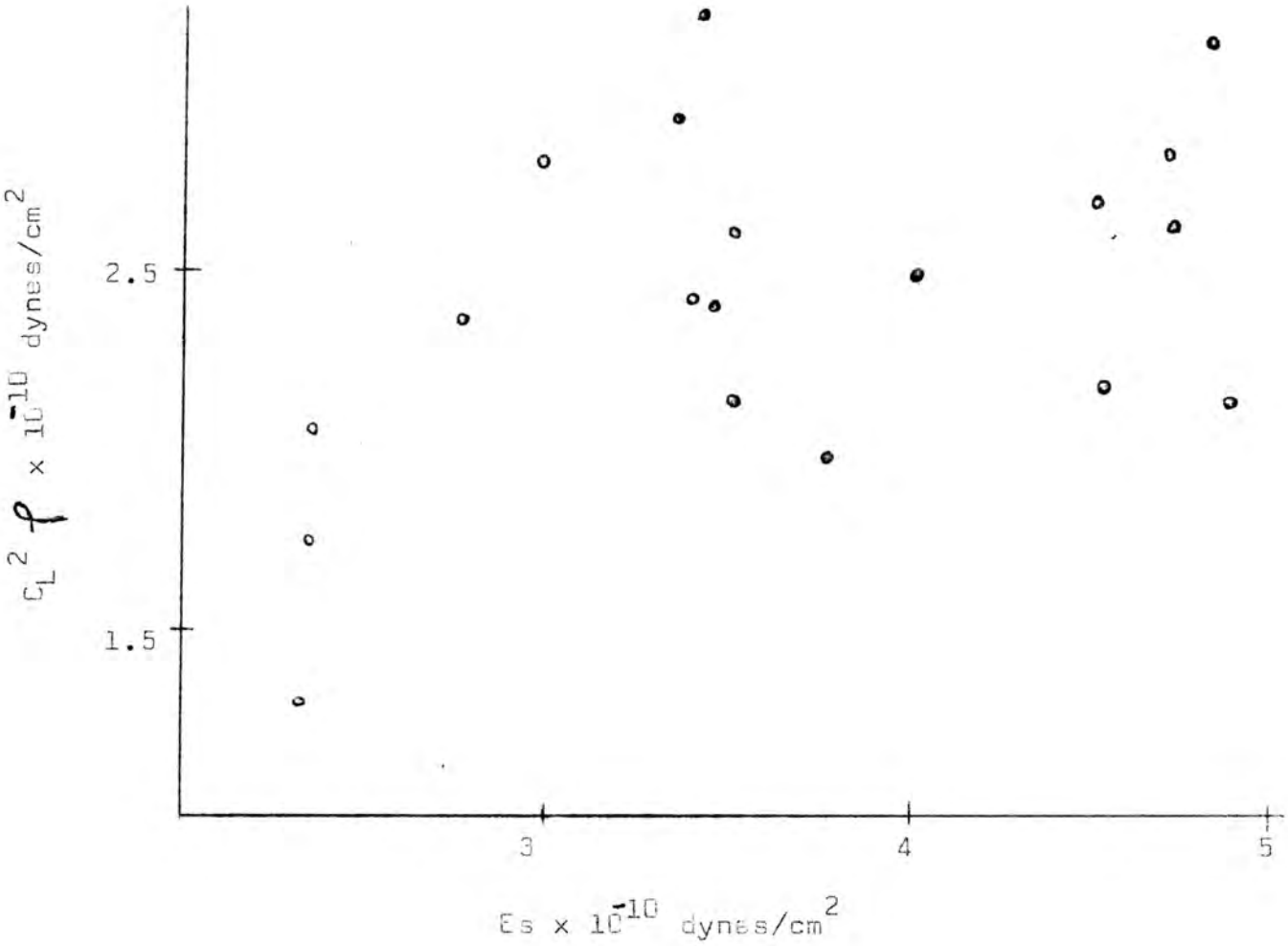

Figure 27. Correlation between ultrasonic longitudinal modulus and stretching modulus for mohair.

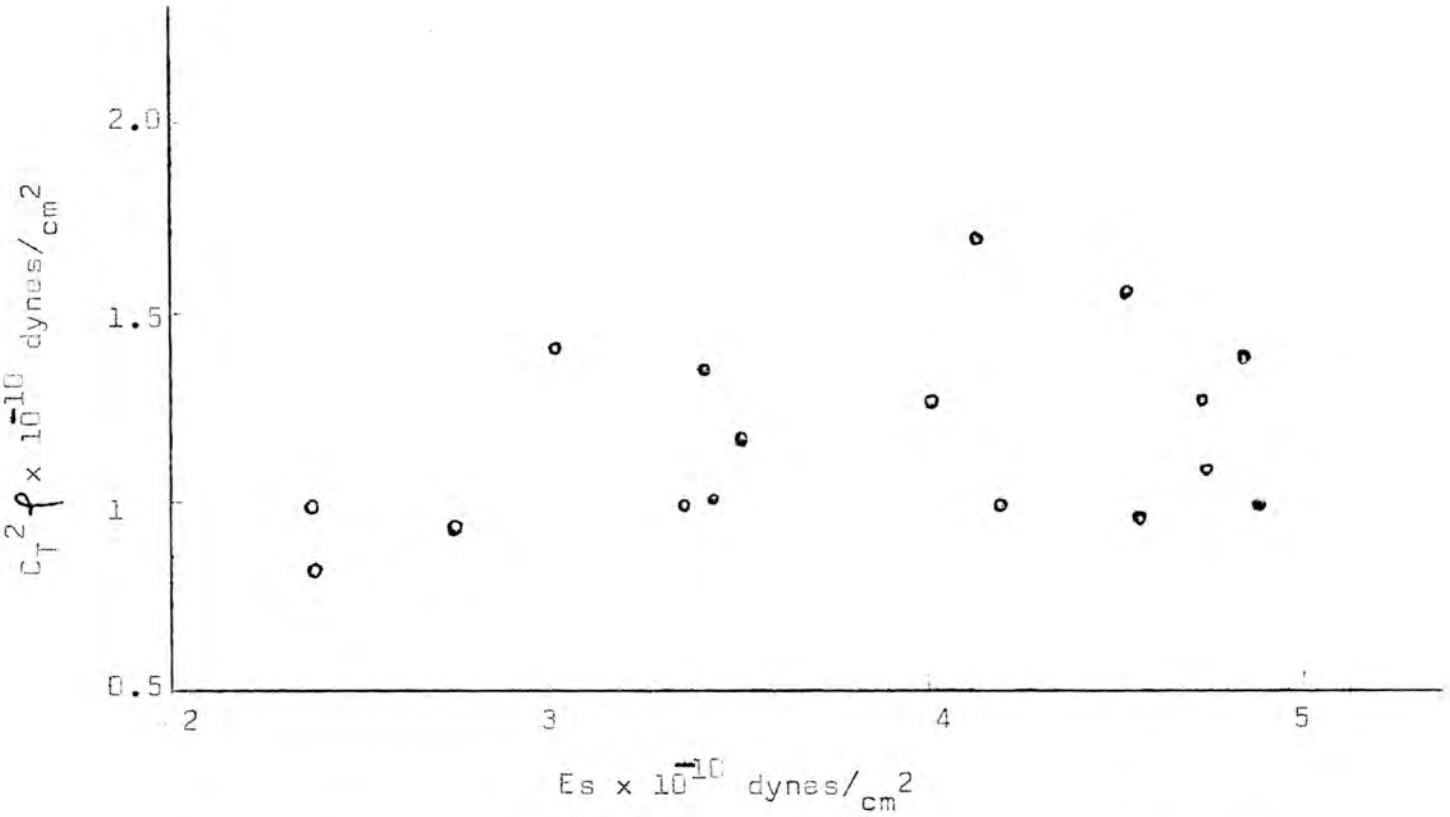

Figure 28. Correlation between ultrasonic torsional modulus and stretching modulus of mohair.

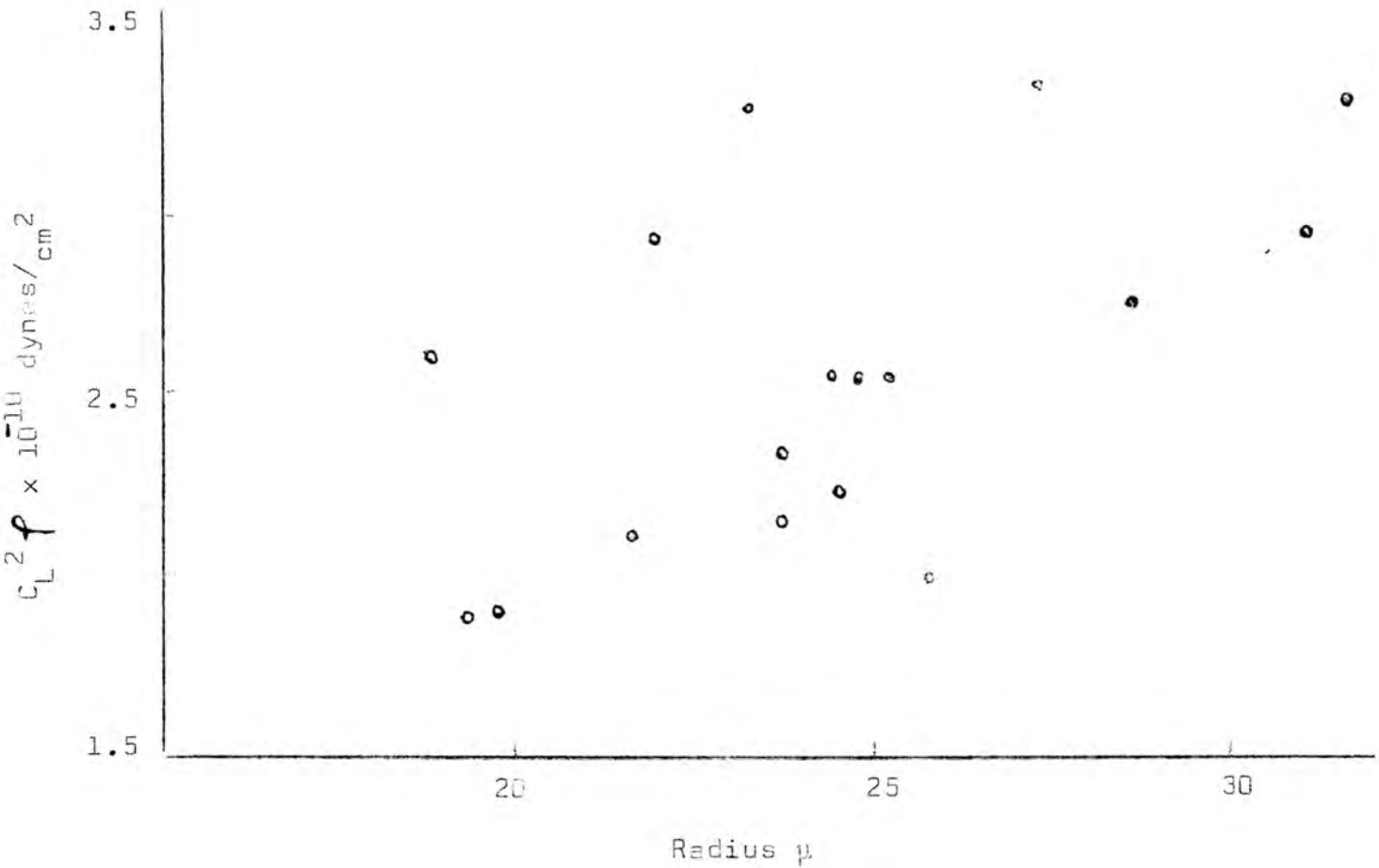

Figure 29. Correlation between longitudinal modulus and fibre radius for mohair.

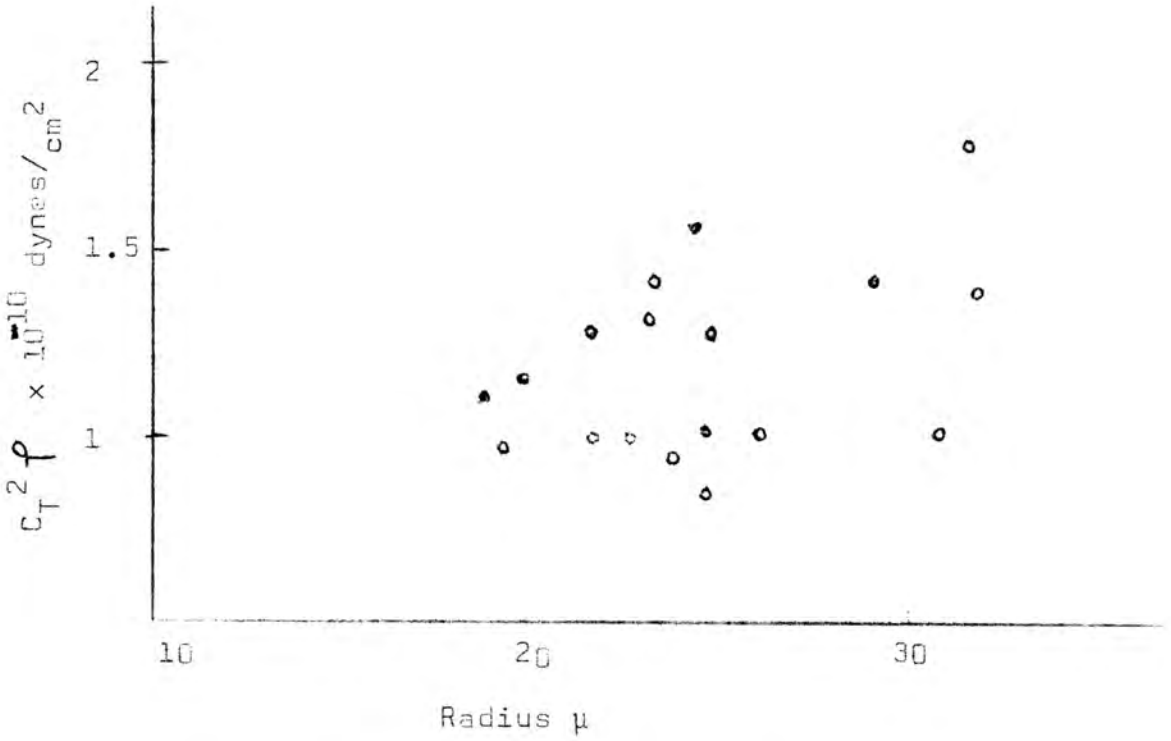

Figure 30. Correlation between torsional modulus and fibre radius for mohair.

modulus measurements were in error since the fibres were under varying amounts of tension before propagation was possible. Also, the delay times (t_o) for each type of transducer were not known so that another error is introduced. E_s results had a large variation. This is because the calculation of E_s involves the inverse of the square of the radius. Fibres with radii with a C. of V. greater than 12% were rejected as in Part II of this thesis in order to minimise the error. It should be noted, however, that E and μ vary over only approximately 1×10^{10} dynes/cm^2, while E_s varies over approximately 3×10^{10} dynes/cm^2. This may be related to fibre structure, since the components responsible for ultrasonic propagation are different from those responsible to extension moduli. It is, however, rather premature to speculate at this stage.

As a result of manipulation difficulties, it was necessary to substitute the transducer holders, with micro-manipulator units, since it was found almost impossible to vary the transducer angle of contact, without either severing the sample or breaking contact with it. The crude adjustment available made propagation a rather "hit and miss" technique and possibly introduced different results on the same fibre as a result of slightly different contact areas as was shown to be the case for fibre mohair 1(c) in Table VI.

4.4 Discussion of results and conclusions

The sequence of presentation of the results above, indicate the difficulties which arose and how they were overcome, in exciting the lowest order longitudinal mode, L(0,1), and the lowest order torsional, T(0), mode in the fibres. At the outset, the major difficulty was that of

the extremely / .....

the extremely high attenuation of the transmitted pulse in the fibre. Ideally, the approach to adopt would have been to commence experiments at a low frequency, increasing fibre diameter until conduction occurred; then increasing the frequency and varying the diameter to determine how rapidly the attenuation changes. From a few such points one could estimate the limits of experimental feasibility. This, however, was not possible since experiments were limited to one particular frequency, which was selected for the reasons given in the introduction of this section.

Very short fibre lengths were employed to begin with, which necessitated the use of the delay plate technique. After conduction has been obtained, it was observed that coupling played an important rôle and, having no success with standard methods, a variety of other coupling techniques were investigated. The results from one of these techniques, viz. a knife edge fixed to the transducer face, indicated velocities were slightly lower than anticipated due to an additional time delay being introduced. This time delay apparently varied with the type of transducer employed, and also with the position of the knife edge to fibre contact for a fixed fibre length (see Table VI). This method of excitation is accomplished relatively simply and quickly. With minor refinements a known tension can be applied to the fibre, consequently this type of coupling seems most suitable for routine measurements of elastic moduli. Mode separation and identification is difficult however. The method of attaching small hooks to the transducer faces, could be refined, but spurious modes were generated which also made identification of the

various lowest / .....

various lowest order modes difficult. This is shown by the results in Table V.

Initially the pressure contact method between transducer face and specimen was subject to large energy losses due mainly to the relatively soft irregular face of the transducer. The polished discs, fixed to the transducer faces, overcame this, but introduced manipulation difficulties when fine diameter specimens were used. This method allowed the identification of the L(0,1), T(0) and F(1,1) modes in a fine copper wire specimen, and equivalent modes in mohair fibres, enabling the values of E and μ to be calculated. Indications are, from the wire specimen results given in Table VII that the time delay factor t_o, as calculated in section 3.3 for the shear and compressional P.Z.T. transducers were in error, and should be of the order of 0.5 μ secs to 1 μ sec. The delay factor t_o appears to be different for different types of transducer coupling.*

At this stage of the investigation the following conclusions have been drawn:-

(i) It is possible to excite mohair, wool and kemp fibres, (amongst others) to act as elastic waveguides and so propagate the lowest order longitudinal L(0,1), and lowest order torsional T(0) modes of vibration in the fibres; and hence to obtain values for Young's modulus E, and shear modulus μ, of the specimen, which are consistent with those

obtained by / .....

* This fact has since been confirmed by the author.

obtained by static determinations, and those of other workers.

(ii) Although poor correlations exist between $C_L^2\rho$, $C_T^2\rho$ and E_s, i.e. E and μ and E_s, this can be accounted for by (a) the large variation in E_s values as a result of diameter variations, (b) the variation of velocity due to an error introduced in measuring the fibre length under tension, and (c) an effect observed where a different velocity is obtained for the same fibre when a different area of contact on the transducer face is used.

A positive correlation between fibre radius and pulse velocity indicates that a tendency exists for thicker fibres to yield higher values of moduli.

(iii) Improvements to the transducer manipulating system are essential if the various modes are to be excited or decoupled*.

(iv) Indications are that with the improvements suggested in (iii) above, it will be possible to excite small diameter wool fibres. With the existing arrangement coarse wool fibres were easily excited, while some results were obtained for fine wool. The main problem with the finer fibres was that severing occurred

with the / .....

* It has been found, since completion of this thesis, that a combination of knife edge coupling and plastic coupling in an ideal means of identifying modes by measuring the slope of a distance versus transit time curve; while simultaneous decoupling of a mode is also possible.

with the slightest amount of manipulation.

(v) The feasibility of developing an instrument for the rapid accurate determination of elastic moduli of high attenuation animal fibres has been demonstrated in the knife edge coupling method. This method has certain advantages over standing wave techniques (S.W.T.). These are:

(a) neither frequency nor length need be varied to calculate the velocity, whereas with S.W.T. at least one of these parameters must be adjustable in order to obtain standing waves;

(b) sample lengths, tension, or degree of stretching can be varied conveniently with pulse techniques, and the most important advantage is

(c) more than one of the elastic constants of the material can be measured during a single excitation.

(vi) Highly medullated fibres show indications of behaving differently to unmedullated types, and a possible group distinction, as found in Part II seems probable.

SUMMARY OF PART II

An apparatus has been built by means of which the static bending modulus of fibres can be determined. By passing known amounts of current through a sensitive galvanometer, with a knife edge attached to the pointer, a known force can be applied to fibres held in a cantilever position. The lengths of the fibres and their deflections under an applied force were measured by means of a travelling microscope, while the diameters were measured on a projection microscope.

Bending moduli E_b, for mohair and kemp were determined. The coefficient of variation of E_b was found to be about 3%.

The bending modulus of mohair was compared with its extension modulus and differences for individual fibres for these two quantities were sometimes very large. However, there was no significant difference between the sample means of E_b and E_s.

Bending of kemp fibres led to two distinct types of fibre, with mean values of E_b differing significantly. The difference is thought to be due to cell filled and partly cell filled medullas. Bending and stretching of the hollow type of kemp do not significantly vary and values are in agreement with those of mohair.

SUMMARY OF PART IV

Excitation of single keratin fibres to act as elastic waveguides and so conduct lowest order longitudinal and torsional modes has been accomplished. Two modes were obtained in the mohair fibres examined which were probably the modes corresponding to Young's modulus E and the shear modulus μ. In order to confirm this, further investigations have been planned and await the arrival of especially cut X-cut and Y-cut Quartz transducers. The main difficulty encountered, was accurate transducer manipulation to make gentle contact with the specimen without severing it; more sensitively adjustable manipulators are also to be employed before further investigations commence. Excitation of fine wool fibres into propagating any particular mode was extremely difficult due to manipulation difficulties and to have attempted thorough investigations would have been time consuming unless the improvements suggested above were carried out. Positive correlations exist between radii and moduli while a poor correlation was found between dynamic moduli and stretching moduli. Experiments in which variations in velocity with frequency are investigated are planned, so that a more accurate picture of attenuation and perhaps optimum operating conditions can be obtained.

APPENDIX I

Correction to Moment of Inertia

(i) For Mohair:-

$$I = \frac{1}{4}\pi r^4$$ where I = Moment of Inertia
r = radius of the fibre
$= \frac{d}{2}$ (diameter)

For a normal distribution of r along the fibre:

$$I = \frac{1}{64}\pi \times \text{Expectation } (d^4)$$

$$= \frac{1}{64}\pi \left[\frac{1}{\sqrt{2\pi}\sigma} \int_{-\infty}^{\infty} d^4 \; e^{\frac{-(d-\bar{d})}{2\sigma^2}} \; d(d) \right]$$

This can be integrated by parts to give (Kendell[64]).

$$\mu_4^1 = \binom{4}{0}\mu_4 + 4\mu_3\mu_1^1 + 6\mu_2\mu_1^{1^2} + 4\mu_1\mu_1^{1^3} + \mu^{1^4}$$

$$= \frac{4!}{4 \times 2} 4 + 6 \frac{2!}{2 \times 1} {}_2m^2 + m^4$$

$$\text{i.e. } I = \pi/64 \left[3\sigma^4 + 6\sigma^2 (\bar{d})^2 + (\bar{d})^4 \right]$$

$$= \pi/64 \; \bar{d}^4 \left[1 + 6 \left(\frac{\sigma}{\bar{d}}\right)^2 + \left(\frac{\sigma}{\bar{d}}\right)^4 \right]$$

In the case of mohair fibre No. 1 (See Table II) we may calculate

$$I = \pi/64 \; \bar{d}^4 \left(1 + 6 \frac{4}{1900} + \ldots\ldots\ldots\right)$$

$$= \underline{\pi/64 \; \bar{d}^4 \; (1.073)}$$

APPENDIX I. (Contd.)

(ii) For a kemp fibre:-

$$I = \pi/64 \left\{ \left[\frac{}{d_1}^4 \left(1 + 6 \left(\frac{\sigma_1}{d_1} \right)^2 + 3 \left(\frac{\sigma_1}{d_1} \right)^4 \right] \right.$$

$$\left. - \left[\frac{}{d_2}^4 \left(1 + 6 \left(\frac{\sigma_2}{d_2} \right)^2 + 3 \left(\frac{\sigma_2}{d_2} \right)^4 \right] \right\}$$

From which we may calculate the Moment of Inertia, for example, for kemp fibres No. 3 (see Table III):-

$$I = \pi/64 \; \bar{d}_1^4 \left(1 + 6 \frac{9}{4900}\right) - \bar{d}_2^4 \left(1 + 6 \frac{25}{1600}\right)$$

$$= \pi/64 \; \bar{d}_1^4 \, (1.01) - \bar{d}_2^4 \, (1.009)$$

where d_2 and d_1 are the inner and outer diameters of the fibre, respectively.

APPENDIX II

Derivation of the wave Equation for unbounded media (See Redwood[54]).

The stress tensor necessary to describe the force on an element of area δs is (See Figure 31)

$$\begin{matrix} \tau_{xx} & \tau_{xy} & \tau_{xz} \\ \tau_{yx} & \tau_{yy} & \tau_{yz} \\ \tau_{zx} & \tau_{zy} & \tau_{zz} \end{matrix}$$

Where the first subscript is regarded as the co-ordinate axis normal to the plane on which the stress acts and the second subscript as the direction of the stress.

However we have that

$$\tau_{xy} = \tau_{yz} \; ; \quad \tau_{zx} = \tau_{xz} \; ; \quad \tau_{yz} = \tau_{zy}$$

by taking moments about the various axes, leaving the six components of stress mentioned in section 3.5.

For small stresses Hooke's law is obeyed, thus each of the six components of stress is a linear function of the six components of strain(e). There are then 36 elastic constants C_{11}, etc.

$$\tau_{xx} = C_{11}\, e_{xx} + C_{12} e_{yy} + C_{13}\, e_{zz} + C_{14} e_{yz} + C_{15} e_{zx} + C_{16} e_{xy}$$

$$\tau_{yy} = C_{21}\, e_{xx} + C_{22} e_{yy} + C_{23}\, e_{zz} + C_{24}\, e_{yz} \ldots\ldots$$

$$\tau_{zz} = C_{31}\, e_{xx} + C_{32} \ldots\ldots\ldots$$

$$\tau_{yz} = C_{41}\, e_{xx} + \ldots\ldots\ldots$$

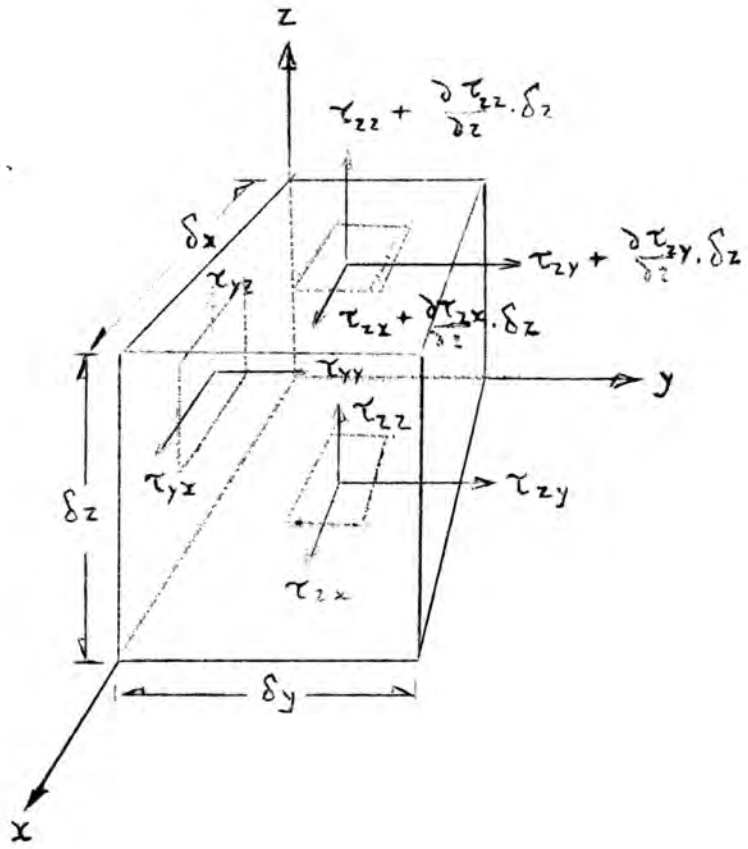

Figure 31. The equilibrium of a solid volume element under stress. Only some of the stresses are shown.

APPENDIX II (Contd.)

$$\tau_{zx} = C_{51}\, e_{xx} + \ldots\ldots$$

$$\tau_{xy} = C_{61}\, e_{xx} + \ldots\ldots \qquad \text{A1}$$

It has been shown[65] that if the elastic energy is single-valued function of strain $C_{jk} = C_{kj}$ and the number of independent constants is 21. For an isotropic solid only two of these constants are needed and they are called the Lamé constants: λ , μ.

$$\lambda = C_{12} = C_{13} = C_{21} = C_{23} = C_{31} = C_{32}$$

$$\mu = C_{44} = C_{55} = C_{66} = \tfrac{1}{2}\,(C_{11} - C_{12})$$

$$\lambda + 2\mu = C_{11} = C_{22} = C_{33}$$

All other coefficients are zero. Thus for the stress we now have

$$\tau_{xx} = \lambda(e_{xx} + e_{yy} + e_{zz}) + 2\mu e_{xx} = \lambda\Delta + 2\mu e_{xx}$$

$$\tau_{yy} = \lambda(e_{xx} + e_{yy} + e_{zz}) + 2\mu e_{yy} = \lambda\Delta + 2\mu e_{yy}$$

$$\tau_{zz} = \lambda(e_{xx} + e_{yy} + e_{zz}) + 2\mu e_{zz} = \lambda\Delta + 2\mu e_{zz}$$

$$\tau_{yz} = \mu e_{yz}; \qquad \tau_{zx} = \mu e_{zx}; \qquad \tau_{xy} = \mu e_{xy} \ldots\ldots \text{A2}$$

where $\Delta = e_{xx} + e_{yy} + e_{zz} = \dfrac{\partial u}{\partial x} + \dfrac{\partial v}{\partial y} + \dfrac{\partial w}{\partial z}$

and is the cubical dilatation.

APPENDIX II (Contd.)

λ and μ completely define the elastic constants of an isotropic solid and are related to E, σ and k by

$$\lambda = \frac{\sigma E}{(1+\sigma)(1-2\sigma)} \quad ; \quad \mu = \frac{E}{2(1+\sigma)} \qquad \text{..... A3}$$

$$E = \frac{\mu(3\lambda + 2\mu)}{\lambda + \mu} \quad ; \quad \sigma = \frac{\lambda}{2(\lambda + \mu)} \quad ; \quad k = \lambda + \frac{2}{3}\mu$$

Note that

$$e_{xx} = \frac{\partial u}{\partial x} \; , \; e_{zy} = \frac{\partial v}{\partial y} \; , \; e_{zz} = \frac{\partial w}{\partial z}$$

$$e_{yz} = \frac{\partial w}{\partial y} + \frac{\partial v}{\partial z} \; ; \; e_{zx} = \frac{\partial u}{\partial z} + \frac{\partial w}{\partial x} \; ; \; e_{xy} = \frac{\partial v}{\partial x} + \frac{\partial u}{\partial y} \qquad \text{..... A4}$$

where (u, v, w) are the co-ordinates which define the displacement of a point P(x,y,z).

Consider the equilibrium of a volume element (Figure 31). The steady forces acting on the body as a whole (such as those due to gravity) are omitted. The x-component of the resultant force on the volume element is:-

$$\left(\tau_{ix} + \frac{\partial \tau_{ix}}{\partial (i)} \delta_i - \tau_{ix} \right) \delta_{si}$$

$$i = x, \; y, \; z$$

where $\delta S_x = (Sy.\delta x)$ etc. This component may therefore be written

$$\left(\frac{\partial \tau_{xx}}{\partial x} + \frac{\partial \tau_{yx}}{\partial y} + \frac{\partial \tau_{zx}}{\partial z}\right).\delta x.\delta y.\delta z.$$

APPENDIX II (Contd.)

By Newton's second law, this force will be equal to:

$\rho \cdot \frac{\partial^2 u}{\partial t^2} \cdot \delta x \, \delta y \, \delta z$. the inertial force in the x-direction

ρ is the linear density of the material. Similar arguments may be applied to the components of force in the y- and z-direction, and we have three equations

$$\rho \frac{\partial^2 u}{\partial t^2} = \frac{\partial \tau_{xx}}{\partial x} + \frac{\partial \tau_{yx}}{\partial y} + \frac{\partial \tau_{zx}}{z}$$

$$\rho \frac{^2 v}{\partial t^2} = \frac{\partial \tau_{xy}}{\partial x} + \frac{\partial \tau_{yy}}{\partial y} + \frac{\partial \tau_{zy}}{\partial z} \qquad \text{..... A5}$$

$$\rho \frac{\partial^2 w}{\partial t^2} = \frac{\partial \tau_{xz}}{\partial x} + \frac{\partial \tau_{yz}}{\partial y} + \frac{\partial \tau_z}{\partial z}$$

These equations are true for both isotropic and anisotropic media. Substituting from Equation A2 into A5 gives three equations of which the first is

$$\frac{\partial^2 u}{\partial t^2} = \frac{\partial}{\partial x}(\lambda \Delta + 2\mu e_{xx}) + \frac{\partial}{\partial y}(\mu e_{yx}) + \frac{\partial}{\partial z}(\mu e_{zx}).$$

or substituting for strains in terms of displacements etc. We have

$$\rho \frac{\partial^2 \mu}{\partial t^2} = (\lambda + \mu) \frac{\partial \Delta}{\partial x} + \mu \nabla^2 \mu.$$

$$\rho \frac{\partial^2 v}{\partial t^2} = (\lambda + \mu) \frac{\partial \Delta}{\partial y} + \mu \nabla^2 v \qquad \text{..... A6}$$

$$\rho \frac{\partial^2 w}{\partial t^2} = (\lambda + \mu) \frac{\partial \Delta}{\partial z} + \mu \nabla^2 w.$$

where ∇^2 is the Laplacian operator: $\left(\frac{\partial^2}{\partial x^2} + \frac{\partial^2}{\partial y^2} + \frac{\partial^2}{\partial z^2}\right)$.

APPENDIX II (Contd.)

The wave equation in terms of potentials ϕ and $\bar{\Psi}$ in rectangular co-ordinates:

The two potential functions, a scalar ϕ and a vector $\bar{\Psi}$ - with components Ψ_x, Ψ_y, Ψ_z are defined by:

$$u = \frac{\partial \phi}{\partial x} + \frac{\partial \Psi_z}{\partial y} - \frac{\partial \Psi_y}{\partial z}$$

$$v = \frac{\partial \phi}{\partial y} + \frac{\partial \Psi_x}{\partial z} - \frac{\partial \Psi_z}{x} \qquad \text{A7}$$

$$w = \frac{\partial \phi}{\partial z} + \frac{\partial \Psi_y}{\partial x} - \frac{\partial \Psi_x}{\partial y}$$

The dilatation is then

$$\Delta = \frac{\partial u}{\partial x} + \frac{\partial v}{\partial y} + \frac{\partial w}{\partial z} = \nabla^2 \phi.$$

Thus the first of the three Equations A6 may be written in the form:

$$\rho \frac{\partial}{\partial x}\left(\frac{\partial^2 \phi}{\partial t^2}\right) + \rho \frac{\partial}{\partial y}\left(\frac{\partial^2 \Psi_z}{\partial t^2}\right) - \rho \frac{\partial}{\partial z}\left(\frac{\partial^2 \Psi_y}{\partial t^2}\right)$$
$$= (\lambda + \mu) \frac{\partial}{\partial x}(\nabla^2 \phi) + \mu \frac{\partial}{\partial y}(\nabla^2 \Psi_z)$$
$$+ \mu \frac{\partial}{\partial x}(\nabla^2 \phi) - \mu \frac{\partial}{\partial z}(\nabla^2 \Psi_y)$$

This equation, and the analogous equations also derived from A6 will be satisfied if the potential functions ϕ and Ψ are solutions of the equations

$$\nabla^2 \phi = \frac{1}{C_d^2} \frac{\partial^2 \phi}{\partial t^2} \qquad \text{A8}$$

APPENDIX II . (Contd.)

$$\nabla^2 \Psi_i = \frac{1}{C_t^2} \frac{\partial^2 \Psi_i}{\partial t^2} \qquad \text{A9}$$

$$i = x, y, z.$$

where

$$C_d^2 = \frac{\lambda + 2\mu}{\rho} = \frac{E(1-\sigma)}{(1+\sigma)(1-2\sigma)} \qquad \text{A10}$$

$$C_t^2 = \frac{\mu}{\rho} \qquad \text{A11}$$

APPENDIX III

Continuous waves in a solid cylinder

In the most general solution of the wave equation for a solid cylinder with cordinates r, θ, and z the particle displacements will be functions of all three variables. "Flexural" waves are found in this category. Two special solutions are of importance. The displacements may be independent of θ - this condition corresponds to "longitudinal" waves - or the displacements in the radial and axial directions may be zero, when torsional waves will be propagated.

Axially symmetrical waves : "longitudinal waves"

(Pochammer-Chree-solutions)

We assume all functions are independent of θ. In cylindrical co-ordinates the wave equations are:

$$\frac{\partial^2 \phi}{\partial r^2} + \frac{1}{r}\frac{\partial \phi}{\partial r} + \frac{\partial^2 \phi}{\partial z^2} = \frac{1}{c_d^2}\frac{\partial^2 \phi}{\partial t^2} \qquad \text{A12}$$

$$\frac{\partial^2 \psi}{\partial r^2} + \frac{1}{r}\frac{\partial \psi}{\partial r} + \frac{\partial^2 \psi}{\partial z^2} = \frac{1}{c_t^2}\frac{\partial^2 \psi}{\partial t^2} \qquad \text{A13}$$

Putting

$$\phi = \phi_0(r)\, e^{-ik_0 z}\, e^{i\omega t} \qquad \text{A14}$$

$$\psi = \psi_0(r)\, e^{-ik_0 z}\, e^{i\omega t} \qquad \text{A15}$$

we obtain two differential equations

$$\frac{\partial^2 \phi_0}{\partial r^2} + \frac{1}{r}\frac{\partial \phi_0}{\partial r} + \left[\left(\frac{\omega}{c_d}\right)^2 - k_0^2\right]\phi_0 = 0 \qquad \text{A16}$$

and

$$\frac{\partial^2 \psi_0}{\partial r^2} + \frac{1}{r}\frac{\partial \psi_0}{\partial r} + \left[\left(\frac{\omega}{c_t}\right)^2 - k_0^2\right]\psi_0 = 0 \qquad \text{A17}$$

APPENDIX III (Contd.)

Each of these may be solved by separating the variables as in the case for a fluid plate. The equations are first order Bessel equations with solutions.

$$\phi = A J_0(k_d r) e^{-k_0 z} e^{i\omega t} \quad \text{A18}$$

$$\psi = C J_0(k_t r) e^{-k_0 z} e^{i\omega t} \quad \text{A19}$$

where

$$k_d^2 = \left(\frac{\omega}{c_d}\right)^2 - k_0^2 \quad \text{A20}$$

and

$$k_t^2 = \left(\frac{\omega}{c_t}\right)^2 - k_0^2 \quad \text{A21.}$$

To find k_d and k_t and A/C in terms of w, the boundary conditions are used. The radial and axial displacements are

$$u_r = \frac{\partial \phi}{\partial r} + \frac{\partial^2 \psi}{\partial r \partial z} \quad \text{A22}$$

$$u_z = \frac{\partial \phi}{\partial z} - \frac{\partial^2 \psi}{\partial r} - \frac{1}{r}\frac{\partial \psi}{\partial r} \quad \text{A23}$$

$$u_r = \left[-k_d A J_1(k_d r) + i k_0 k_t C J_1(k_t r)\right] e^{-ik_0 z} e^{i\omega t} \quad \text{A24}$$

$$u_z = \left[-k_0 A J_0(k_d r) + k_t^2 C J_0(k_t r)\right] e^{-ik_0 z} e^{i\omega t} \quad \text{A25}$$

The stresses are related to the displacements through

$$\tau_{rr} = \lambda\left[\frac{u_r}{r} + \frac{\partial u_r}{\partial r} + \frac{\partial u_z}{\partial z}\right] + 2\mu \frac{\partial u_r}{\partial r} \quad \text{A26}$$

$$\tau_{zr} = \mu\left[\frac{\partial u_r}{\partial z} + \frac{\partial u_z}{\partial r}\right] \quad \text{A27}$$

APPENDIX III (Contd.)

At the boundary (r = a) the stress must be zero. Substitution from A24 and A25 into Equation A26 and putting this equal to zero at r = a, we obtain

$$A\left[-\tfrac{1}{2}(k_t^2-k_0^2)J_0(k_d a)+\frac{k_d}{a}J_1(k_d a)\right] + C\left[ik_0 k_t^2 J_0(k_t a)-\frac{ik_0 k_t}{a}J_1(k_t a)\right] \qquad \text{A28}$$

Putting Equation A27 equal to zero at r = a and using A24 and A25 we have a second equation.

$$A\left[2ik_0 k_d \bar{J}_1(k_d a)\right] - C\left[k_t^3 - k_0^2 k_t\right]\bar{J}_1(k_t a)=0 \qquad \text{A29}$$

If A and C are eliminated from Equations A28 and A29 we obtain the "characteristic equation".

$$k_0^2 \frac{k_t \bar{J}_0(k_t a)}{\bar{J}_1(k_t a)}t\frac{}{} - \tfrac{1}{2}\left(\frac{\omega}{c_t}\right)^2\frac{1}{a} + \left[\tfrac{1}{2}\left(\frac{\omega}{c_t}\right)^2 - k_0^2\right]\frac{\bar{J}_0(k_d a)}{k_d \bar{J}_1(k_d a)} = 0 \qquad \text{A30}$$

If we substitute for $A/_C$ from A29 the equations for μ_r and μ_z became:

$$u_r = iC\left[-\frac{k_0^2-k_t^2}{2k_0}k_t\frac{\bar{J}_1(k_t a)}{\bar{J}_1(k_d a)}\bar{J}_1(k_d r)+k_0 k_t \bar{J}_1(k_t r)\right]e^{-ik_0 z}e^{i\omega t} \qquad \text{A31}$$

and

$$u_z = C\left[\frac{k_0^2-k_t^2}{2k_d}+k_t\cdot\frac{\bar{J}_1(k_t a)}{\bar{J}_1(k_d a)}\bar{J}_0(k_d r)+k_t^2\bar{J}_0(k_t r)\right]e^{-ik_0 z}e^{i\omega t} \qquad \text{A32}$$

The frequency Equation A30 may be solved at any frequency; each root gives the phase velocity of propagation and the displacement functions of a particular mode. These modes are loosely called the "longitudinal modes of vibration". It can be shown that

$$\sin a_d = \frac{c_d}{c_p} = \frac{c_d}{\omega/k_0} \qquad (k_d \text{ real}) \qquad \text{A33}$$

APPENDIX III (Contd.)

and

$$\sin a_t = \frac{c_t}{c_p} = \frac{c_t}{\omega/k_0} \qquad (k_t \text{ real}) \qquad \text{A34}$$

The solutions of the characteristic equation are discussed in the text.

APPENDIX IV

Torsional waves in solid cylinders

Substitution of $U_r = 0$, $U_z = 0$ and U_θ a finite quantity, i.e.

$$u_\theta = u(r)\, e^{-ik_0 z}\, e^{i\omega t} \qquad \text{A35}$$

into Equation A16 or A17 yields one equation of motion

$$\frac{\partial^2 u(r)}{\partial r^2} + \frac{1}{r}\frac{\partial u(r)}{\partial r} - \frac{1}{r^2}u(r) + \left[\left(\frac{\omega}{c_t}\right)^2 - k_0^2\right]u(r) = 0 \qquad \text{A36}$$

The solution to this equation may be written

$$u(r) = A J_1(k_t r) \qquad \text{A37}$$

where as before

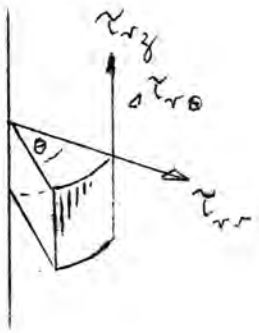

$$k_t^2 = \left(\frac{\omega}{c_t}\right)^2 - k_0^2 \qquad \text{A38}$$

The boundary conditions must also be satisfied. τ_{rr} and τ_{rz} are both zero, and $\tau_{r\theta} = 0$ at $r = a$ if

$$\left[\frac{\partial}{\partial r}\left(\frac{u_\theta}{r}\right)\right]_{r=0} = 0 \qquad \text{A39}$$

This may be written

$$\left[\frac{\partial}{\partial r}\left(\frac{J_1(k_t r)}{r}\right)\right]_{r=0} = 0$$

or

$$\frac{J_0(k_t a)}{J_1(k_t a)} = \frac{2}{k_t a}$$

APPENDIX IV (Contd.)

The roots of this equation are $k_t a = 0, 5.136, 8.418, 11.620$

the solution $k_t a = o$ must be re-examined since $u(r)=o$.

We must rewrite the differential Equation A36 as

$$\frac{\partial^2 u(r)}{\partial r^2} + \frac{1}{r}\frac{\partial u(r)}{\partial r} - \frac{1}{r^2} u(r) = 0 \qquad \text{A40}$$

The solution is $u(r) = Br$ A41

We have thus the solution

$$u_\theta = B.r\, e^{-i\left(\frac{\omega}{c_t}\right)z}\, e^{i\omega t} \qquad \text{when } k_t = o \qquad \text{A42}$$

$$u_\theta = A.J_1(k_t r)\, e^{-ik_0 z}\, e^{i\omega t} \qquad \text{when } k_t \neq o \qquad \text{A43}$$

Equation A42 is the non-dispersive wave mentioned in section 3.9(ii) since $c_t = c_p$ at all frequencies.

REFERENCES

1. Entwistle, D., J. Soc. Dyers & Colourists 37, 12 (1946).
2. Casie, A.B., J. Text. Inst. 37, 154 (1946).
3. Speakman, P.T., J. Text. Inst., Manchester 18, R431 (1927).
4. Speakman, P.T., Proc. Roy. Soc. B., 103, 337 (1928).
5. Sen, G., J. Text. Inst. 37, T339 (1948).
6. Khyatt, R.M. and Chamberlain, N.H., J. Text. Inst. 39, T185 (1948).
7. Meredeth, R., J. Text. Inst. 43, P785 (1952).
8. Van Wyk, C.M., J. Text. Inst. 37, T285 (1946).
9. Winson, C.G., J. Text. Inst. 23, T386 (1932).
10. Schofield, J., J. Text. Inst. 29, T239 (1938).
11. Barker, S.G. and Norris, N.H., J. Text. Inst. 21, T1 (1930).
12. Mitchell, T.W. and Feughelman, M., Text. Res. J. 35, 311 (1965).
13. Simpson, W.S., J. Text. Inst. 56, T675 (1965).
14. Lochner, J., J. Text. Inst. 40, T220 (1949).
15. Guthrie, T.C., Morton, R.H. and Oliver, P.H., J. Text. Inst. 45, T912 (1954).
16. Hermanne, L., Text. Res. J. 19, 61 (1949).
17. Kärrholm, E.M. and Schröder, B., Text. Res. J., 23, 207 (1953).
18. Meredeth, R., Hearle, J.W.S., "Physical methods of investigating textiles", Textile Book Publisher Inc., New York, P217 (1959).
19. Ballou, J.W. and Smith, J.C., J. Appl. Phys. 20, 49 (1949).
20. Lotmar, Helv. Chem. Acta. 19, 68 (1936).
21. Ballou, J.W. and Silverman, S., Text. Res. J., 14, 282 (1944).
22. Hamburger, W.J., Text. Res. J., 18, 102, 105 (1948).
23. Dunell, B.A. and Dillon, J.H., Text. Res. J., 21, 393 (1951).
24. Tipton, H., J. Text. Inst., 46, T322 (1955).
25. Weyland, H.C., Text. Res. J., 31, 629 (1961).

26. Joshi, V.S., Text. Res. J., 34, 732 (1964).

27. Lincoln, B.J., J. Text. Inst., 43, R158 (1952).

28. De Vries, H., Rayon Rev., 10, 53 (1956).

29. Fujino, K., Kawai, H. and Horino, T., Text. Res. J., 25, 722 (1955).

30. Zorowski, C.F. and Murayama, T., Text. Res. J.. 37, 10, 852 (1967).

31. Charch, W.H. and Mosely, W.W., Text. Res. J., 29, 7, 525 (1959)

32. Grover, E.B., Dillon, J.H. and Suppiger, E.W., Text. Res. J., 36, 4, 346 (1966)

33. Morgan, H., "Continuous non-destructive testing of fibres and yarn", presented at Text. Res. Inst. Annual Meeting, April, 1944 and private communication.

34. Wegener, E., Text. Praxi. Internat. II, 33, (1967).

35. Gelles, I.L., J. Acoust. Soc. Americ. 40, 1, 138 (1966).

36. Kinnard, I.F., "Applied electrical measurements", Wiley, New York, (1956).

37. Smith, C.J., "The General properties of matter", Edward Arnold & Co., London, pp. 257, 272 (1953).

38. King, N.E., SAWTRI Techn. Rep. No. 74 (1966).

39. Young, D., "Statistical treatment of experimental data", New York, McGraw Hill Co., pp. 99, 112 (1942).

40. Thorsen, W.J., Text. Res. J., 28, 185 (1958).

41. Von Bergen, N., "Wool Handbook", Vol. I, Third Ed., J.P. Stevens & Co. Inc., 1963.

42. Nosor and Osmin, Vysokomal Soed. 8, 5, 829 (1966).

43. Mason, P., Kolloid Text. 218, 1, 46 (1967).

44. Morton, W.E. and Hearle, J.W.S., "Physical Properties of Textiles", Butterworths, p.31 (1962).

45. Feughelman, M., J. Appl. Polym. Sci. 10, 1937 (1966).

46. Crewther, W.G., Text. Res. J., 35, 10, 867 (1965).

47. Feughelman, M. and Watt, I.C., Text. Res. J. 34, 7, 643 (1964).

48. Oku, M., Kajimoto and Ishibashi, H., J. Text. Inst. 51, T646 (1960).

49. Nolle, A.W., J. Acoust. Soc. America, 19, 1, 194 (1947).

50. Hiller, K.W. and Kolsky, H., Proc. Phys. Soc. 62, 111 (1949).

51. Hiller, K.W., Proc. Phys. Soc. 62, 701 (1949).

52. Bankey, E.C. and Slen, S.B., Text. Res. J. 26, 204 (1956).

53. Ferrous, R.E., M.Sc. Thesis Univ. Manch. (1956).

54. Redwood, M.R., "Mechanical waveguides", Pergamon Press (1960).

55. Kolsky, H., "Stress waves in solids", Oxford Press (1953).

56. Bancroft, D., Phys. Rev. 59, 588 (1941).

57. Davies, R.M., Phil. Trans. Roy. Soc. A240, 375 (1948).

58. Gelles, I.L., Private communication.

59. McSkimin, H.J., J. Acoust. Soc. Am. 28, 484 (1956).

60. Goldman, R.G., "Ultrasonic Technology", Reinhold Publishing Corp., New York, p.182.

61. Gelles, I.L. and Bombhard, C.H., Rev. Sci. Instr. 37, 10, 1345 (1966).

62. Hodgman, C.D., Ed. "Handbook of Chemistry and Physics", Chemical Rubber Publishing Co., 35th Ed., p.2839.

63. Harris, M., Ed. "Handbook of Text. Fibres", Harris Res. Labs. Inc., Washington D.C., p.145 (1954).

64. Kendall, M.C., "The Advanced Theory of Statistics", Vol. I, 4th Ed., Griffin & Co., London (1948).

65. Love, A.E.H., "The Mathematical Theory of elasticity", 4th Ed., Cambridge Univ. Press (1944).

---oOo---